

Supporting information

Elucidating the Molecular Design Principles of *N*-Alkylated Nylons for LCST-Type Phase Separation through a Systematic Polymer Library

Akari Sugano¹, Keitaro Matsuoka^{1,2*}, and Kazuki Sada^{1,2*}

¹ Graduate School of Chemical Sciences and Engineering, Hokkaido University, Sapporo 060-0810, Japan.

² Department of Chemistry, Faculty of Science, Hokkaido University, Sapporo 060-0810, Japan.

Phone: +81-11-706-3473 / Fax: +081-11-706-3474

E-mail: sadatcm@sci.hokudai.ac.jp, ma2oka@sci.hokudai.ac.jp

Contents.

1	General information	2
2	Monomer synthesis procedures and characterization of <i>N</i> -alkylated nylons	3
3	General polymerization procedures and characterization of <i>N</i> -alkylated nylons	5
4	Thermal properties of <i>N</i> -alkylated nylons analyzed by DSC	83
5	Thermo-responsiveness of <i>N</i> -alkylated nylons	87
6	DLS measurement of thermo-responsive behavior of <i>N</i> -Et-4,4 in H ₂ O	103
7	¹ H NMR analysis of thermo-responsive behavior of <i>N</i> -Et-4,4 in D ₂ O	104
8	Concentration dependence of <i>N</i> -alkylated nylons on the LCST-type phase separation	105
9	Supplementary references	108

1 General information

All reactions were carried out in flame-dried glassware under a nitrogen atmosphere unless otherwise noted. Commercially available dichloromethane (DCM, Wako Ltd., Super Dehydrated grade) and triethylamine (TEA, Sigma-Aldrich $\geq 99.5\%$) were used without further manipulation unless otherwise stated. Commercially available monomer *N,N'*-dimethylethylenediamine (TCI Co., Ltd.), *N,N'*-diethylethylenediamine (TCI Co., Ltd.), *N,N'*-diethyl-1,3-propanediamine (Wako Ltd.), *N,N'*-diisopropylethylenediamine (TCI Co., Ltd.), Malonyl chloride (Sigma-Aldrich), Succinyl chloride (TCI Co., Ltd.), Glutaryl chloride (TCI Co., Ltd.), Adipoyl chloride (TCI Co., Ltd.), Pimeloyl chloride (Sigma-Aldrich), and Suberoyl chloride (TCI Co., Ltd.) were commercially available and used as received unless otherwise noted. The monomer of *N,N'*-diethyl-1,4-diaminobutane, *N,N'*-di-*n*-propylethylenediamine and 3-Methyl-glutaryl chloride^[1] were synthesized according to the literature. All other reagents were commercially available and used as received unless otherwise noted.

¹H NMR and ¹³C NMR spectra were recorded on JEOL JNM-ECZ400 spectrometers. Chemical shifts were reported in the scale relative to CHCl₃ (7.26 ppm for ¹H NMR), and CDCl₃ (77.0 ppm for ¹³C NMR) as an internal reference, respectively.

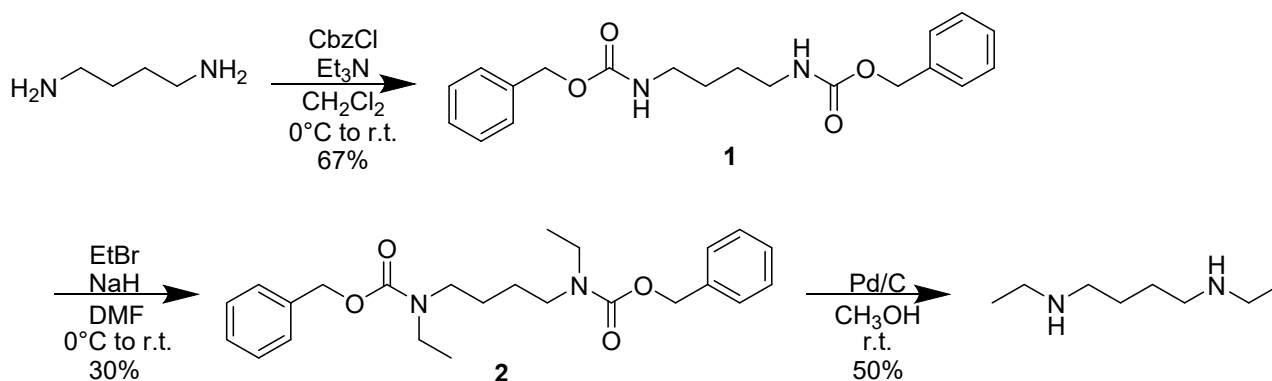
Size exclusion chromatography (SEC) Measurements were performed on a polystyrene gel column Shodex K-803L and K-805L connected to a SHIMADZU CTO-20A with LC-20AD gradient pump, SPD-20A UV detector, and RID-20A refractive detector. CHCl₃ was used as an eluent at 40 °C (flow rate of 1.0 mL/min). The calibrations were made against linear polystyrene standards for CHCl₃. Number average molecular weight (M_n), weight average molecular weight (M_w), and polydispersity index (\mathcal{D}) were determined by SEC Measurements.

Differential scanning calorimetry (DSC) was performed on a METTLER TOLEDO STAR^e System DSC 1 at a heating rate of 10 °C/min under a nitrogen flow of 60 mL/min.

Transmittance Measurements at 800 nm were recorded on a Jasco V-750 spectrophotometer with a Jasco ETC-505T temperature controller, and the temperature scan rate was 1.5 °C/min. Cloud point (T_{cp}) was determined by the Transmittance measurement using UV-vis as the temperature at which %Transmittance = 90 in the heating process. Dynamic light scattering (DLS) data were collected on a Malvern Nano-S light scattering system with a 633 nm He/Ne laser at 20 °C.

2 Monomer synthesis procedures and characterization of *N*-alkylated nylons

N,N'-diethyl-1,4-butanediamine



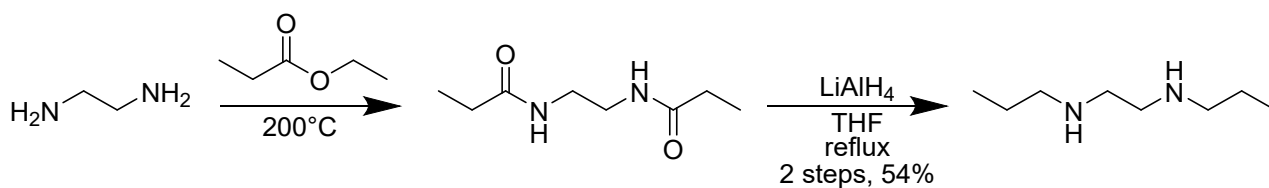
Benzyl chloroformate (10.5 mL, 73.5 mmol) in CH₂Cl₂ (40 mL) was added dropwise to a solution of 1,4-butanediamine (3.50 mL, 35.0 mmol) and triethylamine (12.0 mL, 86.7 mmol) in CH₂Cl₂ (80 mL) at 0 °C. The reaction mixture was stirred at 0 °C for 1 h and then at room temperature overnight. The solvent was removed under reduced pressure, and the crude product was washed with water. The resulting solid was collected by filtration and dried under vacuum to afford compound **1**.

NaH (60% dispersion in Paraffin Liquid, 2.81 g, 70.0 mmol) was added to a solution of **1** (8.32 g, 23.3 mmol) in DMF (120 mL) at 0 °C, and the mixture was stirred at 0 °C for 1 h. Ethyl bromide (5.20 mL, 70.0 mmol) was then added, and the reaction mixture was stirred at room temperature overnight. The reaction mixture was diluted with sat. aq. NaHCO₃ (30 mL) and water (200 mL), and extracted with ethyl acetate (100 mL × 3). The combined organic layers were washed with water (100 mL × 2) and brine (100 mL), dried over MgSO₄, filtered, and concentrated under reduced pressure to give the crude product. Purification by silica gel column chromatography (10% ethyl acetate in CH₂Cl₂) afforded compound **2**.

Pd/C (10 % on carbon, 285 mg) was added to a solution of **2** in methanol (25 mL), and the mixture was stirred under a hydrogen atmosphere at room temperature overnight. The catalyst was removed by filtration, and the solvent was evaporated under reduced pressure. The residue was purified by vacuum distillation to afford *N,N'*-diethyl-1,4-butanediamine.

¹H NMR (CDCl₃, 400 MHz) δ = 2.57-2.70 (m, 8 H), 1.53 (q, 4 H), 1.11 (t, 6 H).

N,N'-di-*n*-propylethylenediamine

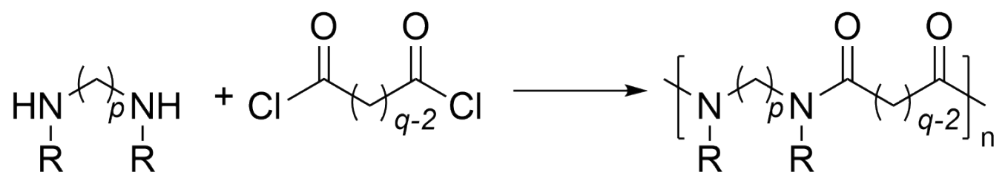


Ethylenediamine (2.20 mL, 32.6 mmol) and ethyl propionate (20 mL) were placed in an autoclave and heated at 200°C for 12 h. After cooling to room temperature, the crude product was washed with ethyl propionate and purified by recrystallization (ethanol/acetone/hexane = 0.5:1:10) to afford the corresponding solid.

The obtained solid was dissolved in THF (150 mL) and cooled to 0°C . LiAlH_4 (4.82 g, 127 mmol) was added, and the reaction mixture was refluxed for 2 days. After cooling to 0°C , an excess of $\text{Na}_2\text{SO}_4 \cdot 10\text{H}_2\text{O}$ was carefully added to quench the reaction. The mixture was filtered, and the filtrate was washed with THF. The organic solution was concentrated under reduced pressure. The residue was purified by vacuum distillation to afford *N,N'*-di-*n*-propylethylenediamine.

^1H NMR (CDCl_3 , 400 MHz) δ = 2.72 (s, 4 H), 2.58 (t, 4 H), 1.51 (sext, 4 H), 0.92 (t, 6 H).

3 General polymerization procedures and characterization of *N*-alkylated nylons



To a stirred solution of *N,N'*-dialkyl- α,ω -alkyldiamine (1.0 equiv.) and triethylamine (2.0 equiv.) in DCM (0.4 M) was added α,ω -diacid chloride (1.0 equiv.) dropwise at 0 °C for 15-30 min. The reaction mixture was stirred at 0 °C for 30 min. and warmed to room temperature. After stirring for 2 h, the solvent was removed *in vacuo*. The residue was purified by dialysis against water for 3–5 days using a dialysis membrane (Spectra/Por® 3, 3.5 kD) and freeze-drying to afford *N*-alkylated nylons.

N,N'-diethylnylon-2,4 (*N*-Et-2,4)

Polymerization of *N,N'*-diethylethylenediamine (1.50 mL, 10.5 mmol) and Succinyl chloride (1.18 mL, 10.4 mmol) afforded *N*-Et-2,4 (217 mg, 55% yield) as a brown solid.

^1H NMR (CDCl_3 , 400 MHz) δ = 3.18-4.03 (m, 8 H), 2.40-3.00 (m, 4 H), 0.92-1.35 (m, 6 H).

^{13}C NMR (CDCl_3 , 100 MHz) δ = 171.7, 45.1, 44.8, 43.8, 43.3, 28.0, 14.2, 13.0.

SEC (CHCl_3): $M_n = 2.3 \times 10^3$, $D = 1.6$.

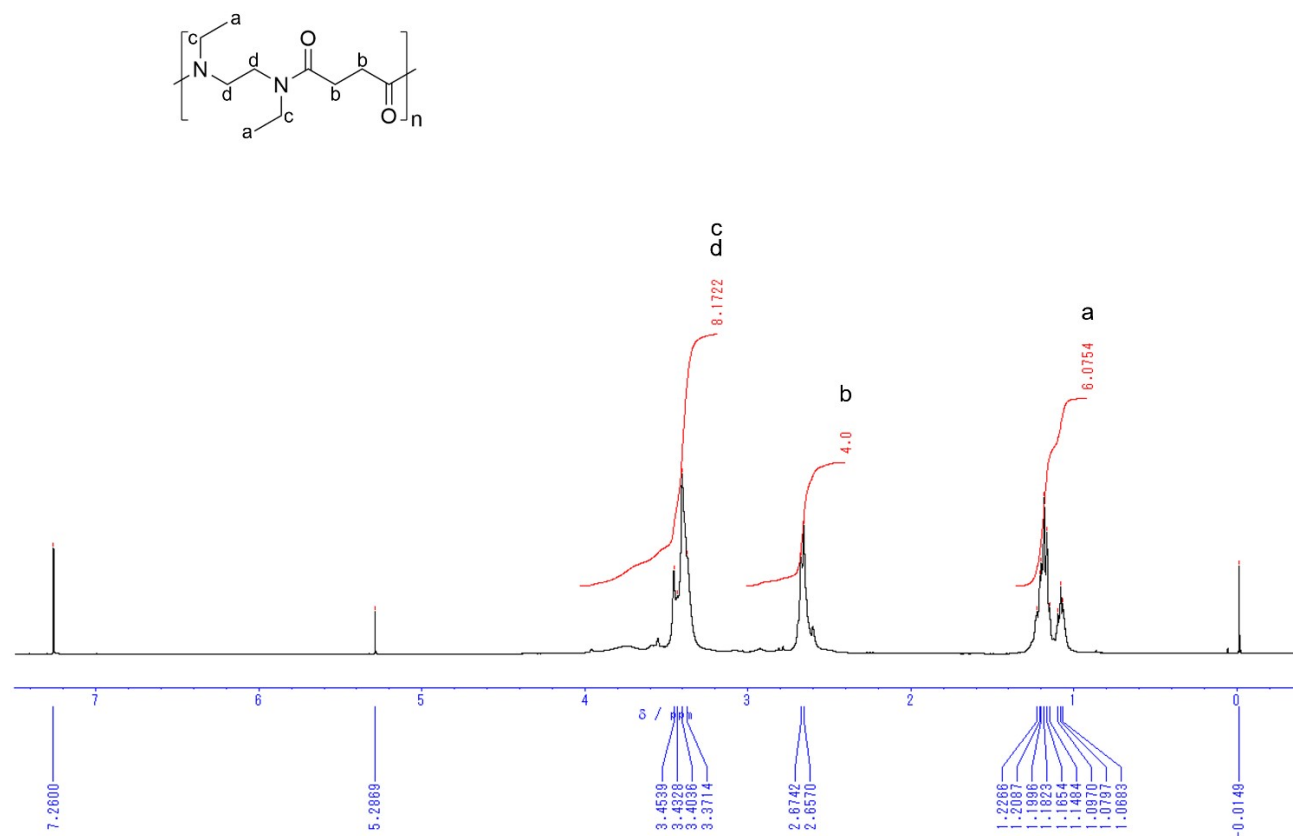


Figure S1. ^1H NMR spectrum of *N*-Et-2,4

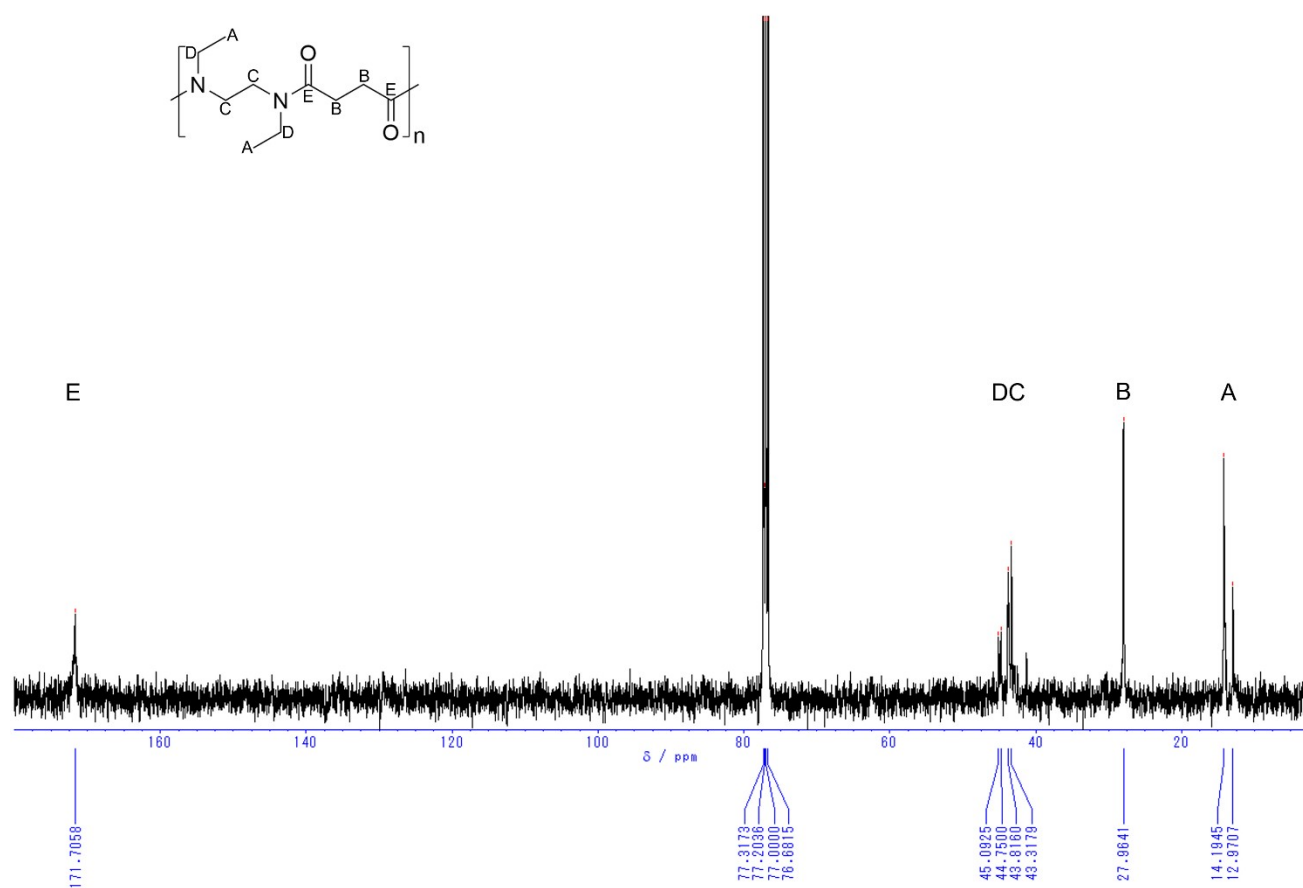


Figure S2. ^{13}C NMR spectrum of *N*-Et-2,4

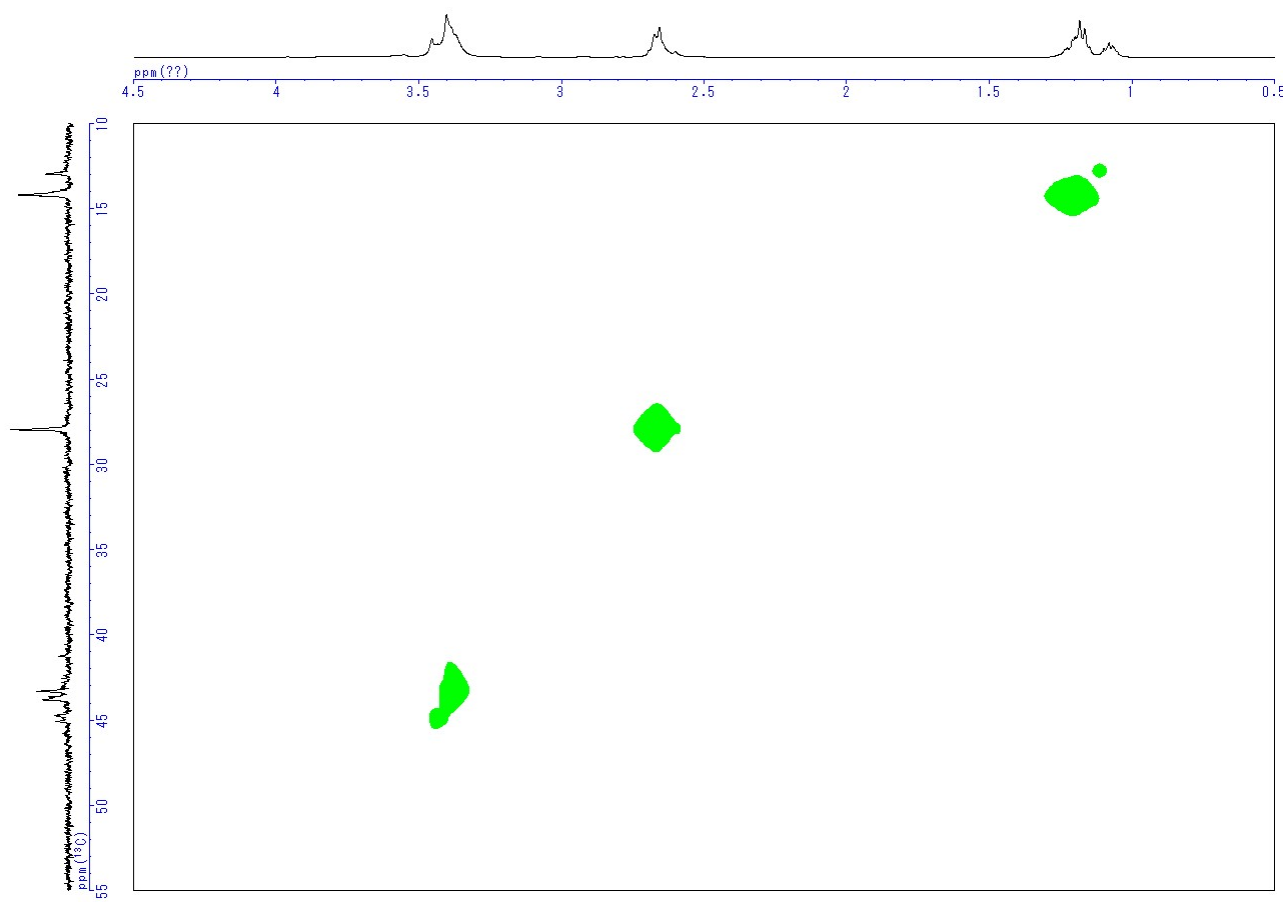


Figure S3. HMQC spectrum of *N*-Et-2,4

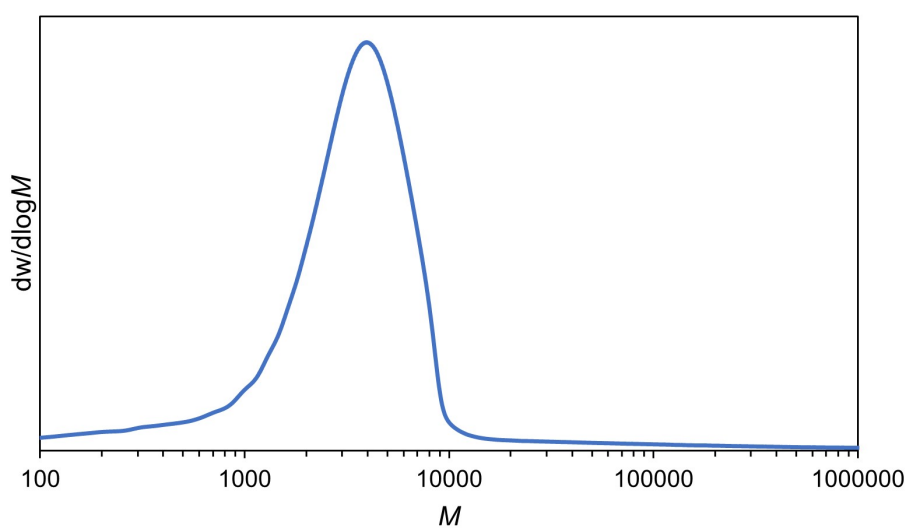


Figure S4. SEC chromatogram of *N*-Et-2,4

N,N'-diethylnylon-2,5 (*N*-Et-2,5)

Polymerization of *N,N'*-diethylethylenediamine (287 μ L, 2.00 mmol) and Glutaryl chloride (258 μ L, 2.00 mmol) afforded *N*-Et-2,5 (143 mg, 34% yield) as a brown solid.

^1H NMR (CDCl_3 , 400 MHz) δ = 3.22-3.57 (m, 8 H), 2.29-2.51 (m, 4 H), 1.86-2.08 (m, 2 H), 1.03-1.27 (m, 6 H).

^{13}C NMR (CDCl_3 , 100 MHz) δ = 172.2, 44.7, 43.4, 43.2, 31.9, 20.5, 14.2, 13.0.

SEC (CHCl_3): M_n = 5.0×10^3 , \bar{D} = 2.4.

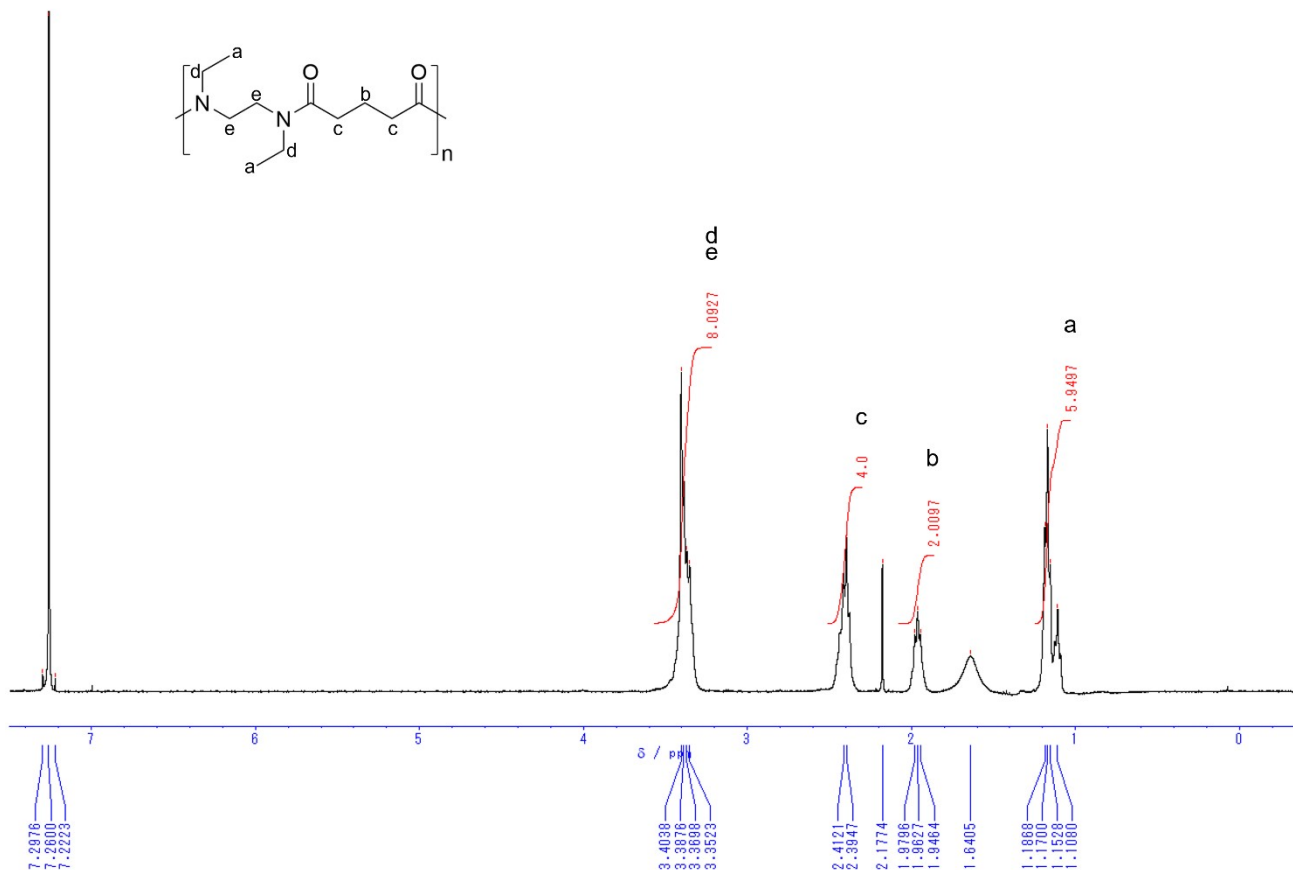


Figure S5. ^1H NMR spectrum of *N*-Et-2,5

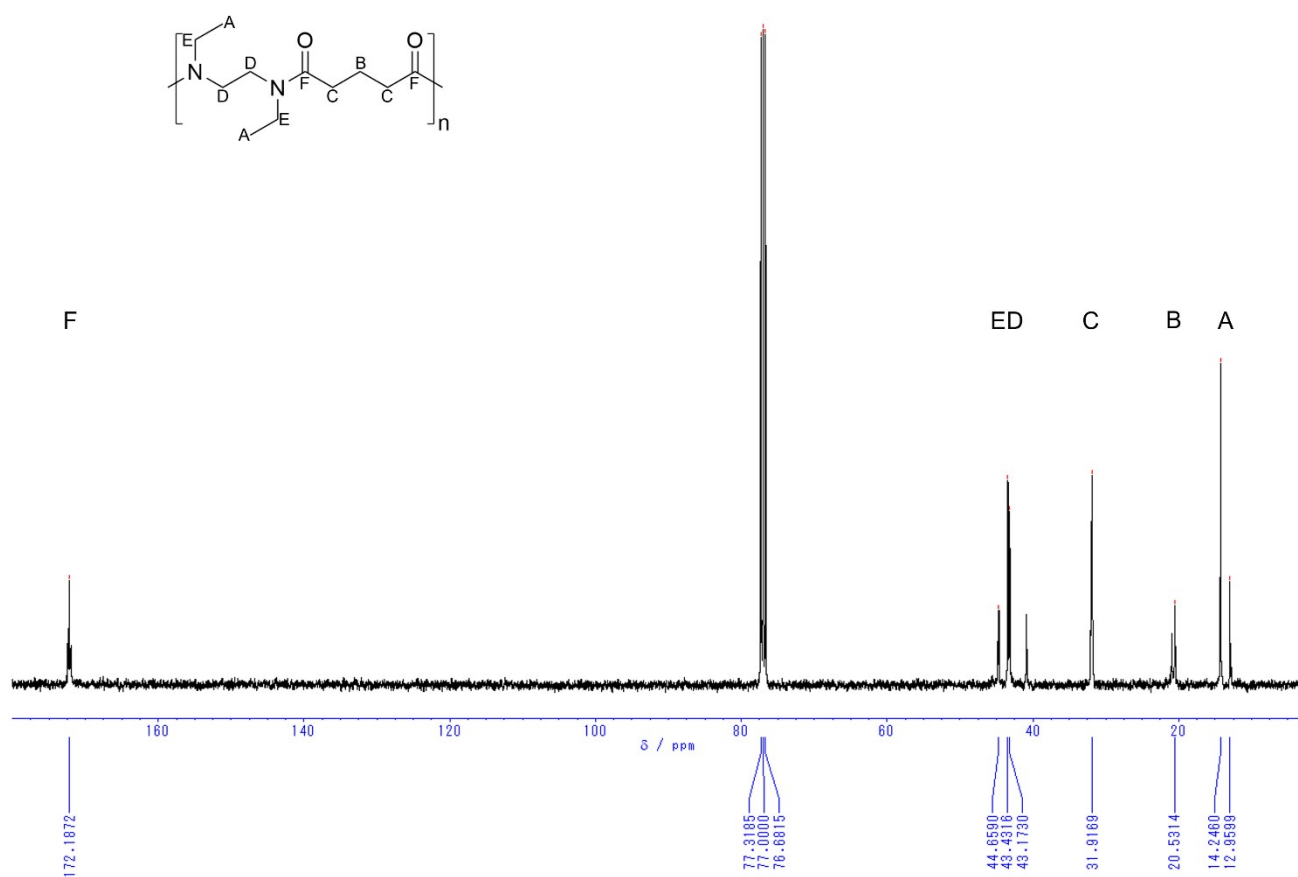


Figure S6. ¹³C NMR spectrum of *N*-Et-2,5

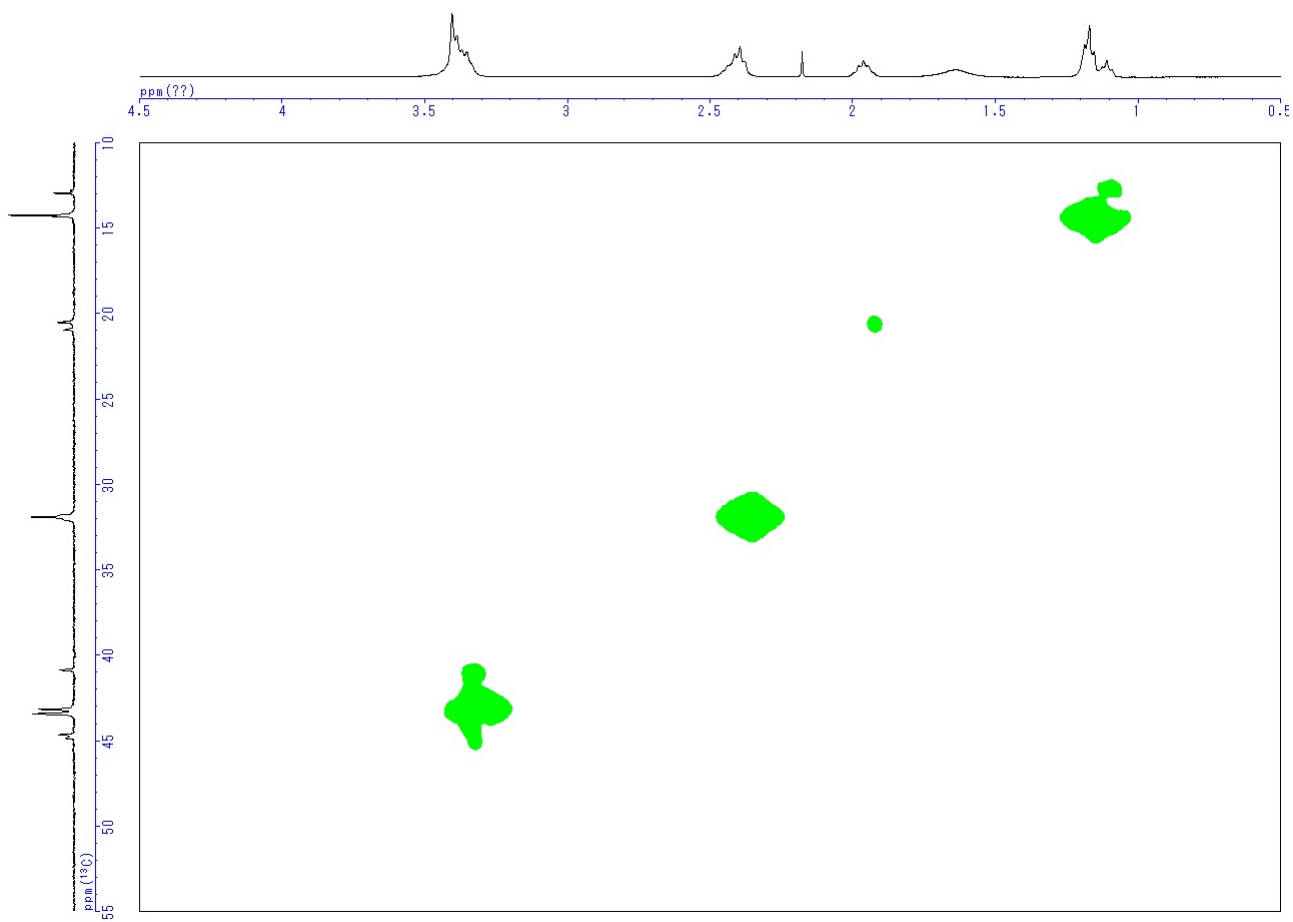


Figure S7. HMPC spectrum of *N*-Et-2,5

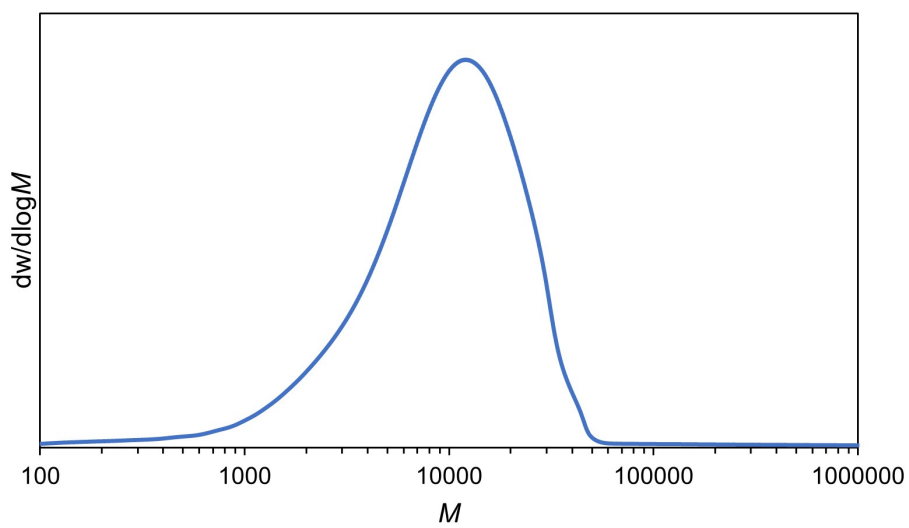


Figure S8. SEC chromatogram of *N*-Et-2,5

N,N'-diethylnylon-2,6 (*N*-Et-2,6)

Polymerization of *N,N'*-diethylethylenediamine (287 μ L, 2.00 mmol) and Adipoyl chloride (291 μ L, 2.00 mmol) afforded *N*-Et-2,6 (60.2 mg, 13% yield) as a yellow solid.

^1H NMR (CDCl_3 , 400 MHz) δ = 3.04-3.66 (m, 8 H), 2.26-2.44 (m, 4 H), 1.56-1.82 (m, 4 H), 0.98-1.30 (m, 6 H).

^{13}C NMR (CDCl_3 , 100 MHz) δ = 172.5, 43.5, 43.3, 32.7, 25.0, 14.5, 14.4, 13.0.

SEC (CHCl_3): M_n = 5.1×10^3 , D = 1.7.

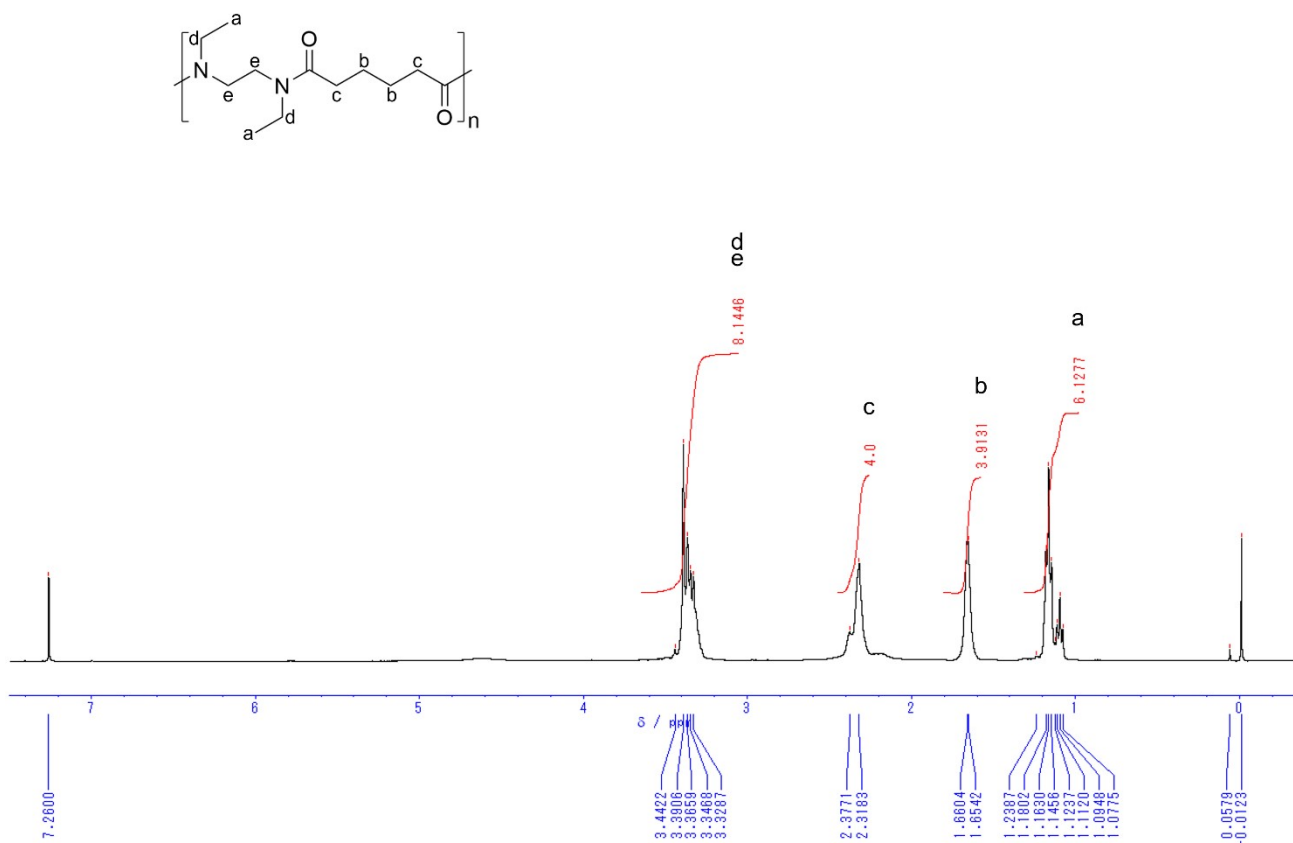


Figure S9. ^1H NMR spectrum of *N*-Et-2,6

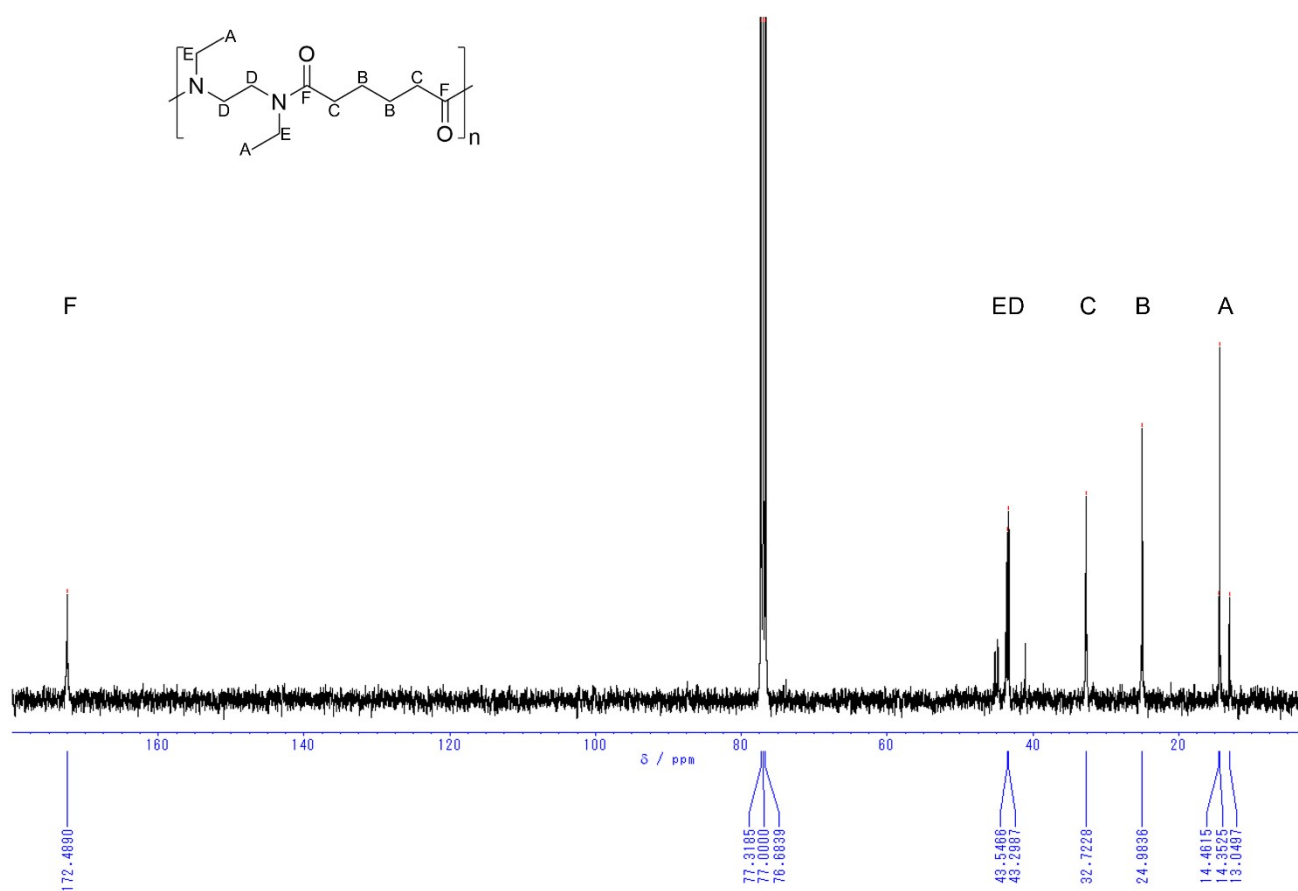


Figure S10. ¹³C NMR spectrum of *N*-Et-2,6

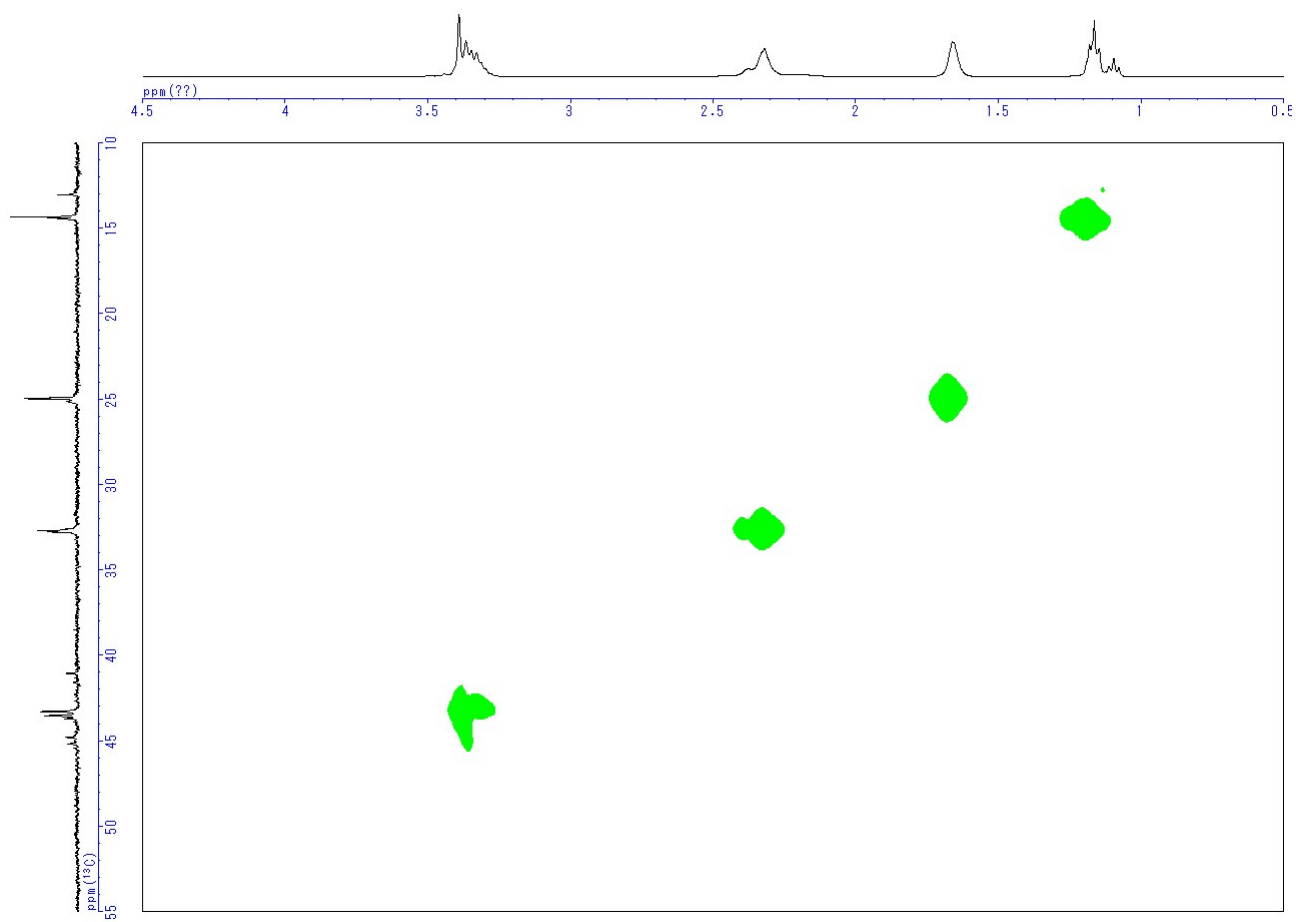


Figure S11. HMQC spectrum of *N*-Et-2,6

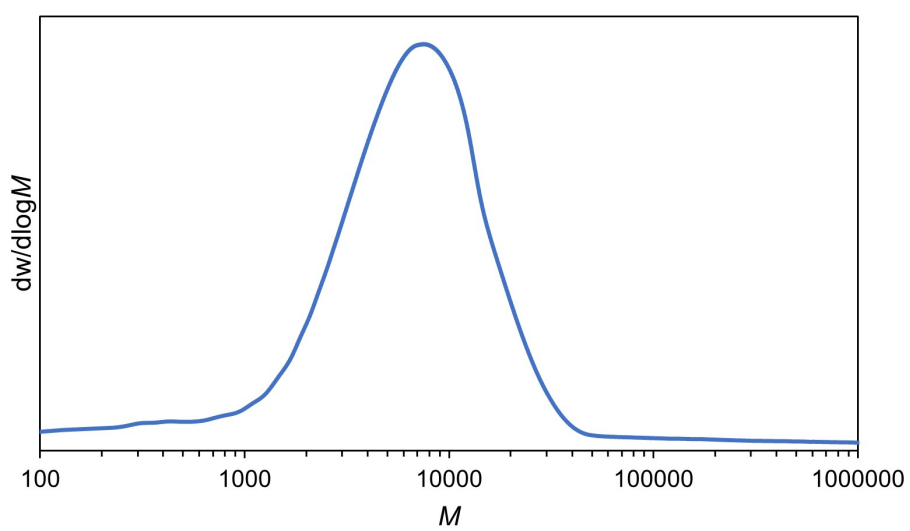


Figure S12. SEC chromatogram of *N*-Et-2,6

N,N'-diethylnylon-2,7 (*N*-Et-2,7)

Polymerization of *N,N'*-diethylethylenediamine (287 μ L, 2.00 mmol) and Pimeloyl chloride (326 μ L, 2.00 mmol) afforded *N*-Et-2,7 (265 mg, 55% yield) as a yellow solid.

^1H NMR (CDCl_3 , 400 MHz) δ = 3.16-3.53 (m, 8 H), 2.22-2.46 (m, 4 H), 1.57-1.78 (m, 4 H), 1.31-1.48 (m, 2 H), 1.04-1.24 (m, 6 H).

^{13}C NMR (CDCl_3 , 100 MHz) δ = 172.7, 13.4, 13.2, 32.7, 29.2, 14.3, 13.0.

SEC (CHCl_3): M_n = 6.9×10^3 , Đ = 2.0.

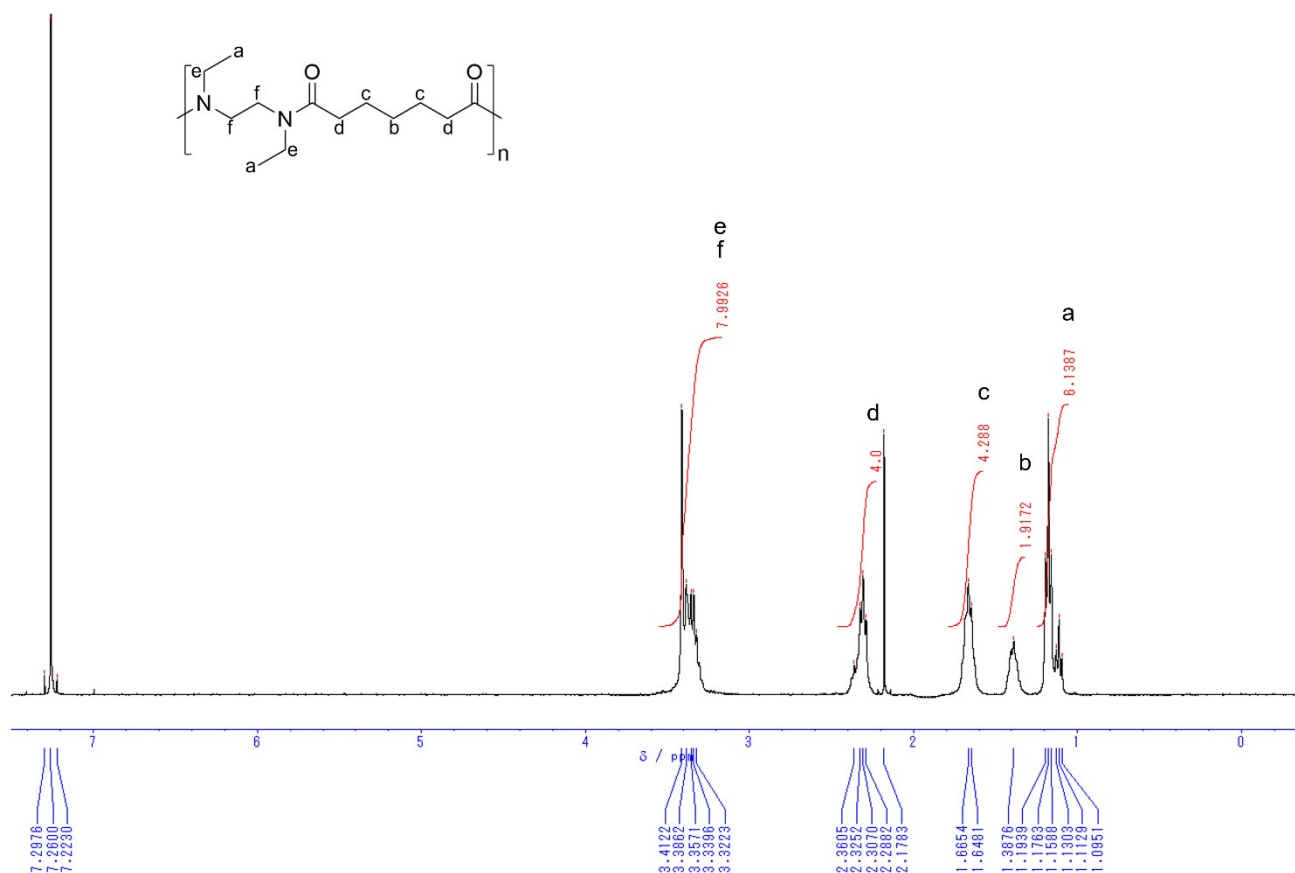


Figure S13. ^1H NMR spectrum of *N*-Et-2,7

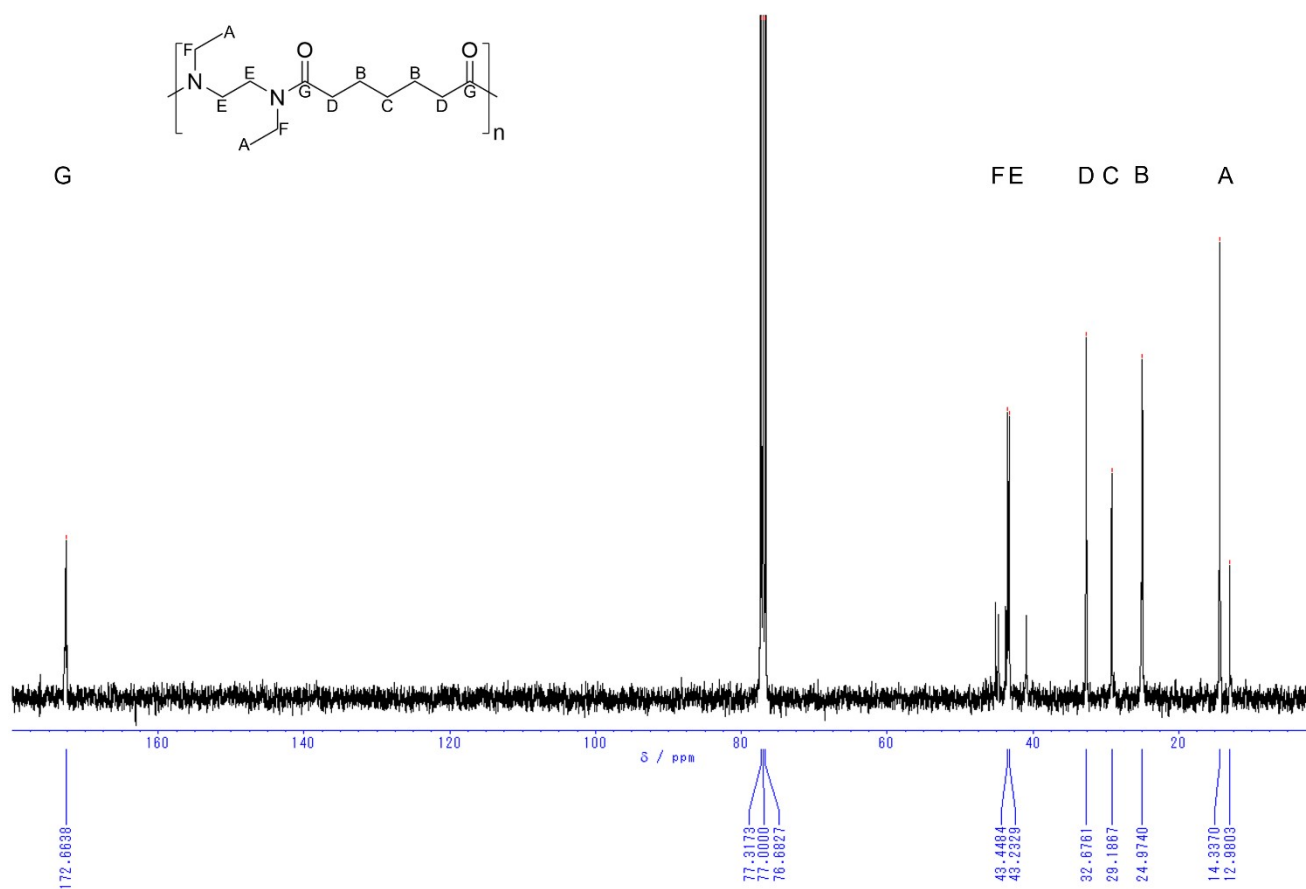


Figure S14. ¹³C NMR spectrum of *N*-Et-2,7

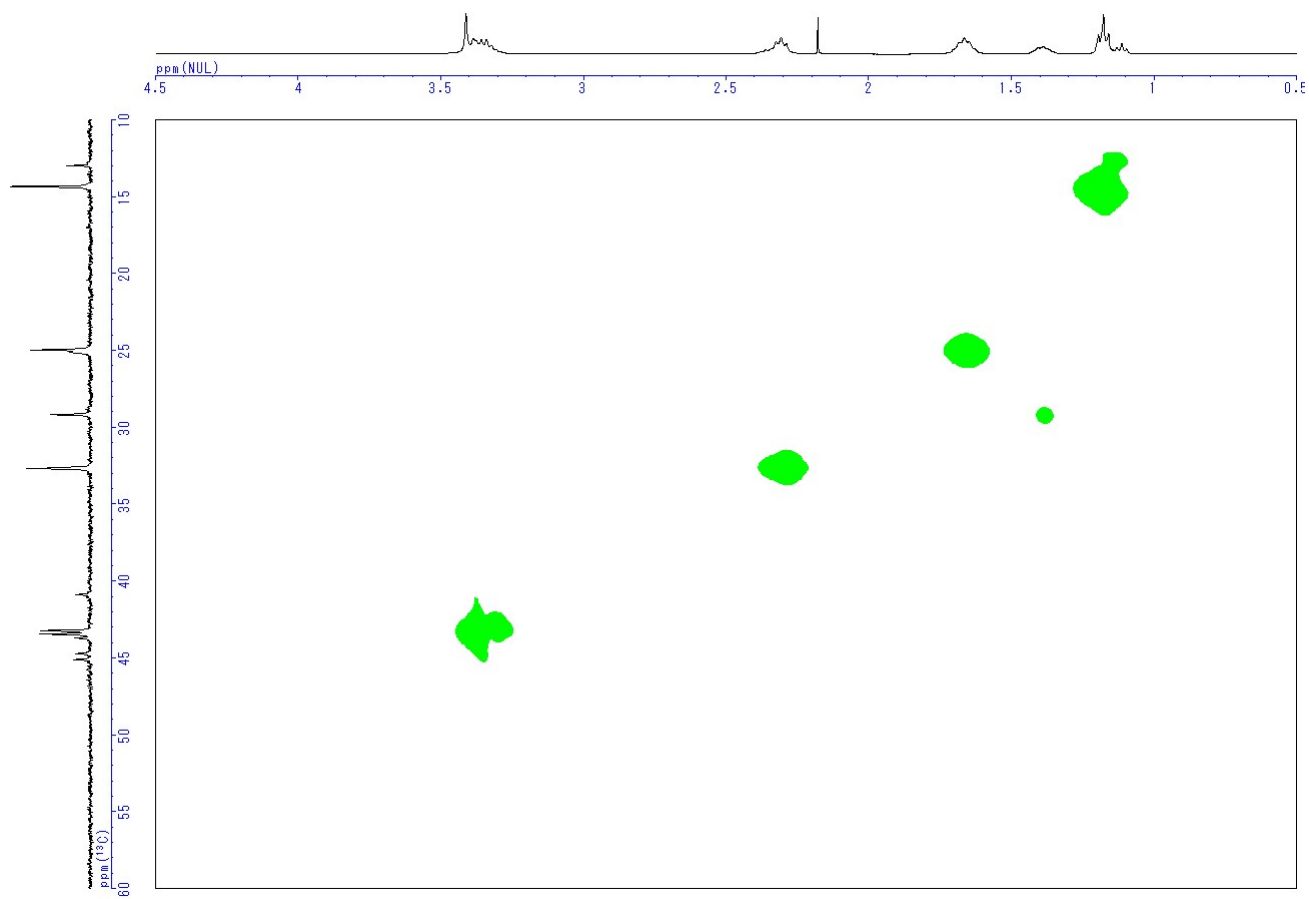


Figure S15. HMQC spectrum of *N*-Et-2,7

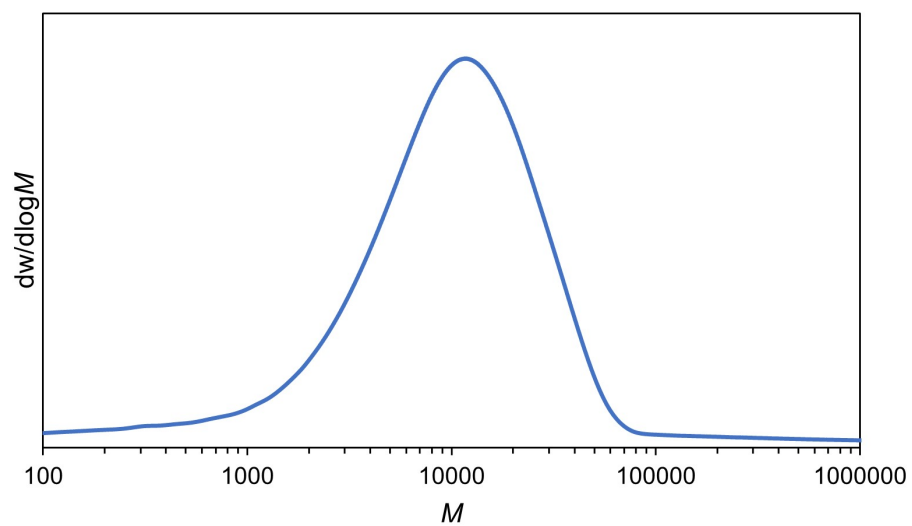


Figure S16. SEC chromatogram of *N*-Et-2,7

N,N'-diethylnylon-2,8 (*N*-Et-2,8)

Polymerization of *N,N'*-diethylethylenediamine (287 μL , 2.00 mmol) and Suberoyl chloride (361 μL , 2.00 mmol) afforded *N*-Et-2,8 (237 mg, 47% yield) as a yellow solid.

^1H NMR (CDCl_3 , 400 MHz) δ = 3.17-3.49 (m, 8 H), 2.16-2.43 (m, 4 H), 1.53-1.76 (m, 4 H), 1.27-1.46 (m, 4 H), 1.06-1.25 (m, 6 H).

^{13}C NMR (CDCl_3 , 100 MHz) δ = 172.8, 43.4, 43.2, 32.8, 29.3, 25.1, 14.3, 13.0.

SEC (CHCl_3): M_n = 1.4×10^4 , \bar{D} = 1.7.

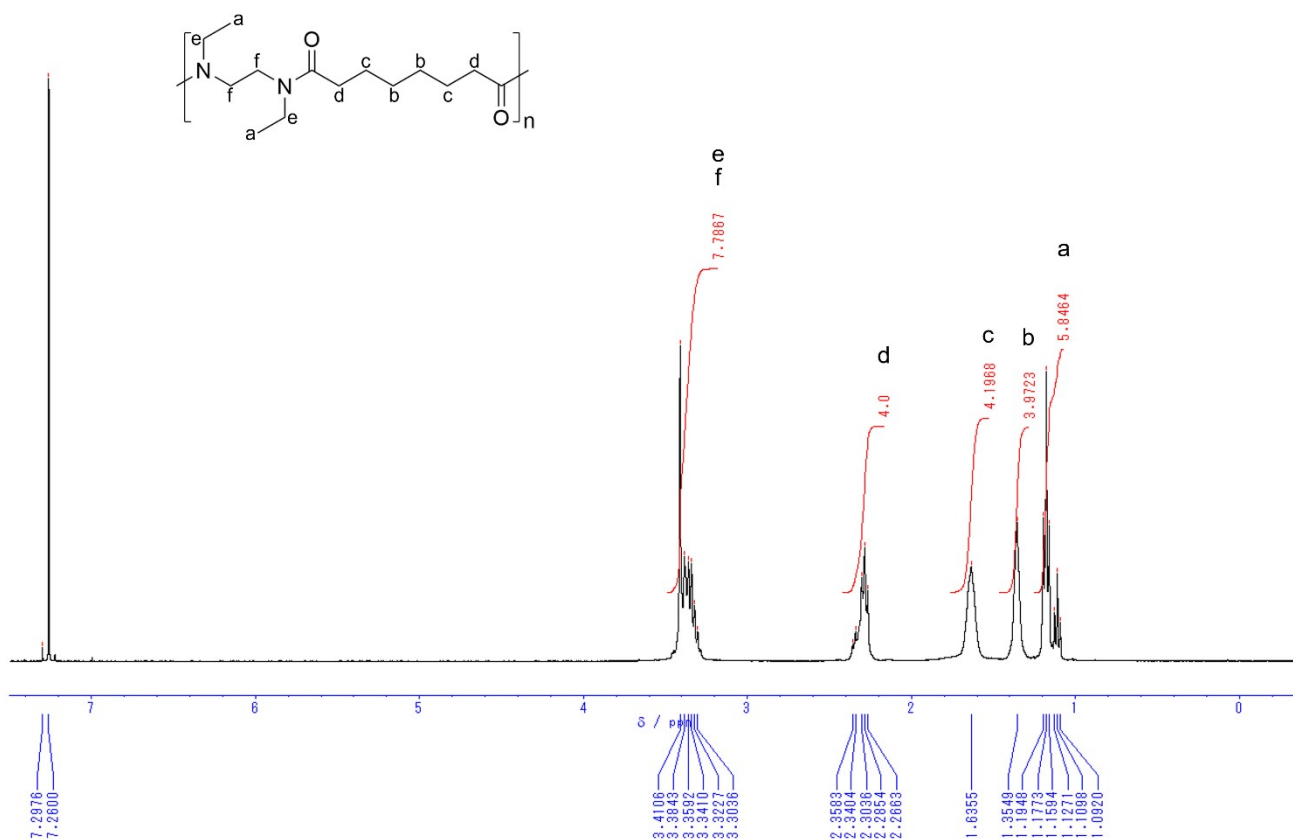


Figure S17. ^1H NMR spectrum of *N*-Et-2,8

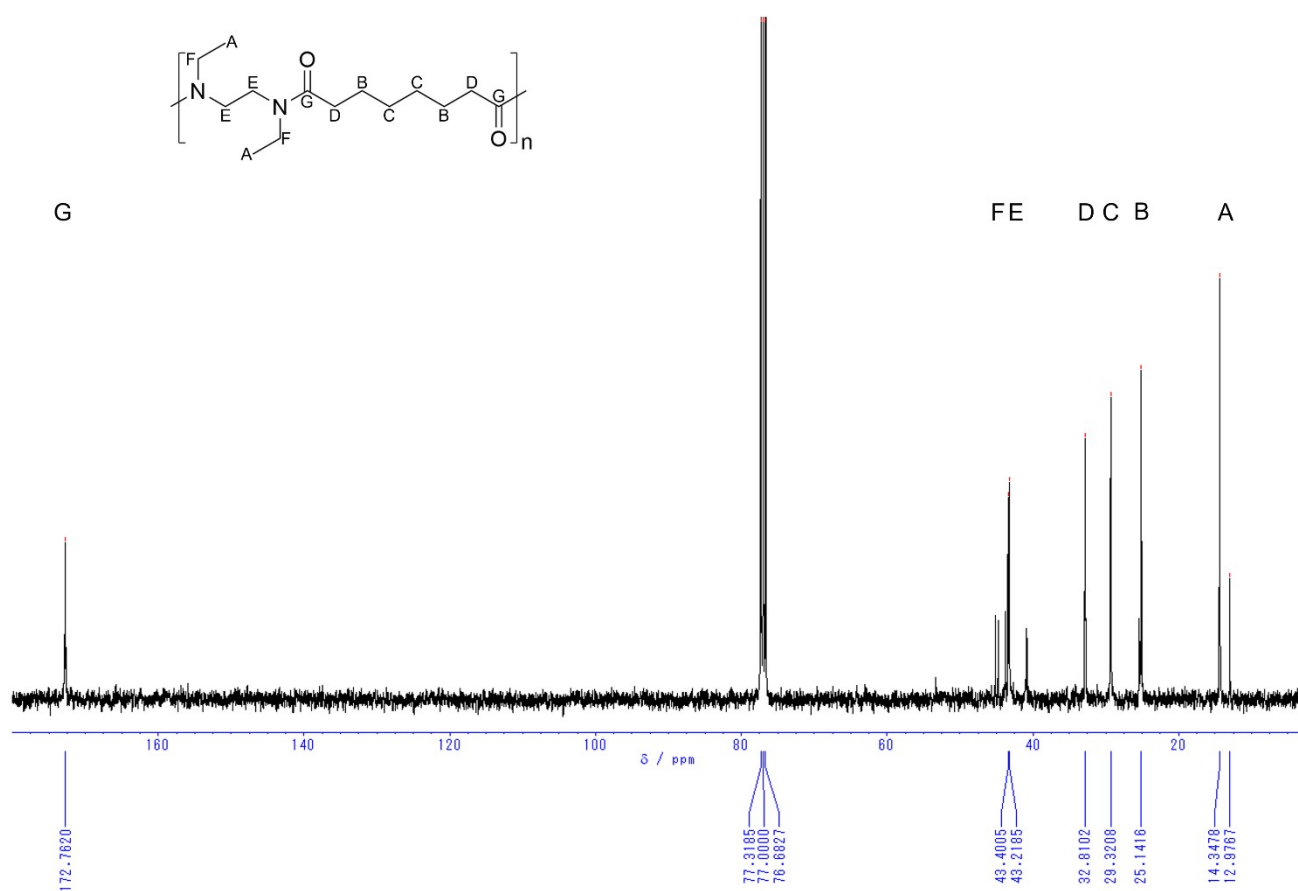


Figure S18. ¹³C NMR spectrum of *N*-Et-2,8

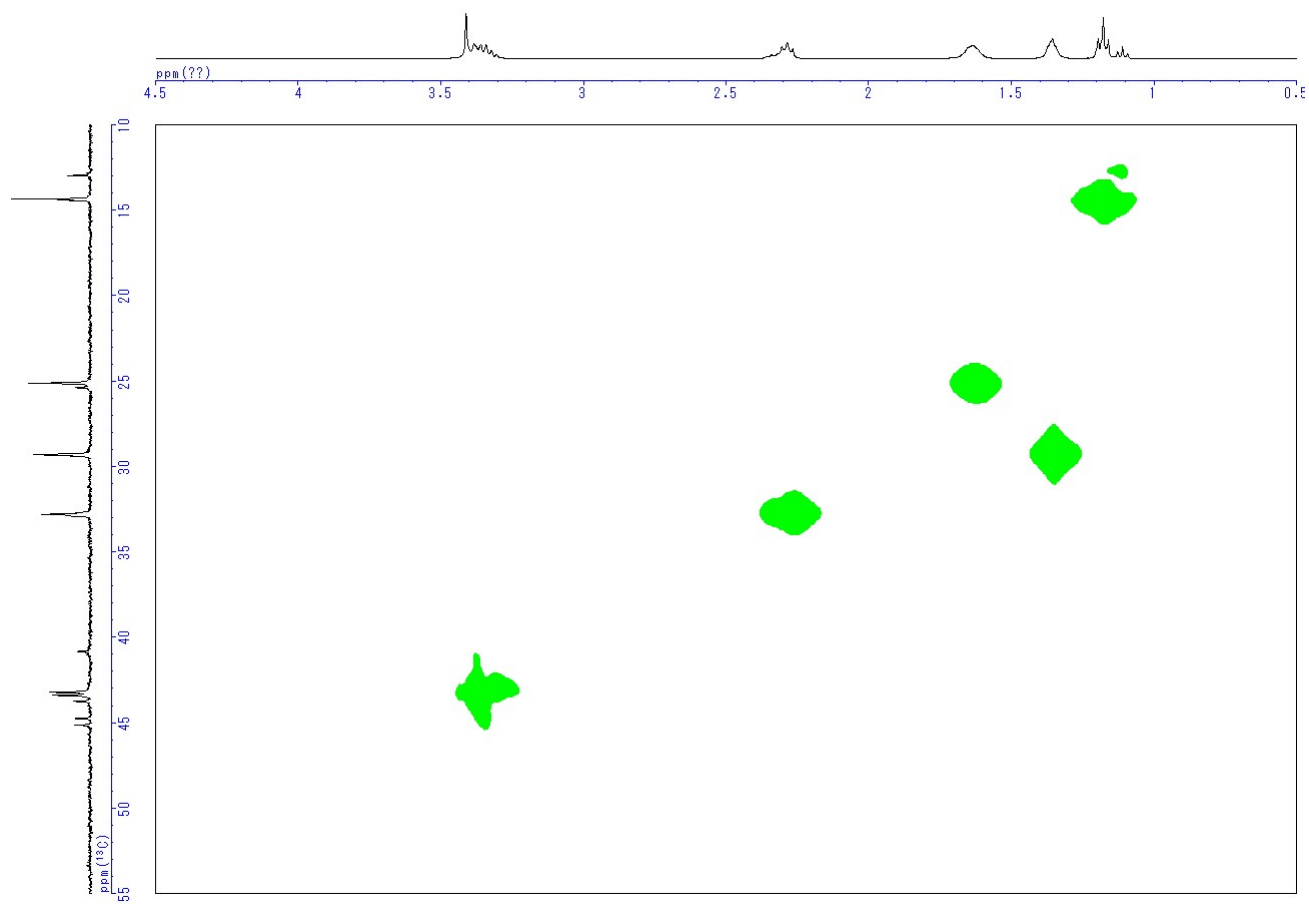


Figure S19. HMQC spectrum of *N*-Et-2,8

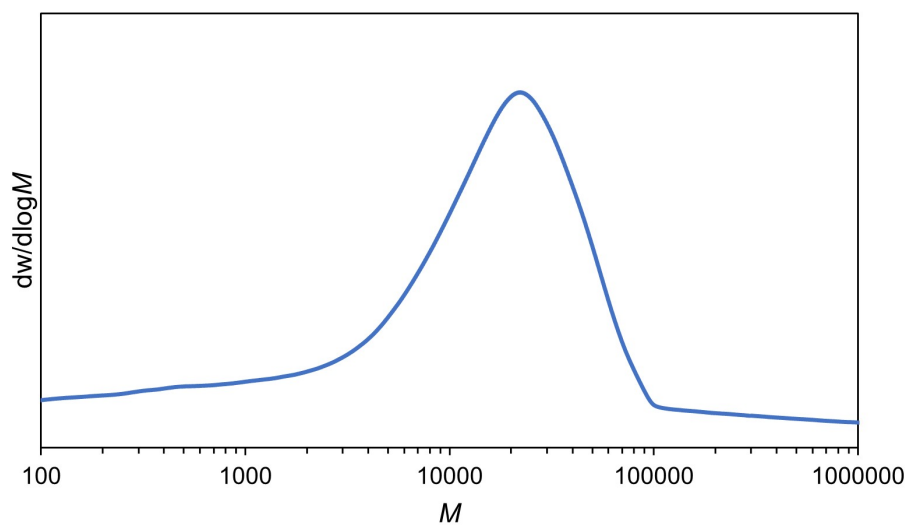


Figure S20. SEC chromatogram of *N*-Et-2,8

N,N'-diethylnylon-3,3 (*N*-Et-3,3)

Polymerization of *N,N'*-diethyl-1,3-propanediamine (318 μ L, 2.00 mmol) and Malonyl chloride (194 μ L, 2.00 mmol) afforded *N*-Et-3,3 (144 mg, 36% yield) as a yellow solid.

^1H NMR (CDCl_3 , 400 MHz) δ = 3.60-3.98 (m, 2 H), 2.88-3.60 (m, 8 H), 1.65-2.14 (m, 2 H), 0.95-1.50 (m, 6 H).

^{13}C NMR (CDCl_3 , 100 MHz) δ = 166.6, 45.8, 45.5, 43.1, 40.8, 40.6, 14.0, 13.8, 12.8, 11.3.

SEC (CHCl_3): M_n = 1.8×10^3 , D = 2.4.

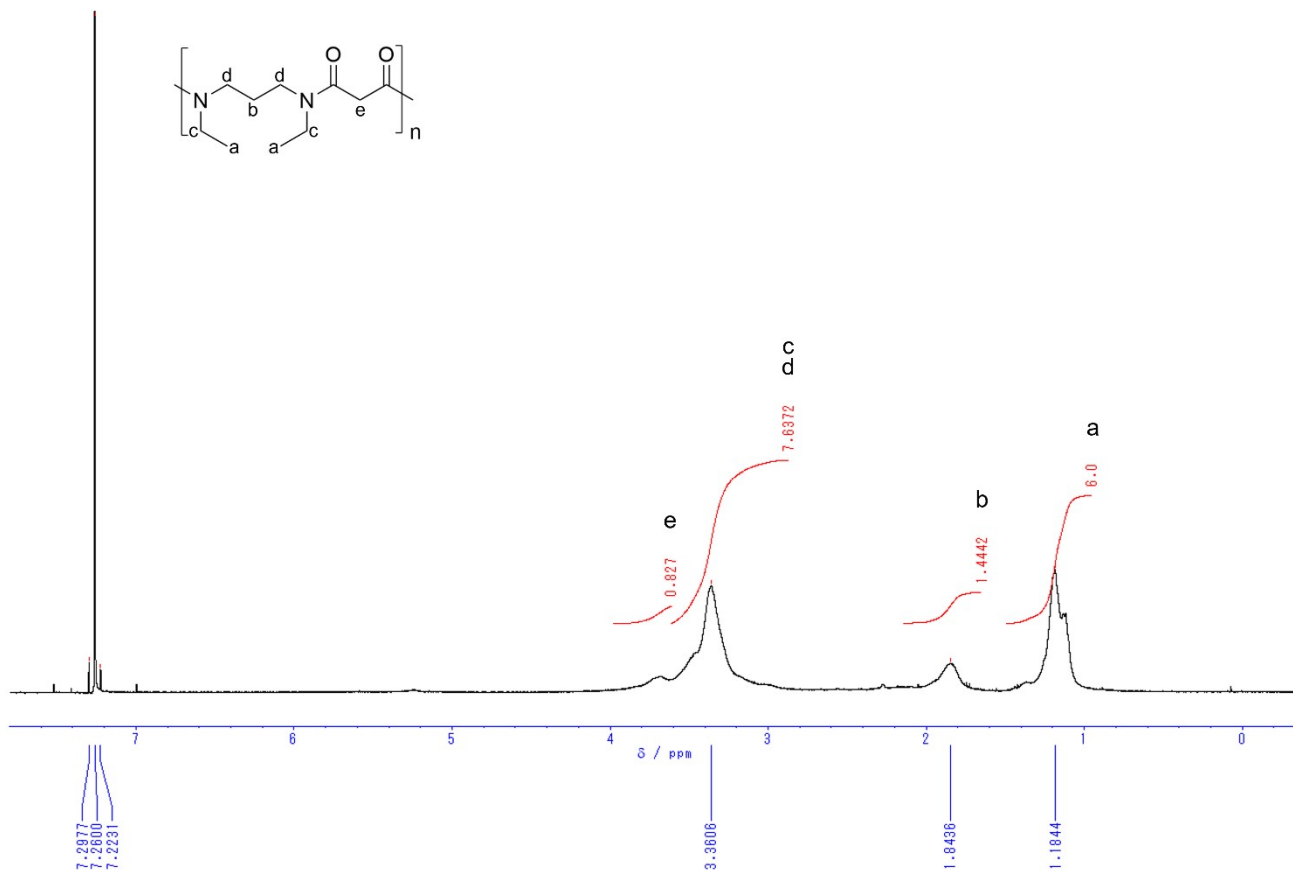


Figure S21. ^1H NMR spectrum of *N*-Et-3,3

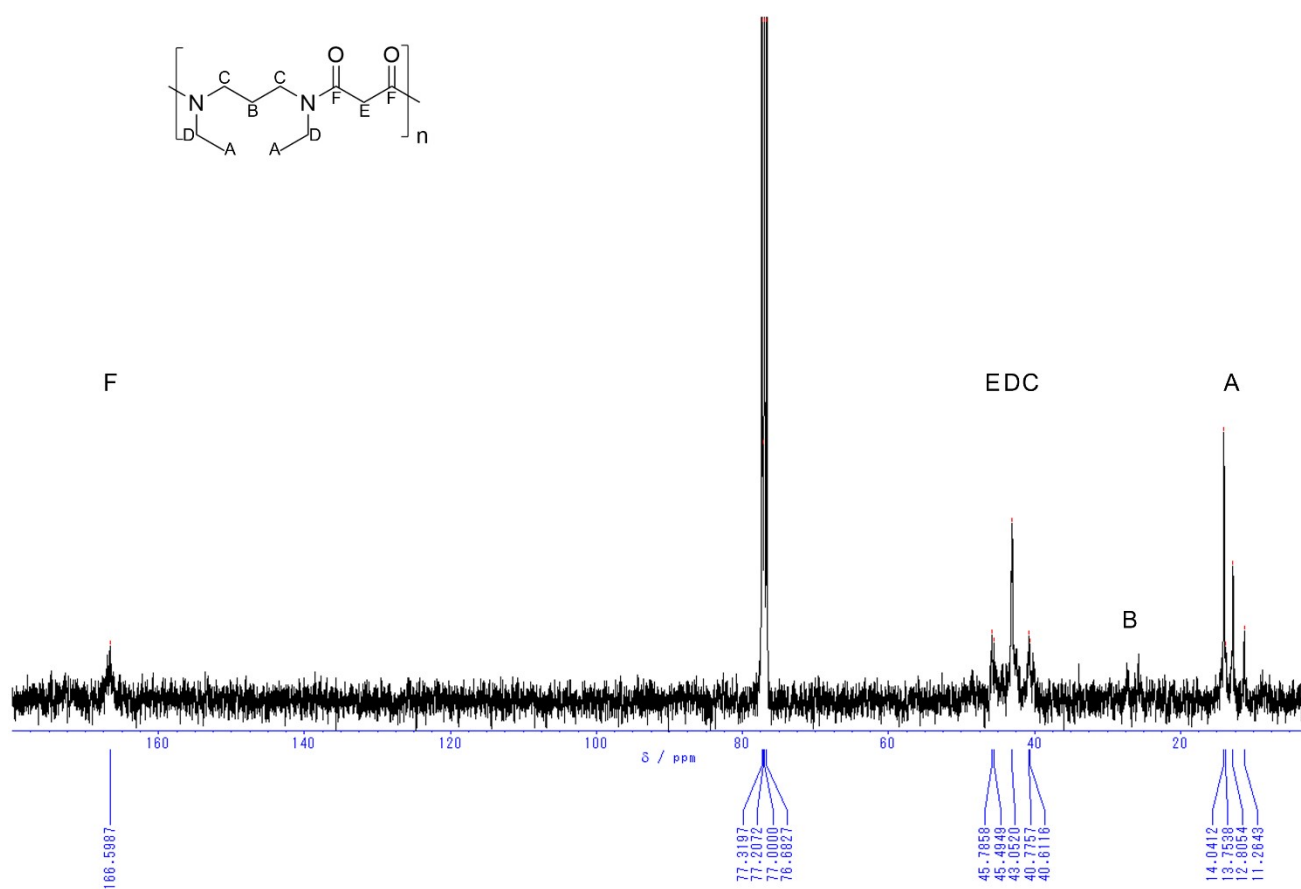


Figure S22. ¹³C NMR spectrum of *N*-Et-3,3

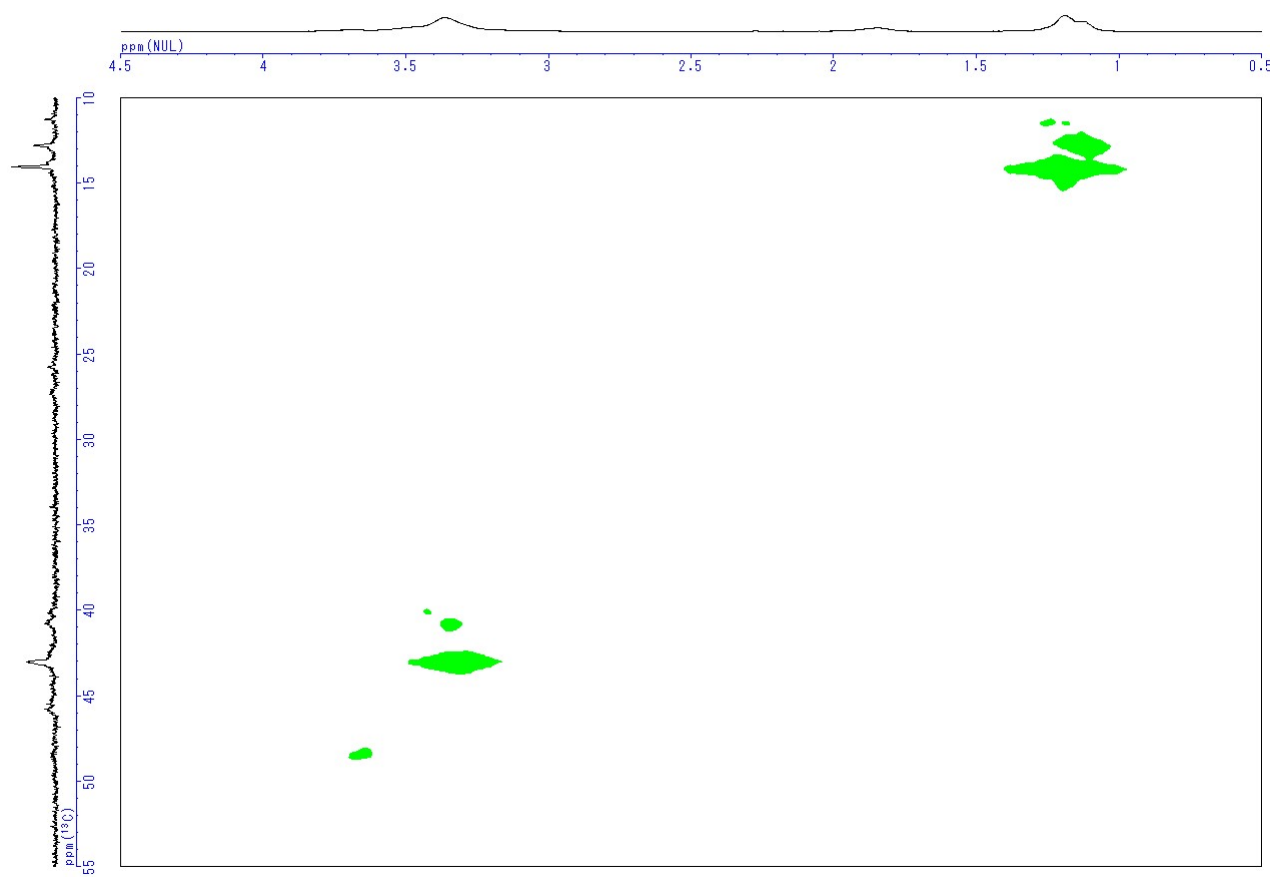


Figure S23. HMQC spectrum of *N*-Et-3,3

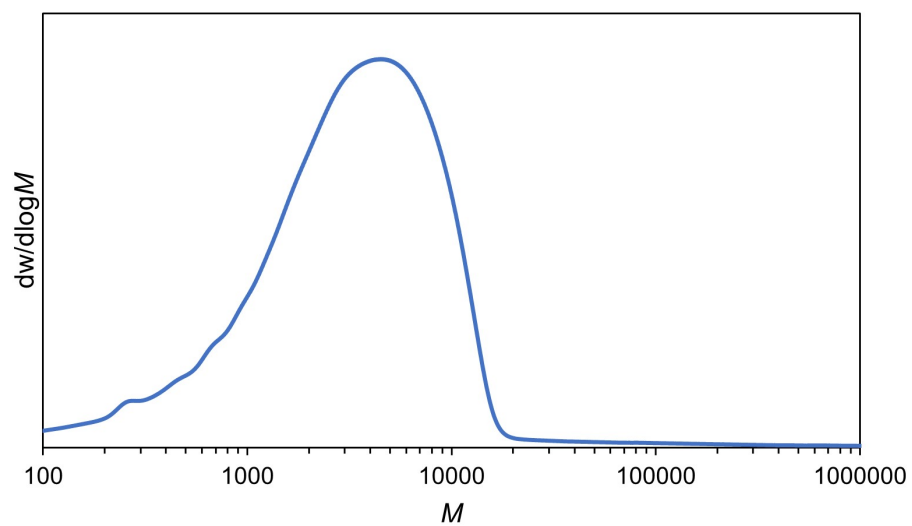


Figure S24. SEC chromatogram of *N*-Et-3,3

N,N'-diethylnylon-3,4 (*N*-Et-3,4)

Polymerization of *N,N'*-diethyl-1,3-propanediamine (318 μ L, 2.00 mmol) and Succinyl chloride (226 μ L, 2.00 mmol) afforded *N*-Et-3,4 (75.5 mg, 18% yield) as a brown solid.

^1H NMR (CDCl_3 , 400 MHz) δ = 3.01-3.76 (m, 8 H), 2.49-3.00 (m, 4 H), 1.61-2.23 (m, 2 H), 0.96-1.38 (m, 6 H).

^{13}C NMR (CDCl_3 , 100 MHz) δ = 171.2, 47.1, 45.2, 42.3, 40.7, 28.2, 28.1, 26.4, 25.3, 14.1, 14.0, 12.9.

SEC (CHCl_3): M_n = 1.9×10^3 , \bar{D} = 2.1.

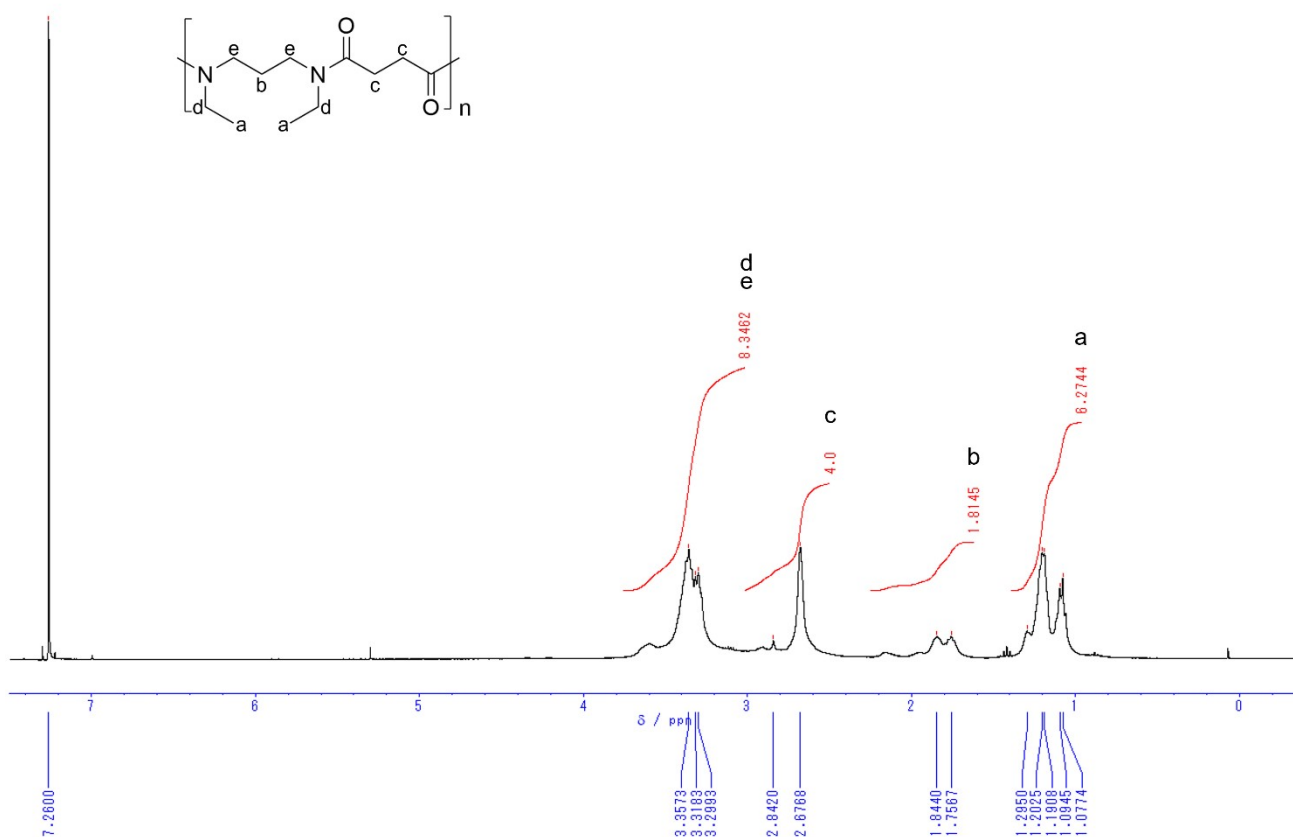


Figure S25. ^1H NMR spectrum of *N*-Et-3,4

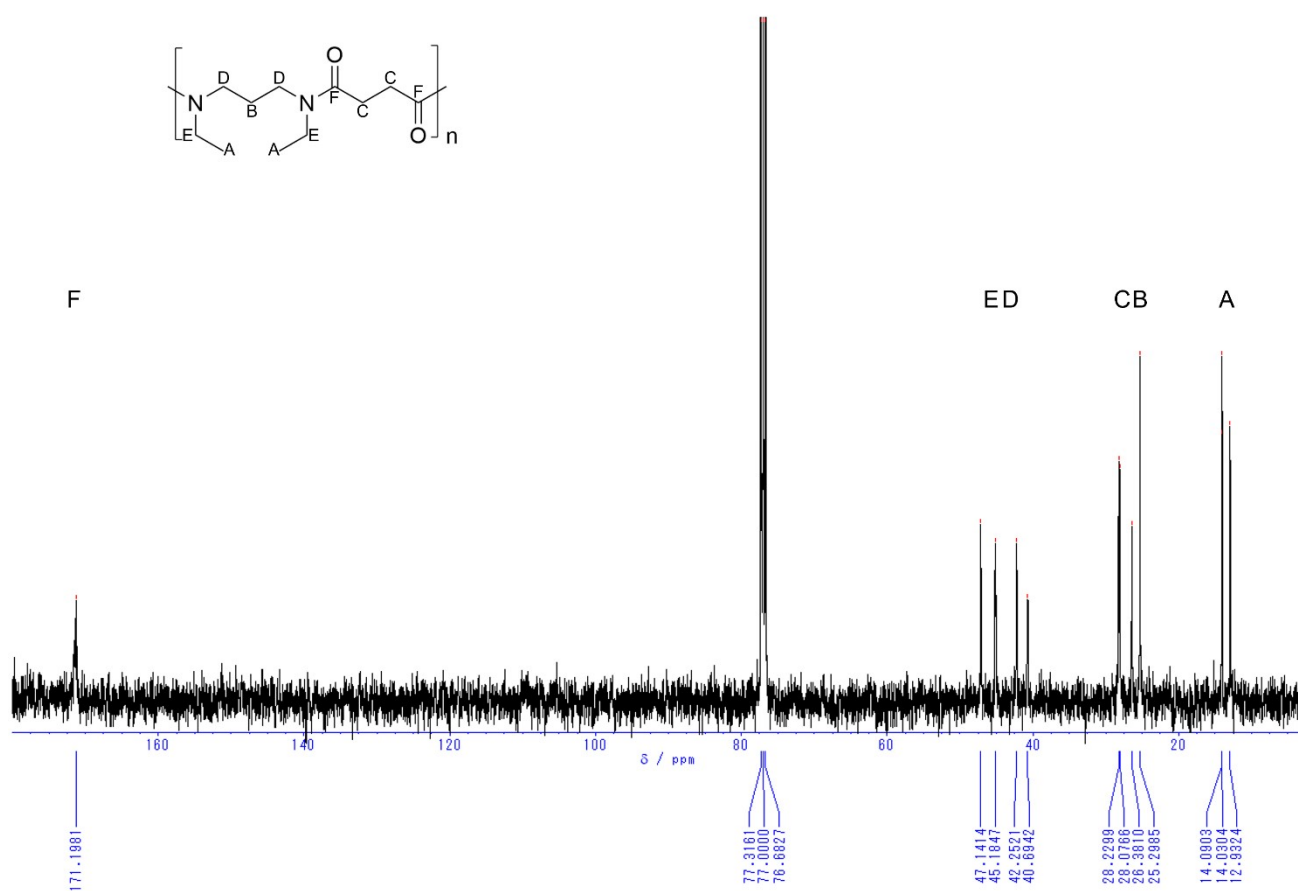


Figure S26. ¹³C NMR spectrum of *N*-Et-3,4

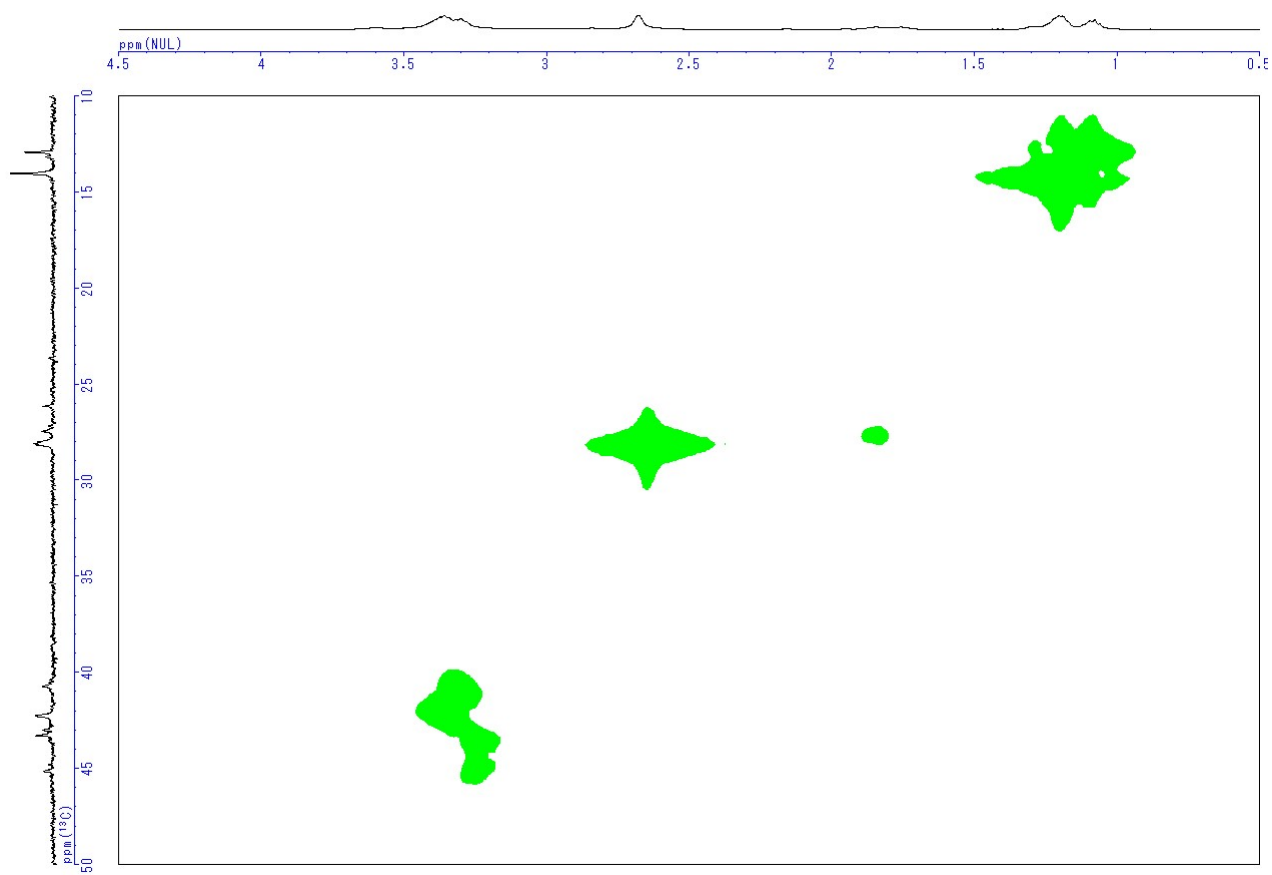


Figure S27. HMQC spectrum of *N*-Et-3,4

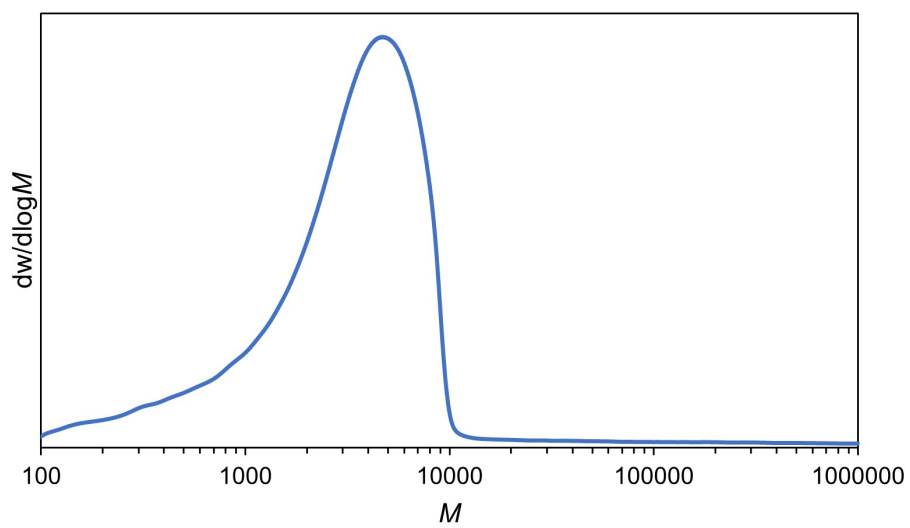


Figure S28. SEC chromatogram of *N*-Et-3,4

N,N'-diethylnylon-3,5 (*N*-Et-3,5)

Polymerization of *N,N'*-diethyl-1,3-propanediamine (318 μ L, 2.00 mmol) and Glutaryl chloride (258 μ L, 2.00 mmol) afforded *N*-Et-3,5 (165 mg, 37% yield) as a yellow solid.

^1H NMR (CDCl_3 , 400 MHz) δ = 3.16-3.45 (m, 8 H), 2.30-2.54 (m, 4 H), 1.88-2.03 (m, 2 H), 1.69-1.88 (m, 2 H), 1.03-1.23 (m, 6 H).

^{13}C NMR (CDCl_3 , 100 MHz) δ = 171.7, 44.9, 42.7, 42.1, 41.9, 40.1, 31.9, 27.3, 25.8, 20.7, 20.6, 13.9, 12.7.

SEC (CHCl_3): M_n = 7.6×10^3 , \mathcal{D} = 1.5.

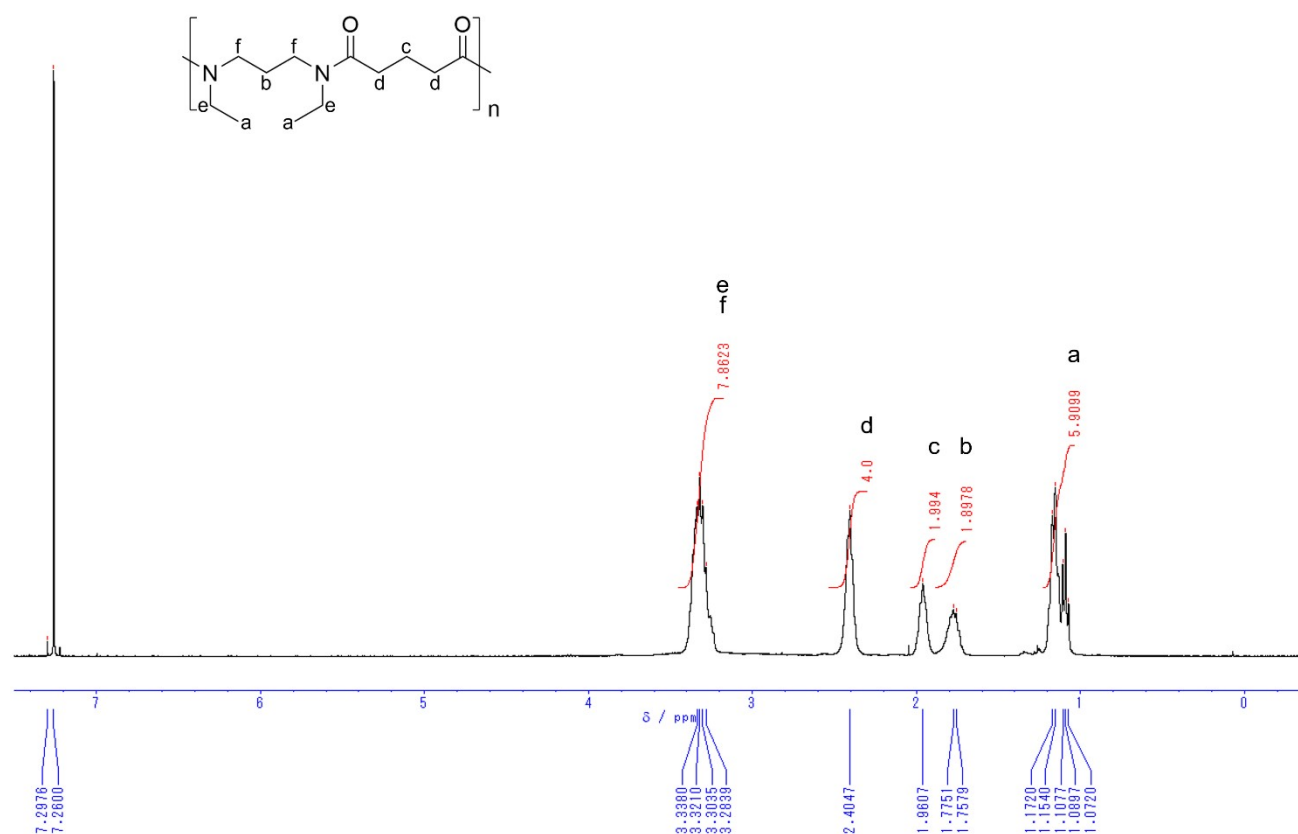


Figure S29. ^1H NMR spectrum of *N*-Et-3,5

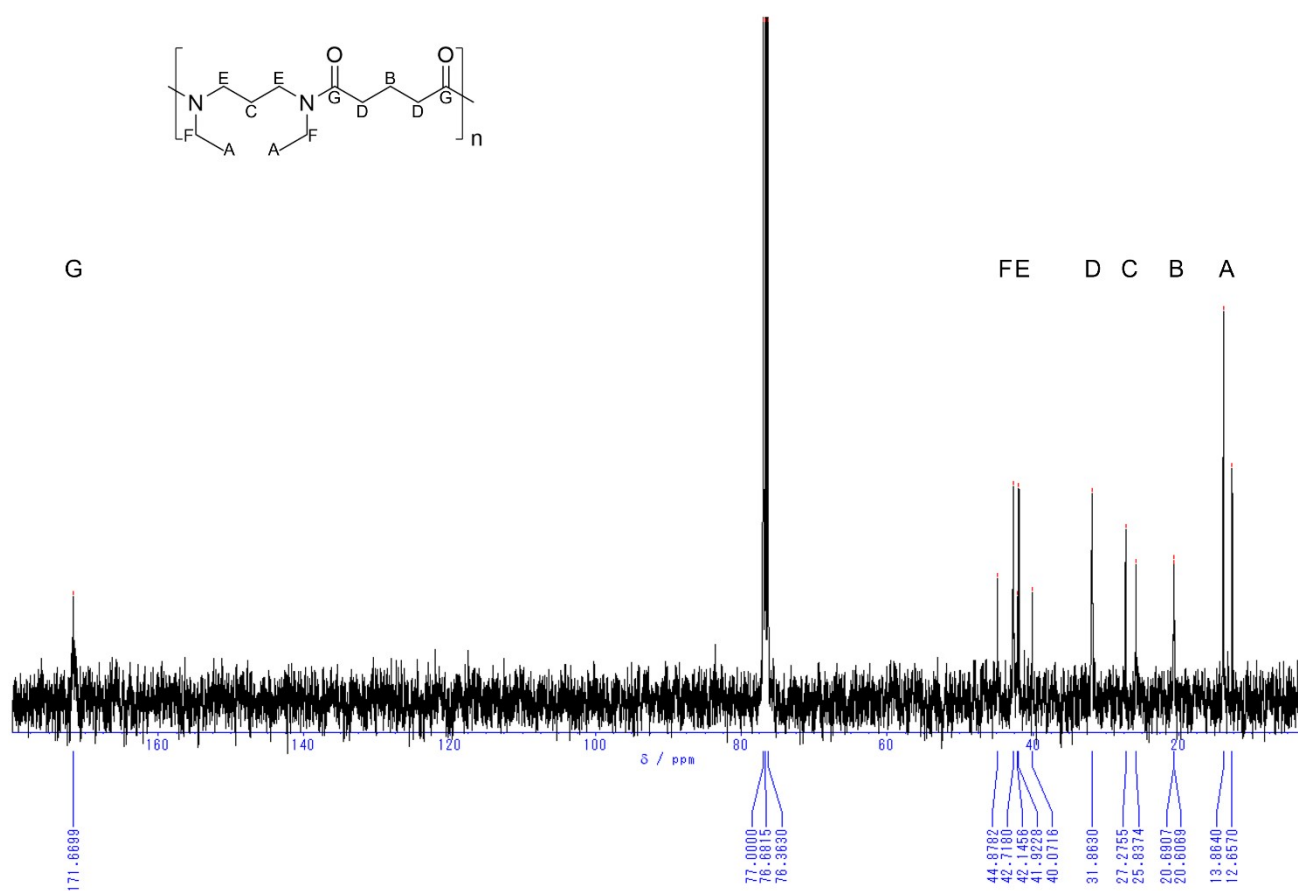


Figure S30. ¹³C NMR spectrum of *N*-Et-3,5

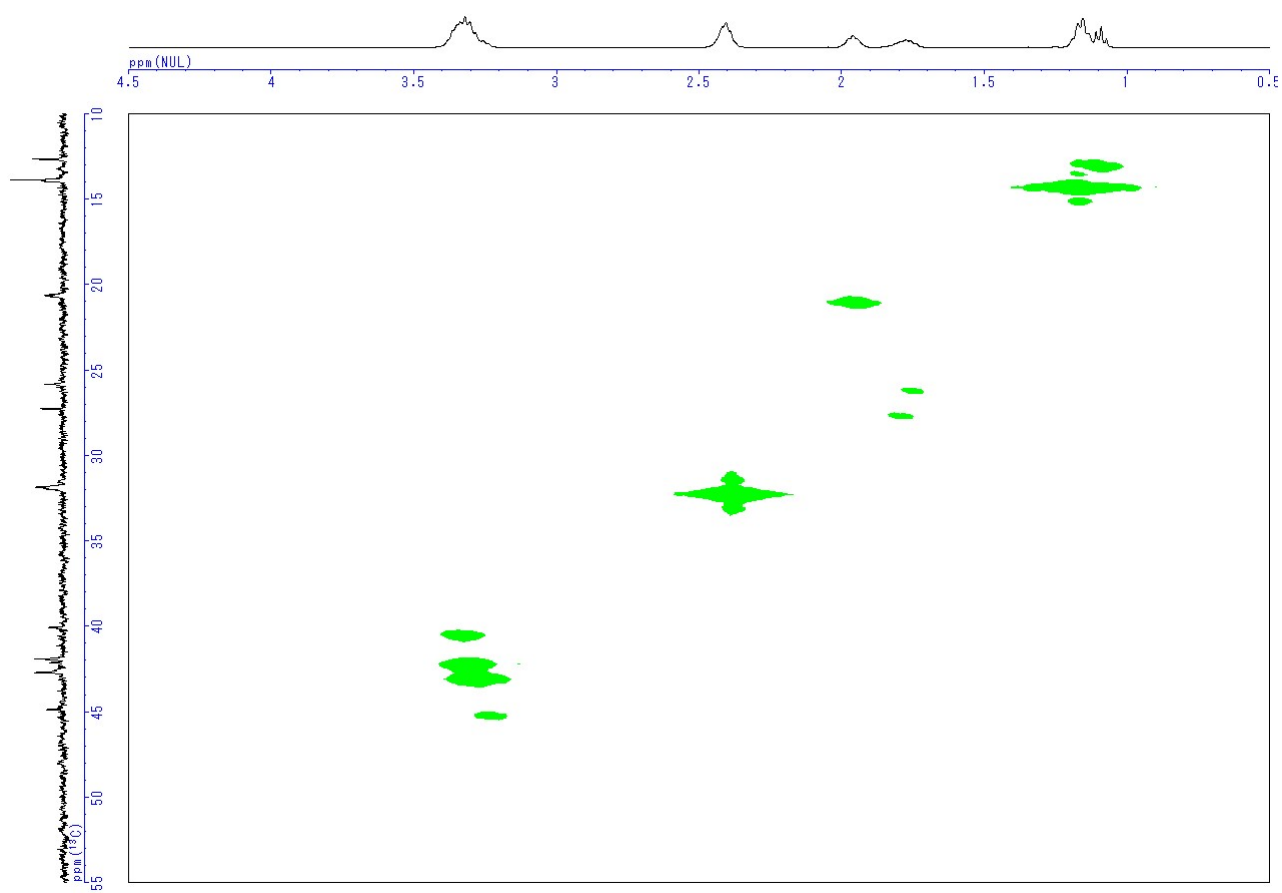


Figure S31. HMQC spectrum of *N*-Et-3,5

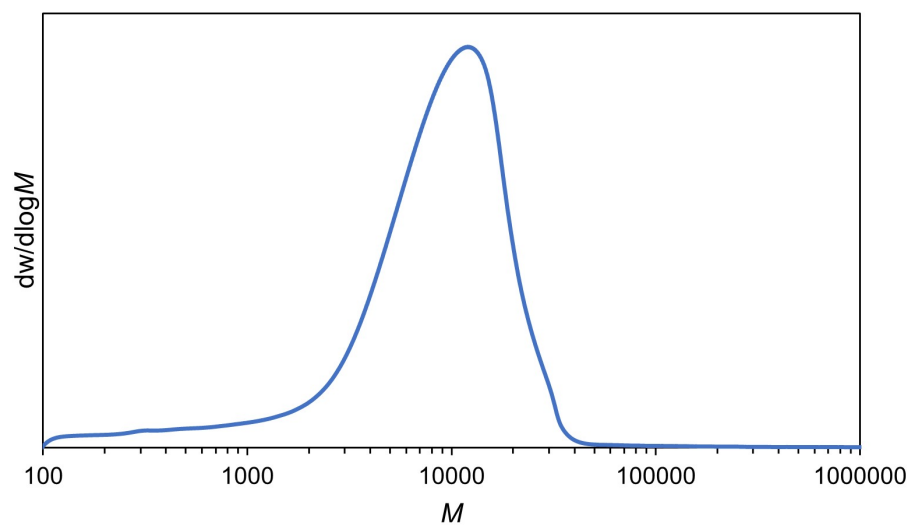


Figure S32. SEC chromatogram of *N*-Et-3,5

N,N'-diethylnylon-3,6 (*N*-Et-3,6)

Polymerization of *N,N'*-diethyl-1,3-propanediamine (318 μ L, 2.00 mmol) and Adipoyl chloride (291 μ L, 2.00 mmol) afforded *N*-Et-3,6 (113 mg, 24% yield) as a yellow solid.

^1H NMR (CDCl_3 , 400 MHz) δ = 3.13-3.56 (m, 8 H), 2.14-2.41 (m, 4 H), 1.73-1.92 (m, 2 H), 1.58-1.73 (m, 4 H), 1.03-1.26 (m, 6 H).

^{13}C NMR (CDCl_3 , 100 MHz) δ = 172.2, 45.3, 43.1, 42.5, 42.3, 40.5, 32.9, 27.7, 26.1, 25.2, 14.3, 14.2, 13.0.

SEC (CHCl_3): M_n = 4.0×10^3 , \mathcal{D} = 1.6.

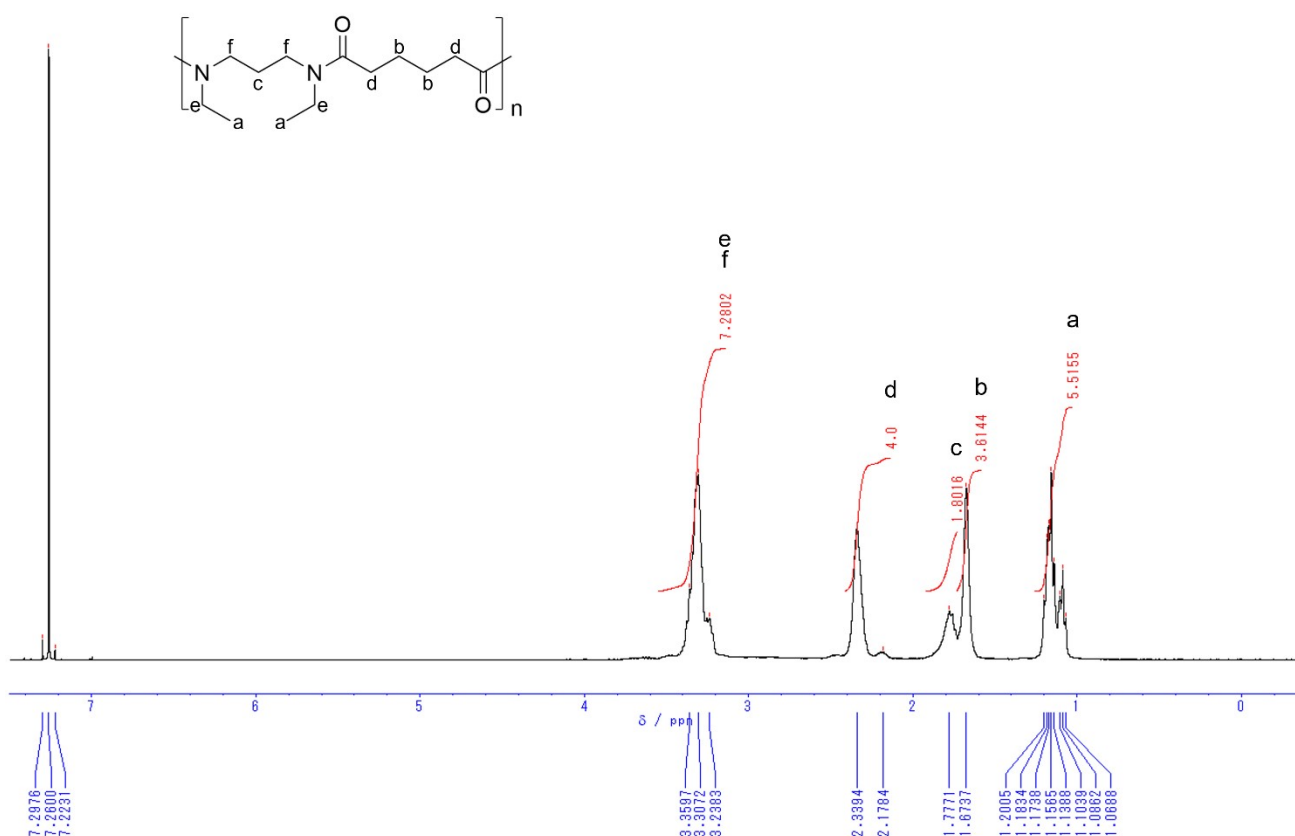


Figure S33. ^1H NMR spectrum of *N*-Et-3,6

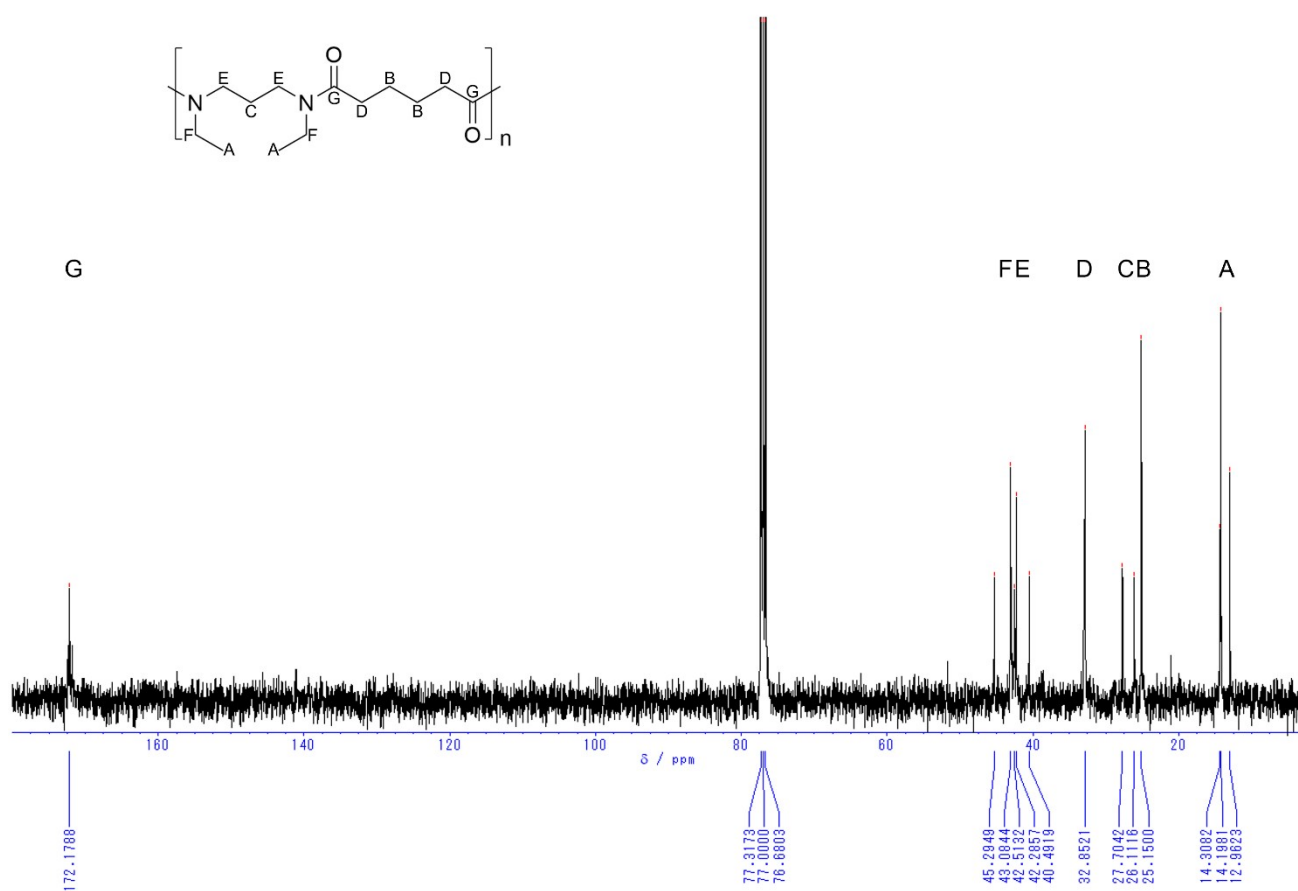


Figure S34. ¹³C NMR spectrum of *N*-Et-3,6

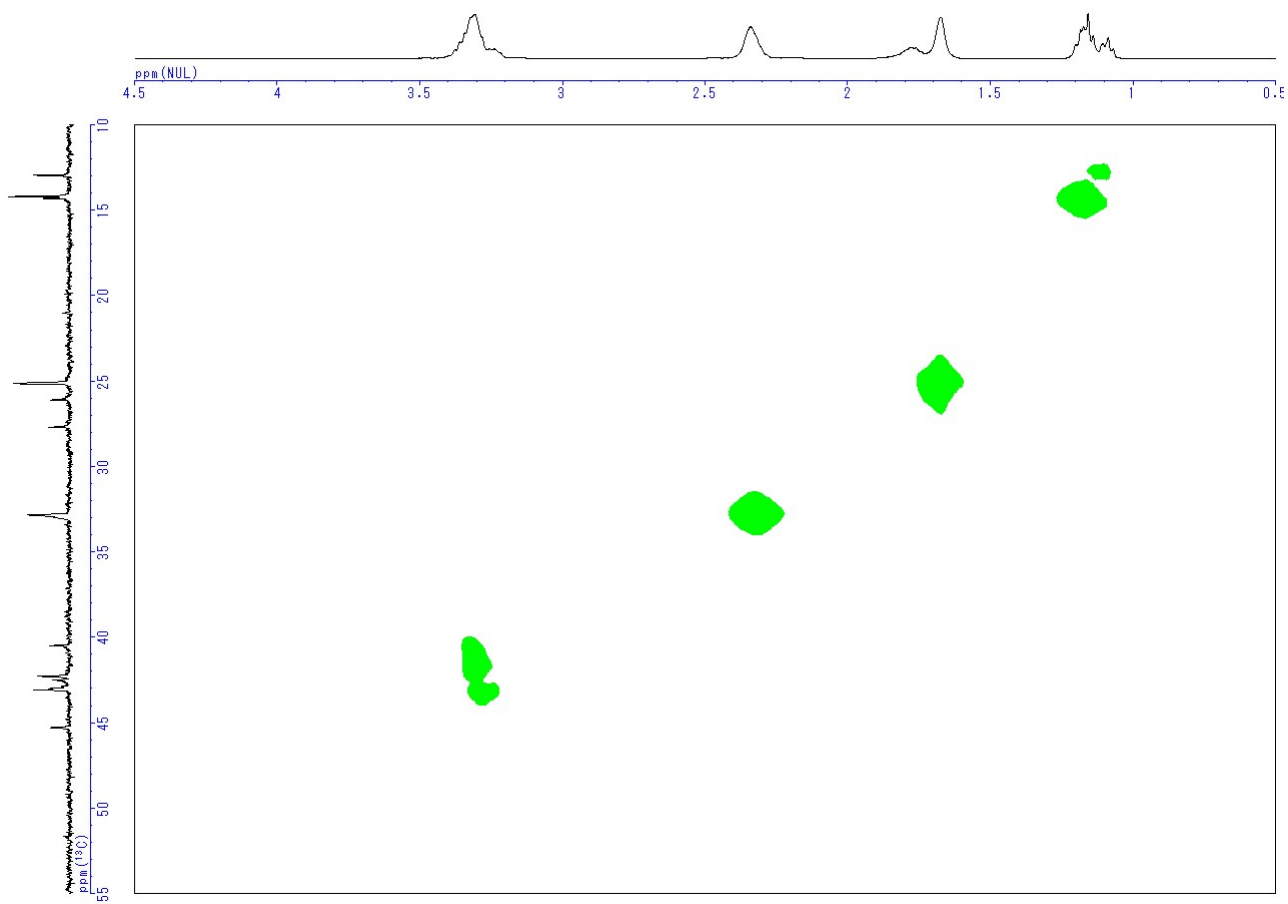


Figure S35. HMQC spectrum of *N*-Et-3,6

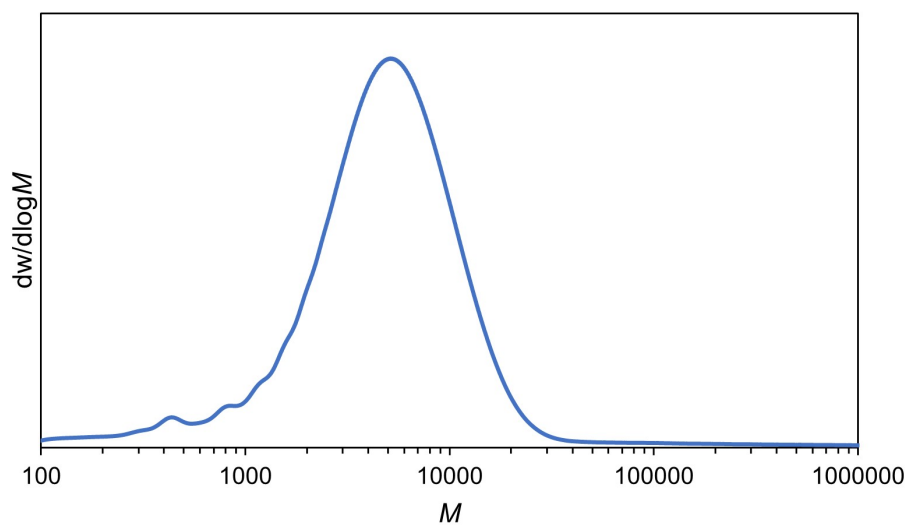


Figure S36. SEC chromatogram of *N*-Et-3,6

N,N'-diethylnylon-3,7 (*N*-Et-3,7)

Polymerization of *N,N'*-diethyl-1,3-propanediamine (318 μ L, 2.00 mmol) and Pimeloyl chloride (326 μ L, 2.00 mmol) afforded *N*-Et-3,7 (139 mg, 27% yield) as a yellow solid.

^1H NMR (CDCl_3 , 400 MHz) δ = 3.16-3.45 (m, 8 H), 2.23-2.42 (m, 4 H), 1.73-1.91 (m, 2 H), 1.58-1.73 (m, 4 H), 1.33-1.48 (m, 2 H), 1.01-1.24 (m, 6 H).

^{13}C NMR (CDCl_3 , 100 MHz) δ = 172.6, 43.1, 42.4, 33.0, 29.4, 25.3, 14.5, 14.3, 13.1.

SEC (CHCl_3): $M_n = 7.2 \times 10^3$, $D = 1.6$.

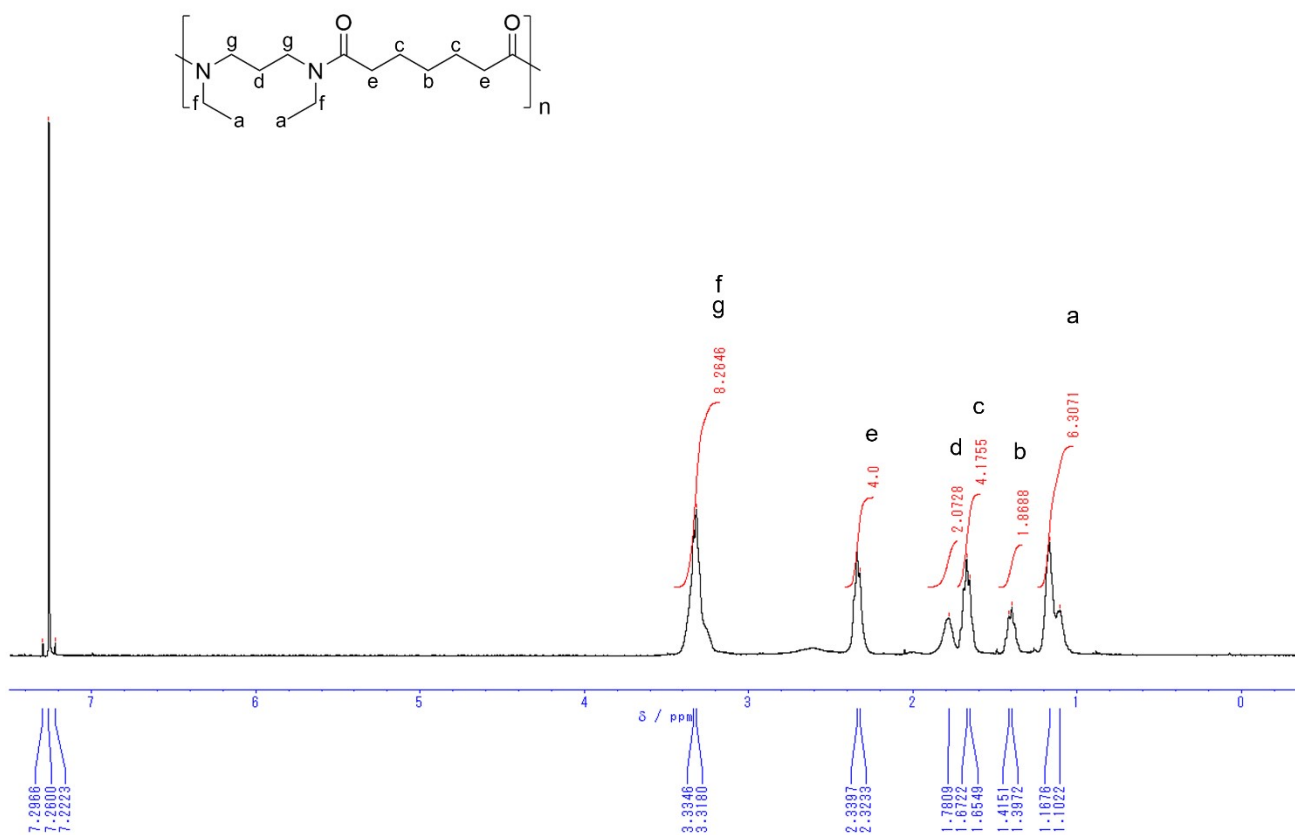


Figure S37. ^1H NMR spectrum of *N*-Et-3,7

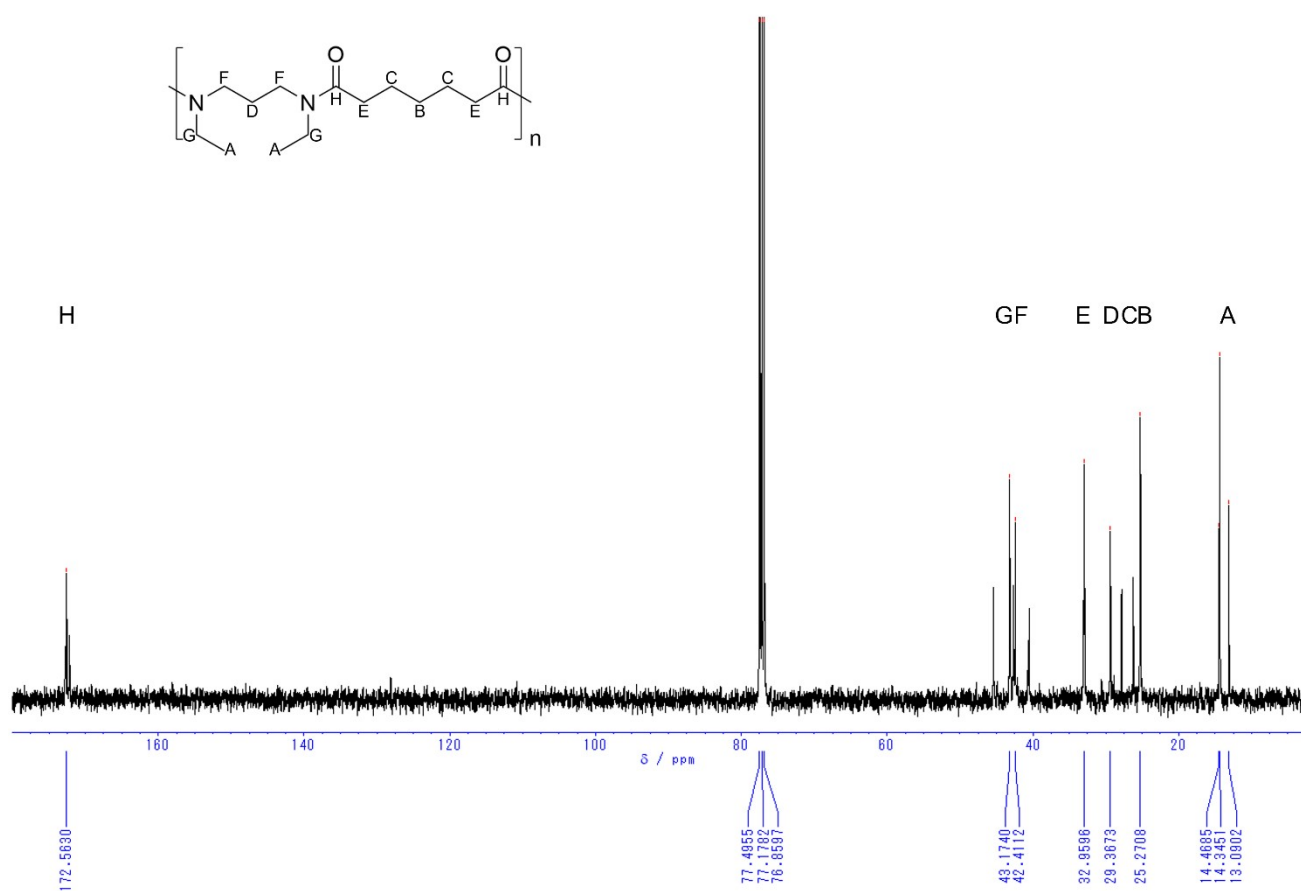


Figure S38. ¹³C NMR spectrum of *N*-Et-3,7

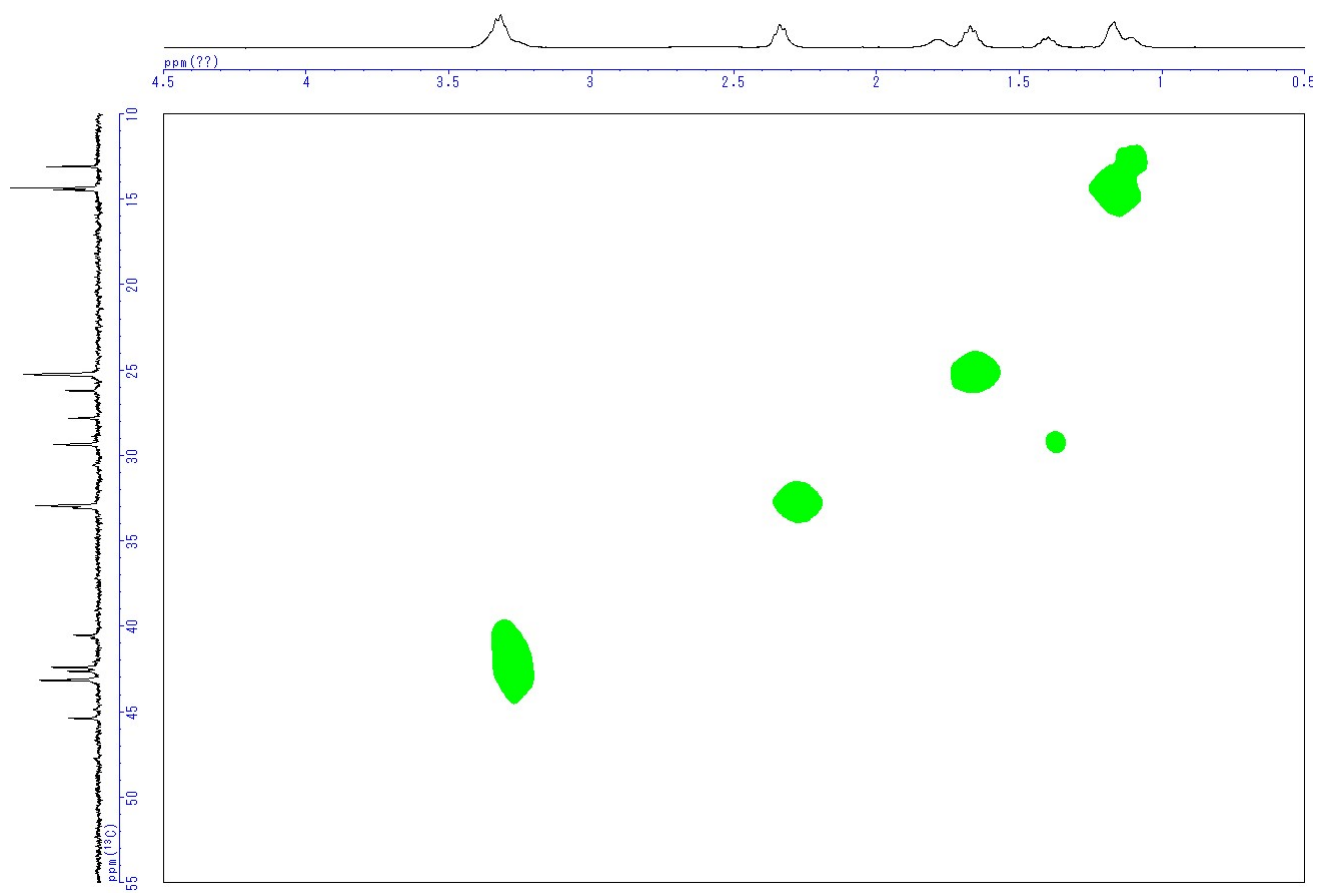


Figure S39. HMQC spectrum of *N*-Et-3,7

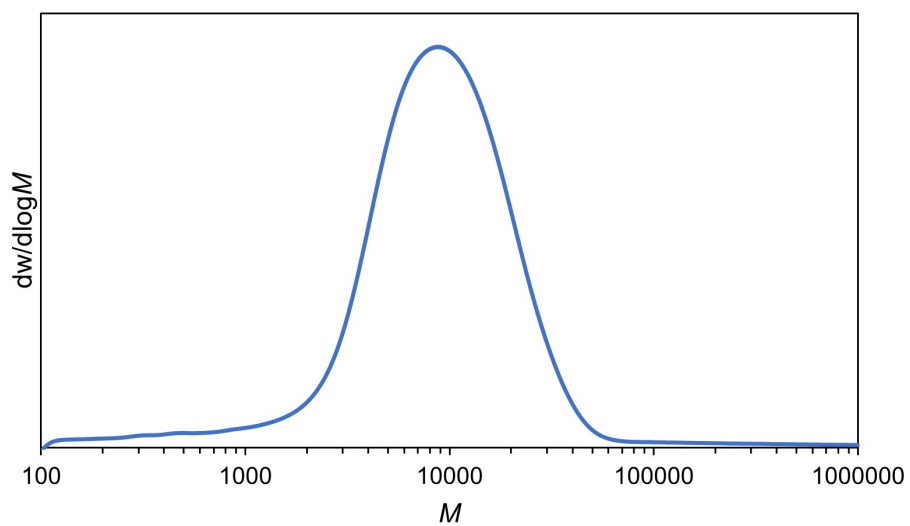


Figure S40. SEC chromatogram of *N*-Et-3,7

N,N'-diethylnylon-4,3 (*N*-Et-4,3)

Polymerization of *N,N'*-diethyl-1,4-butanediamine (356 μ L, 2.00 mmol) and Malonyl chloride (194 μ L, 2.00 mmol) afforded *N*-Et-4,3 (64.9 mg, 15% yield) as a yellow solid.

^1H NMR (CDCl_3 , 400 MHz) δ = 3.56-3.91 (m, 2 H), 2.82-3.56 (m, 8 H), 1.37-2.14 (m, 4 H), 0.96-1.37 (m, 6 H).

^{13}C NMR (CDCl_3 , 100 MHz) δ = 165.6, 47.8, 44.9, 42.9, 40.7, 25.0, 14.1, 12.8, 11.3.

SEC (CHCl_3): M_n = 3.3×10^3 , D = 2.3.

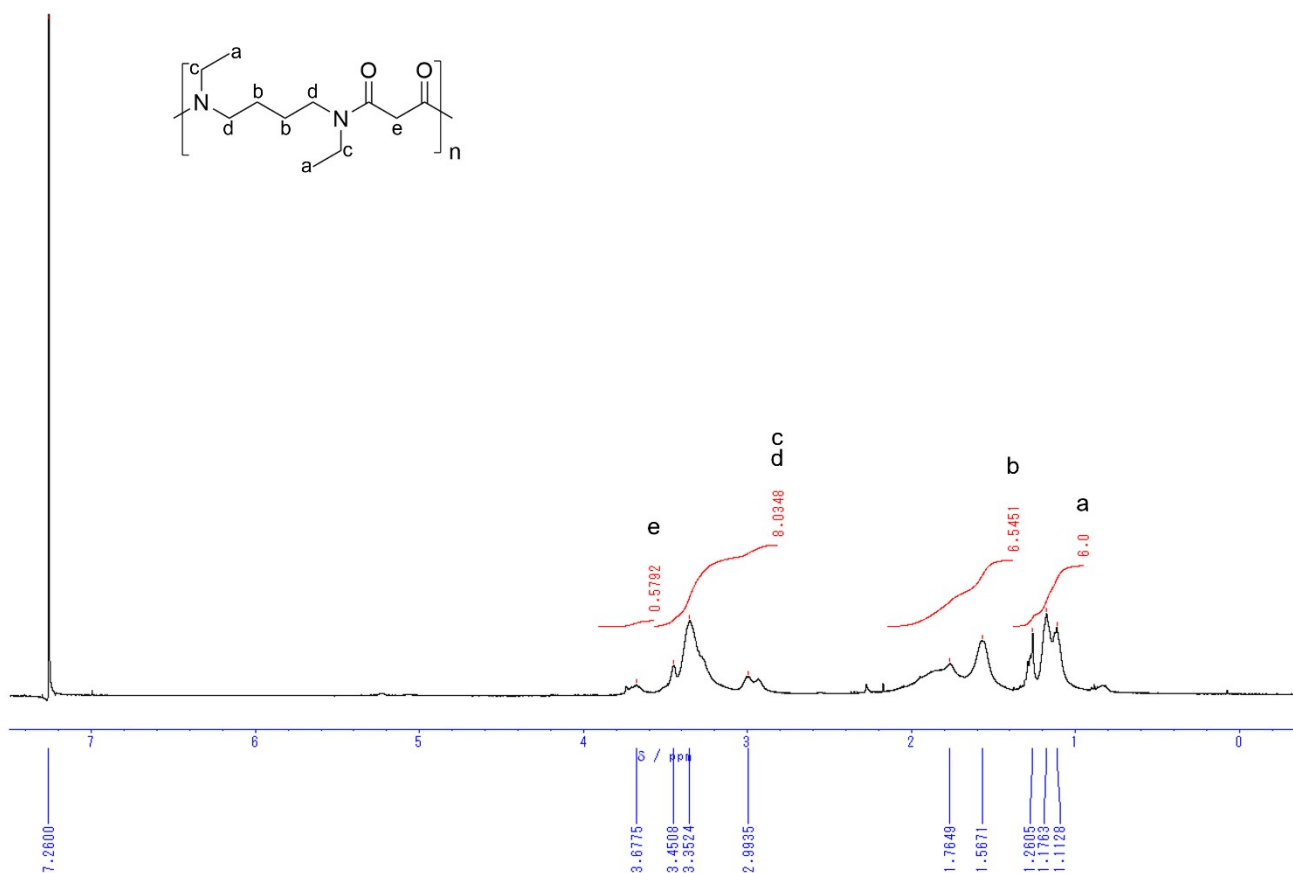


Figure S41. ^1H NMR spectrum of *N*-Et-4,3

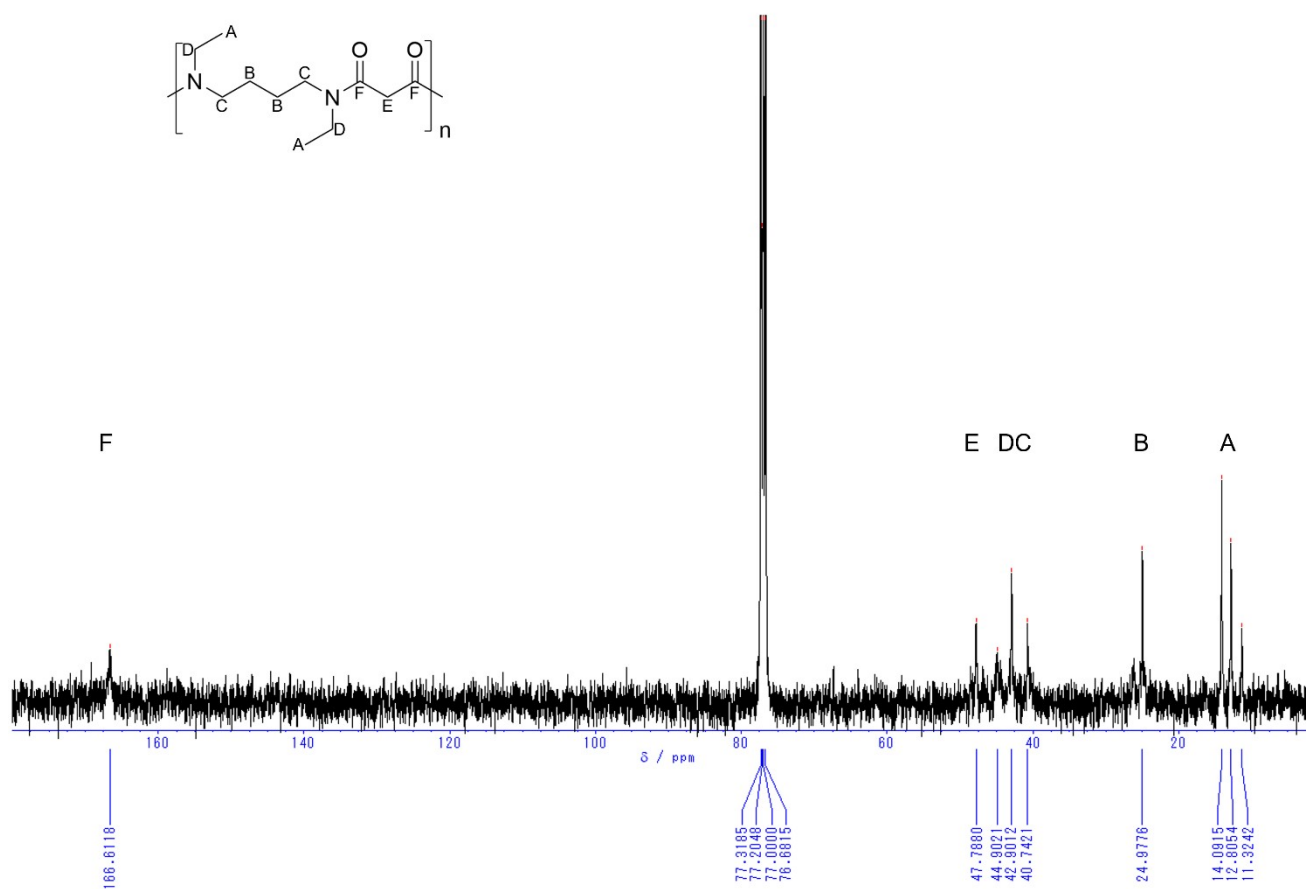


Figure S42. ¹³C NMR spectrum of *N*-Et-4,3

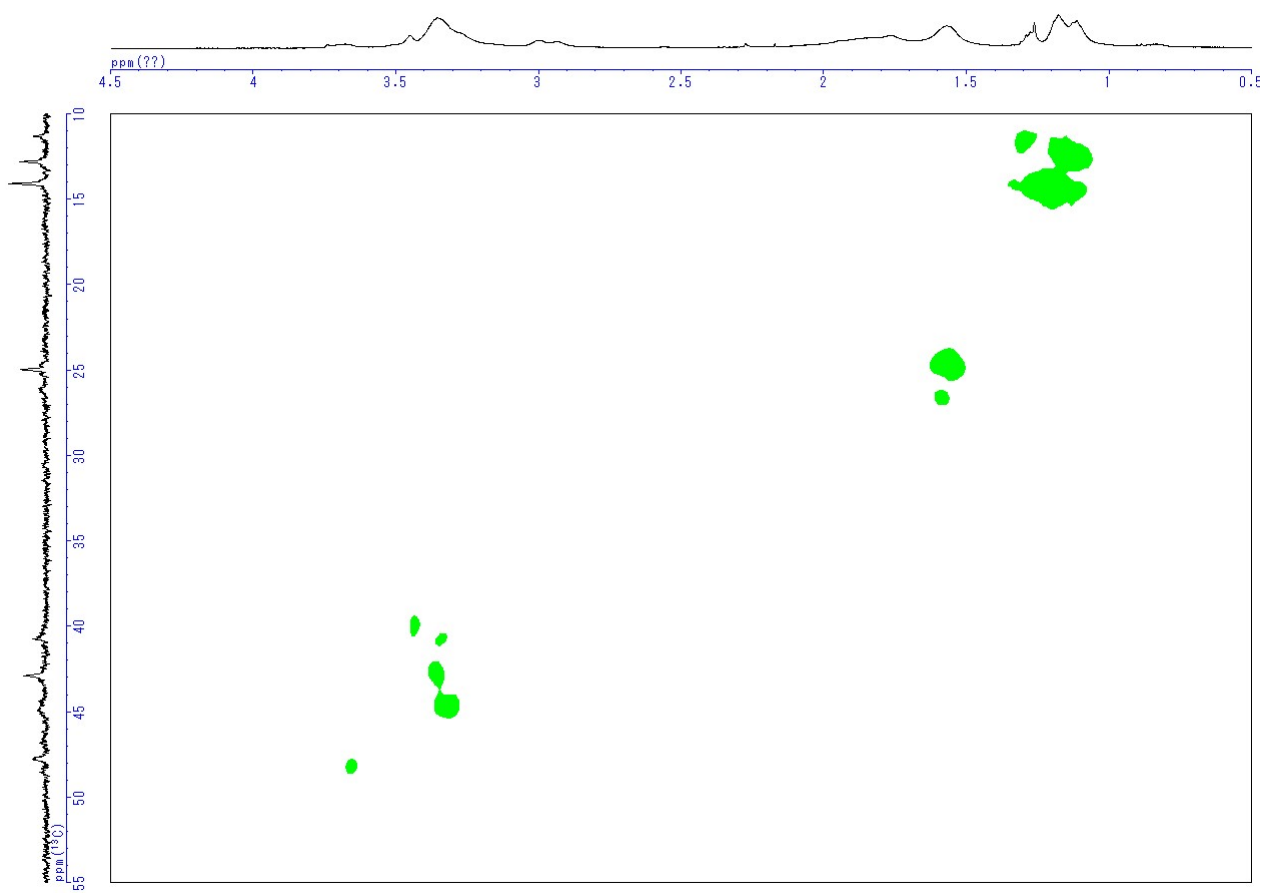


Figure S43. HMQC spectrum of *N*-Et-4,3

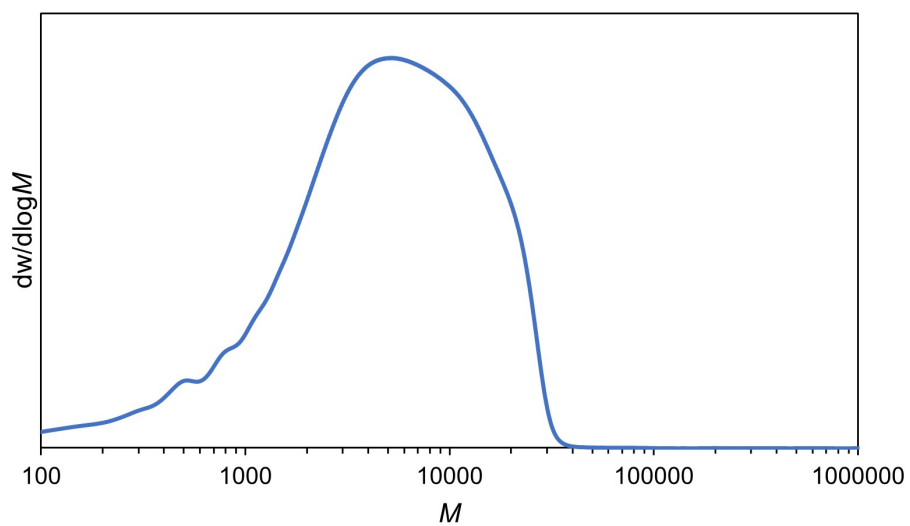


Figure S44. SEC chromatogram of *N*-Et-4,3

N,N'-diethylnylon-4,4 (*N*-Et-4,4)

Polymerization of *N,N'*-diethyl-1,4-butanediamine (356 μ L, 2.00 mmol) and Succinyl chloride (226 μ L, 2.00 mmol) afforded *N*-Et-4,4 (224 mg, 50% yield) as a brown solid.

^1H NMR (CDCl_3 , 400 MHz) δ = 3.10-3.44 (m, 8 H), 2.37-2.72 (m, 4 H), 1.33-1.66 (m, 4 H), 0.96-1.33 (m, 6 H).

^{13}C NMR (CDCl_3 , 100 MHz) δ = 171.2, 47.1, 45.2, 42.3, 40.7, 28.2, 28.1, 26.4, 25.3, 14.1, 14.0, 12.9.

SEC (CHCl_3): M_n = 8.0×10^3 , \mathcal{D} = 2.0.

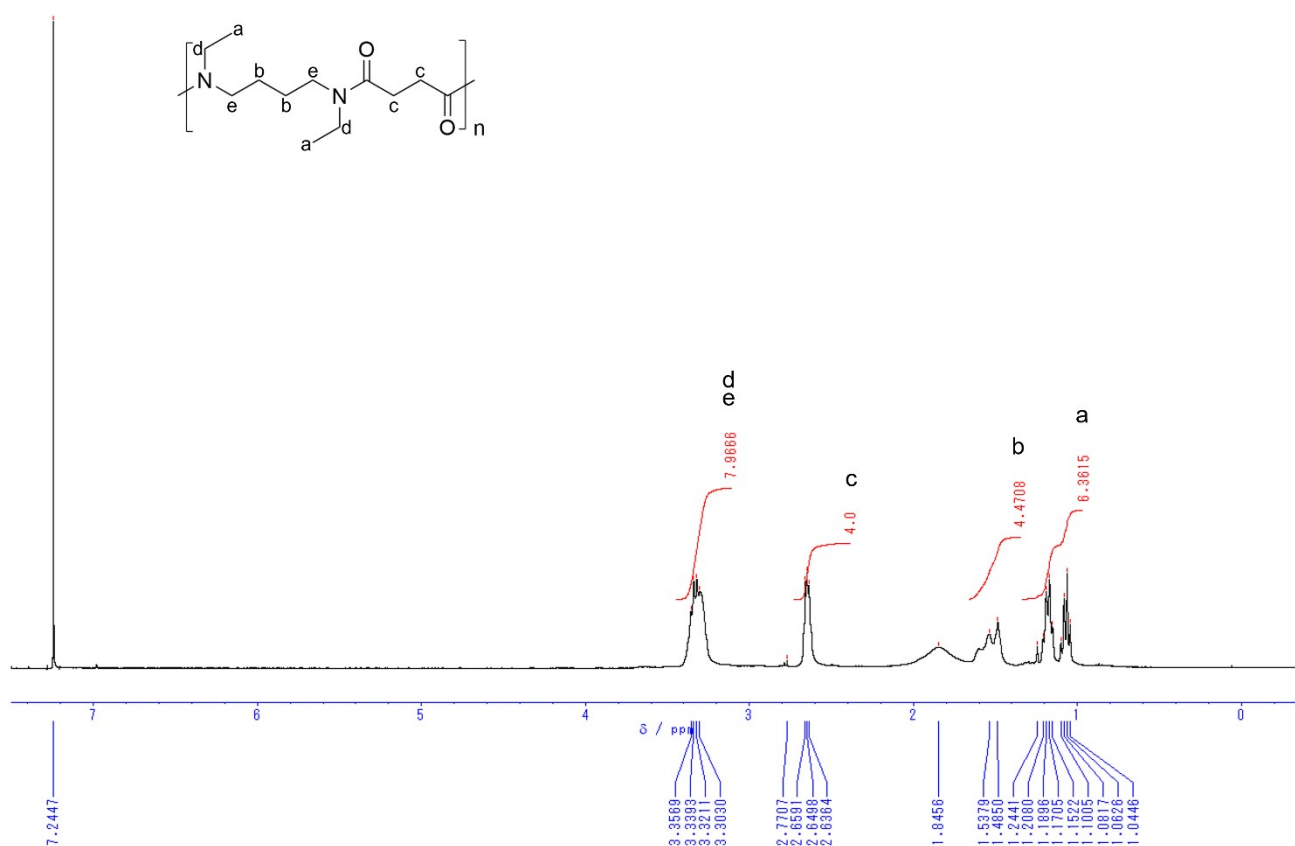


Figure S45. ^1H NMR spectrum of *N*-Et-4,4

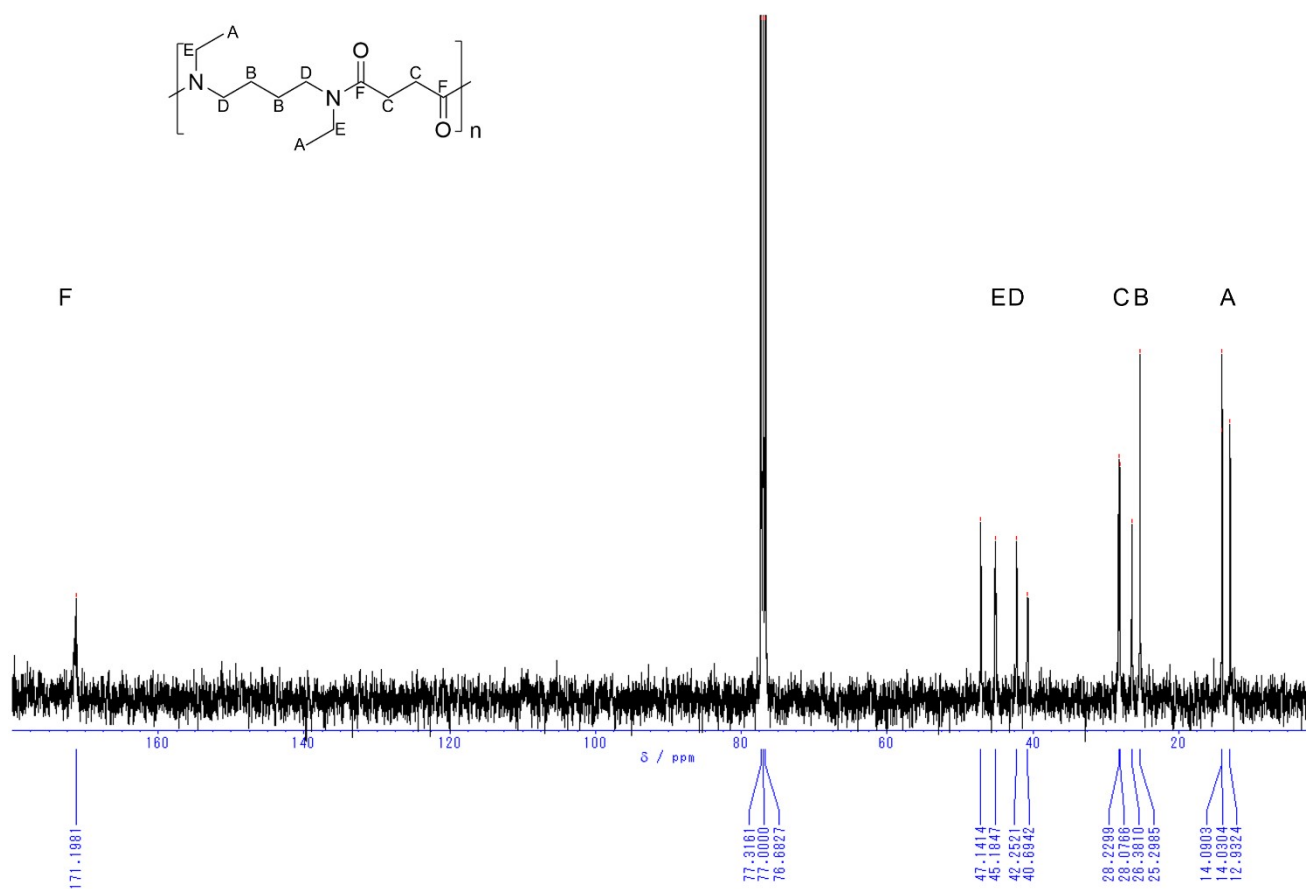


Figure S46. ¹³C NMR spectrum of *N*-Et-4,4

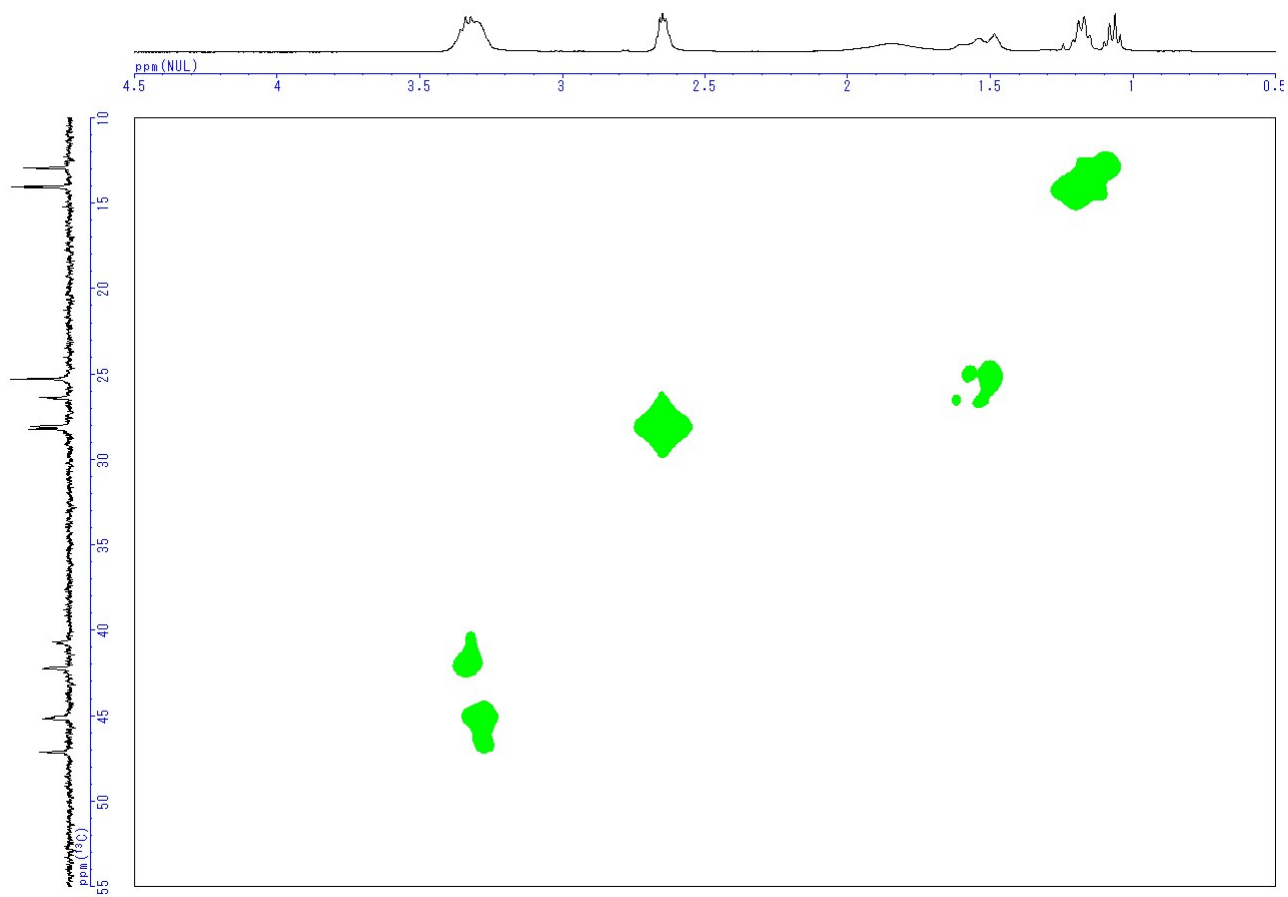


Figure S47. HMQC spectrum of *N*-Et-4,4

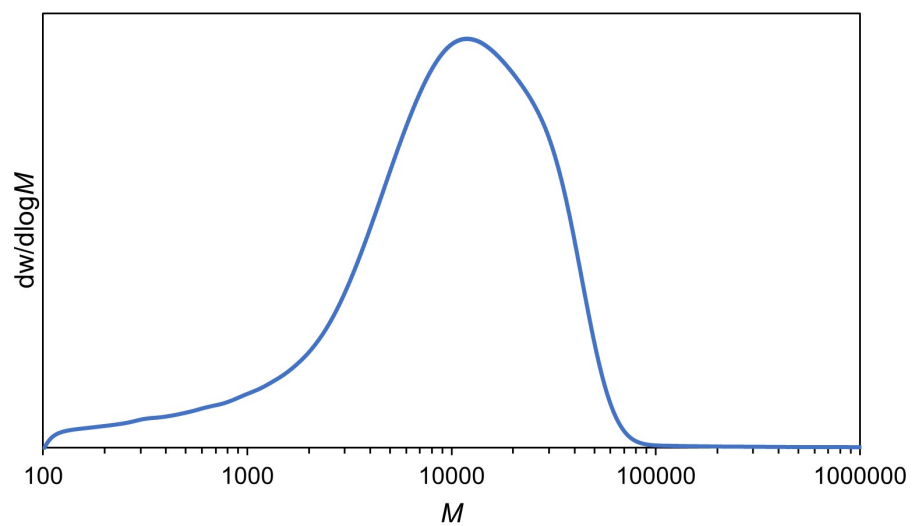


Figure S48. SEC chromatogram of *N*-Et-4,4

N,N'-diethylnylon-4,5 (*N*-Et-4,5)

Polymerization of *N,N'*-diethyl-1,4-butanediamine (356 μ L, 2.00 mmol) and Glutaryl chloride (258 μ L, 2.00 mmol) afforded *N*-Et-4,5 (231 mg, 48% yield) as a yellow solid.

^1H NMR (CDCl_3 , 400 MHz) δ = 3.17-3.45 (m, 8 H), 2.30-2.48 (m, 4 H), 1.89-2.03 (m, 2 H), 1.42-1.58 (m, 4 H), 1.03-1.23 (m, 6 H).

^{13}C NMR (CDCl_3 , 100 MHz) δ = 171.9, 47.1, 44.9, 42.2, 40.4, 32.2, 26.5, 25.3, 25.2, 21.1, 14.2, 14.2, 13.0.

SEC (CHCl_3): M_n = 1.0×10^4 , \mathcal{D} = 1.7.

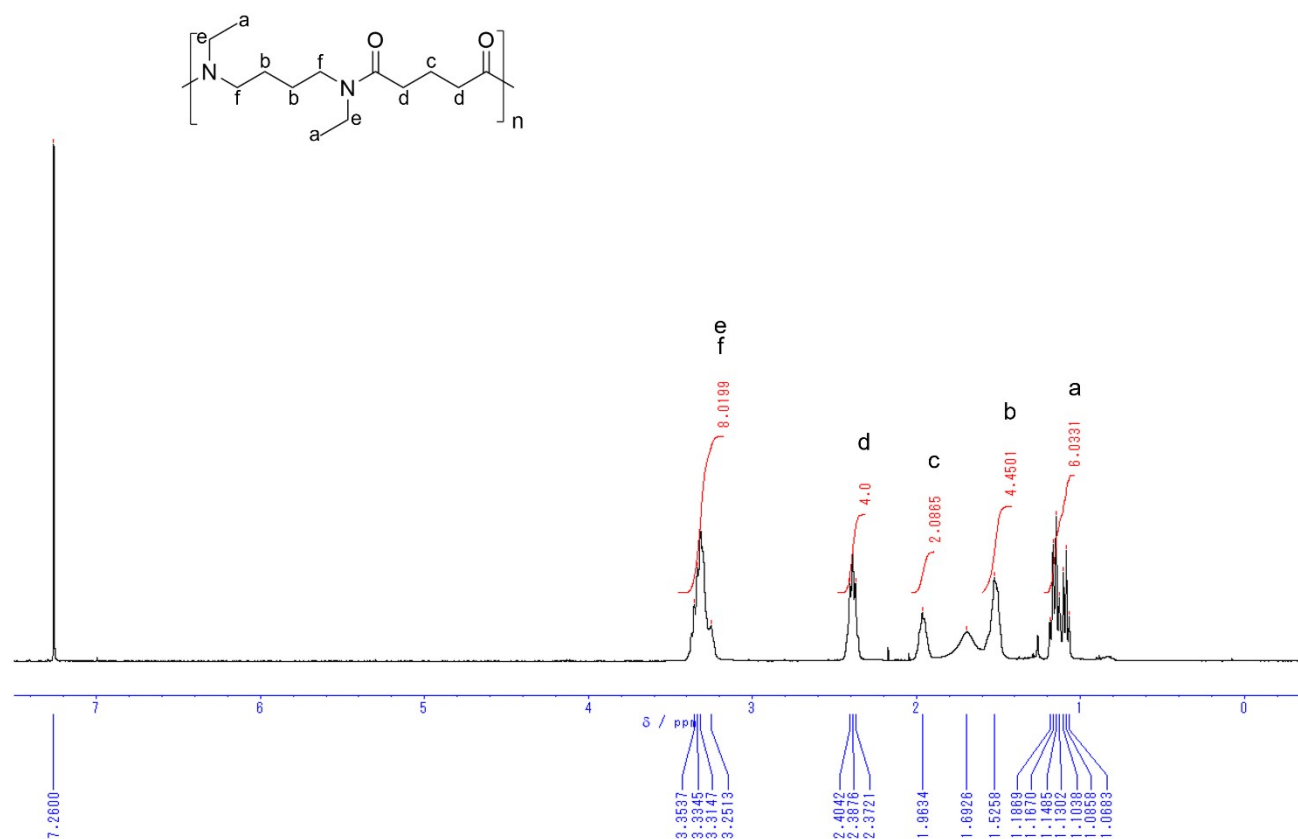


Figure S49. ^1H NMR spectrum of *N*-Et-4,5

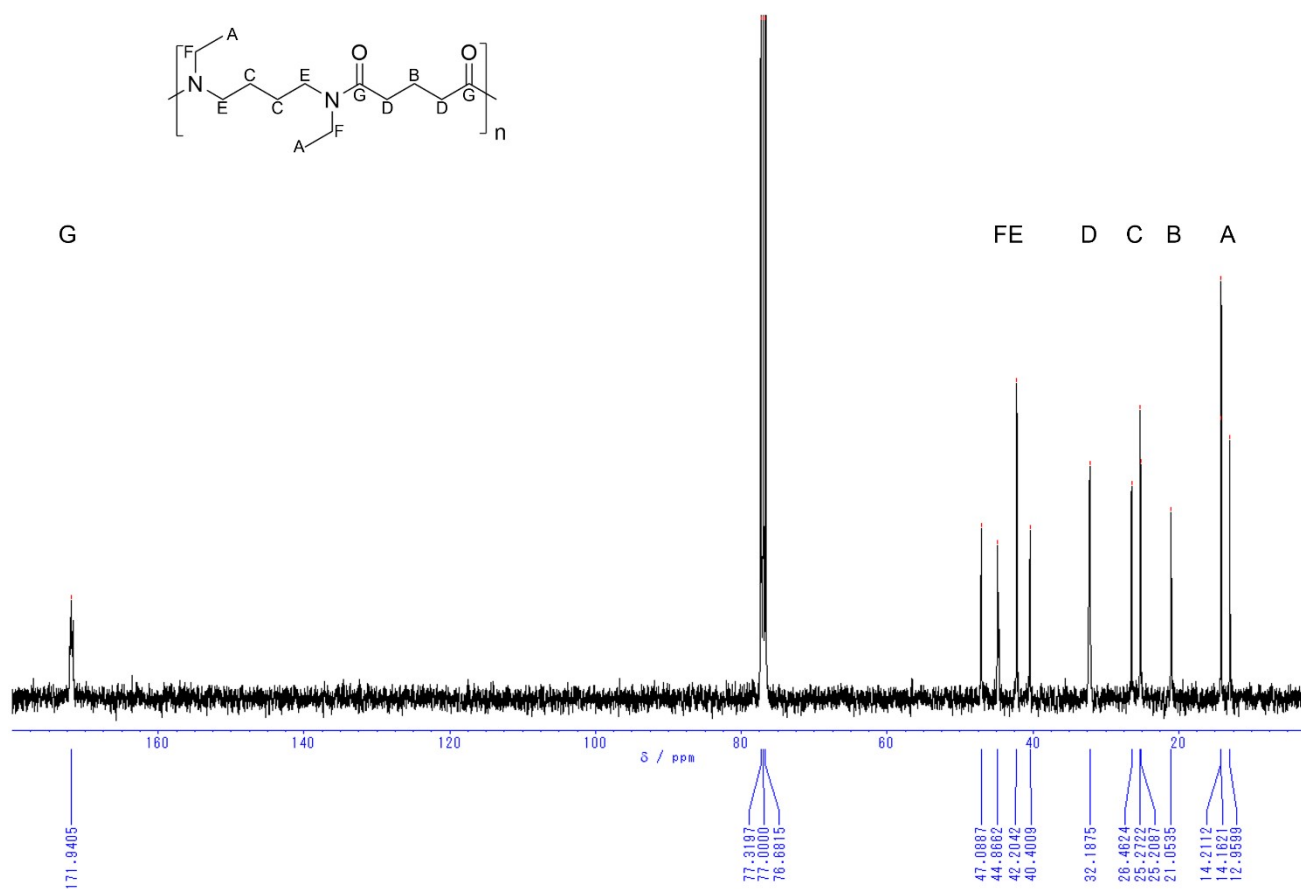


Figure S50. ¹³C NMR spectrum of *N*-Et-4,5

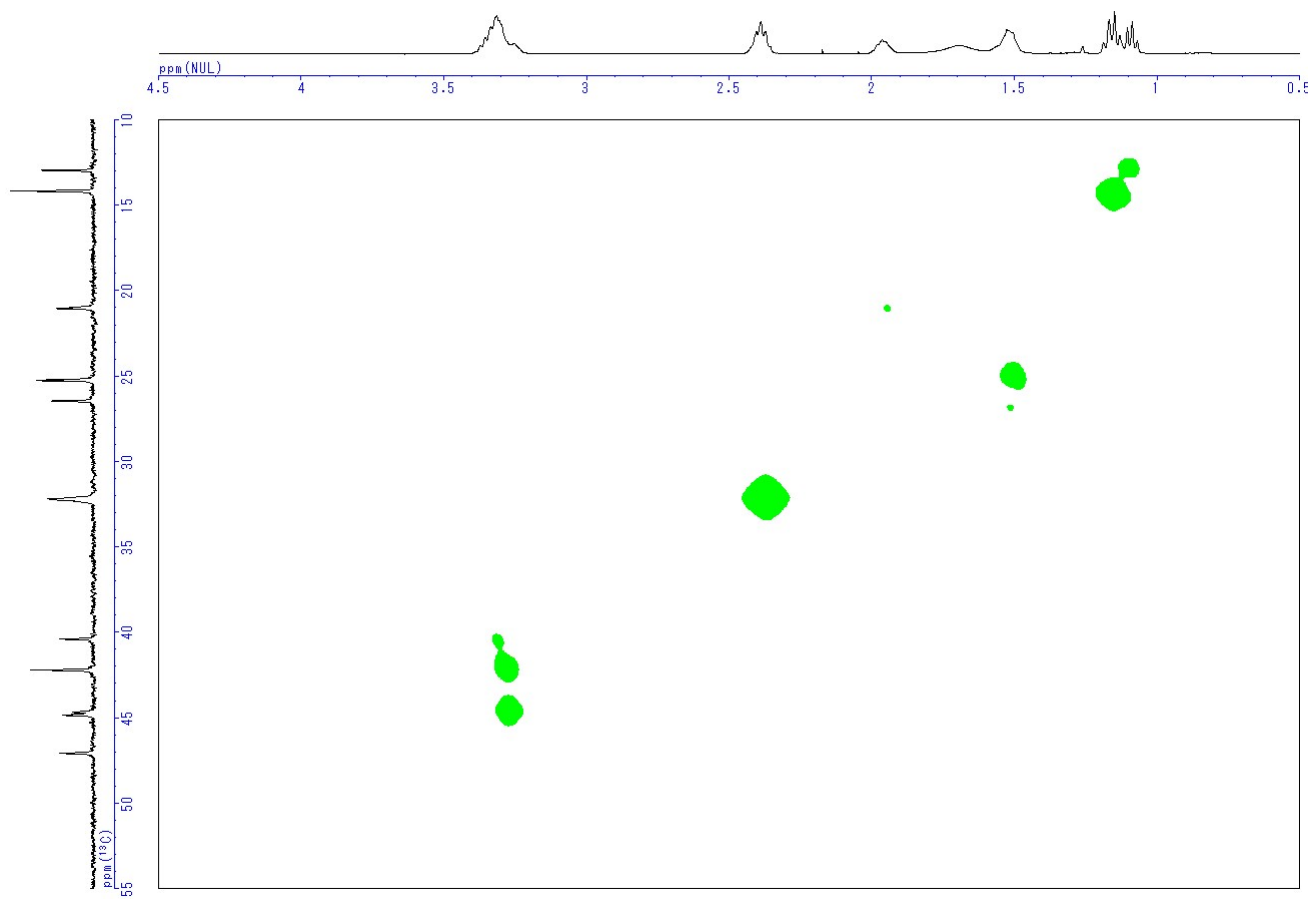


Figure S51. HMQC spectrum of *N*-Et-4,5

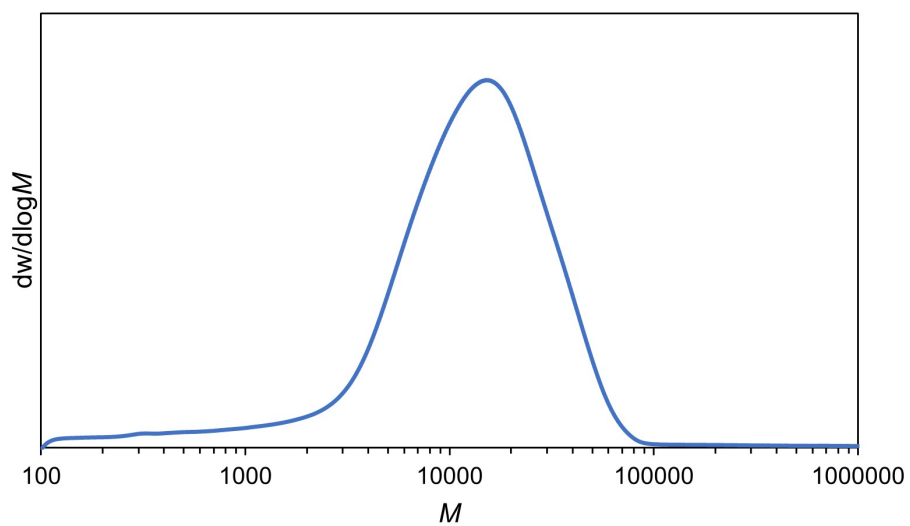


Figure S52. SEC chromatogram of *N*-Et-4,5

N,N'-diethylnylon-4,6 (*N*-Et-4,6)

Polymerization of *N,N'*-diethyl-1,4-butanediamine (356 μ L, 2.00 mmol) and Adipoyl chloride (291 μ L, 2.00 mmol) afforded *N*-Et-4,6 (116 mg, 23% yield) as a white solid.

^1H NMR (CDCl_3 , 400 MHz) δ = 2.97-3.46 (m, 8 H), 2.03-2.31 (m, 4 H), 1.31-1.52 (m, 4 H), 0.87-1.24 (m, 6 H).

^{13}C NMR (CDCl_3 , 100 MHz) δ = 172.0, 47.4, 44.8, 44.7, 42.2, 40.4, 32.7, 32.7, 26.4, 25.1, 14.1, 14.1, 12.8.

SEC (CHCl_3): M_n = 7.1×10^3 , D = 1.5.

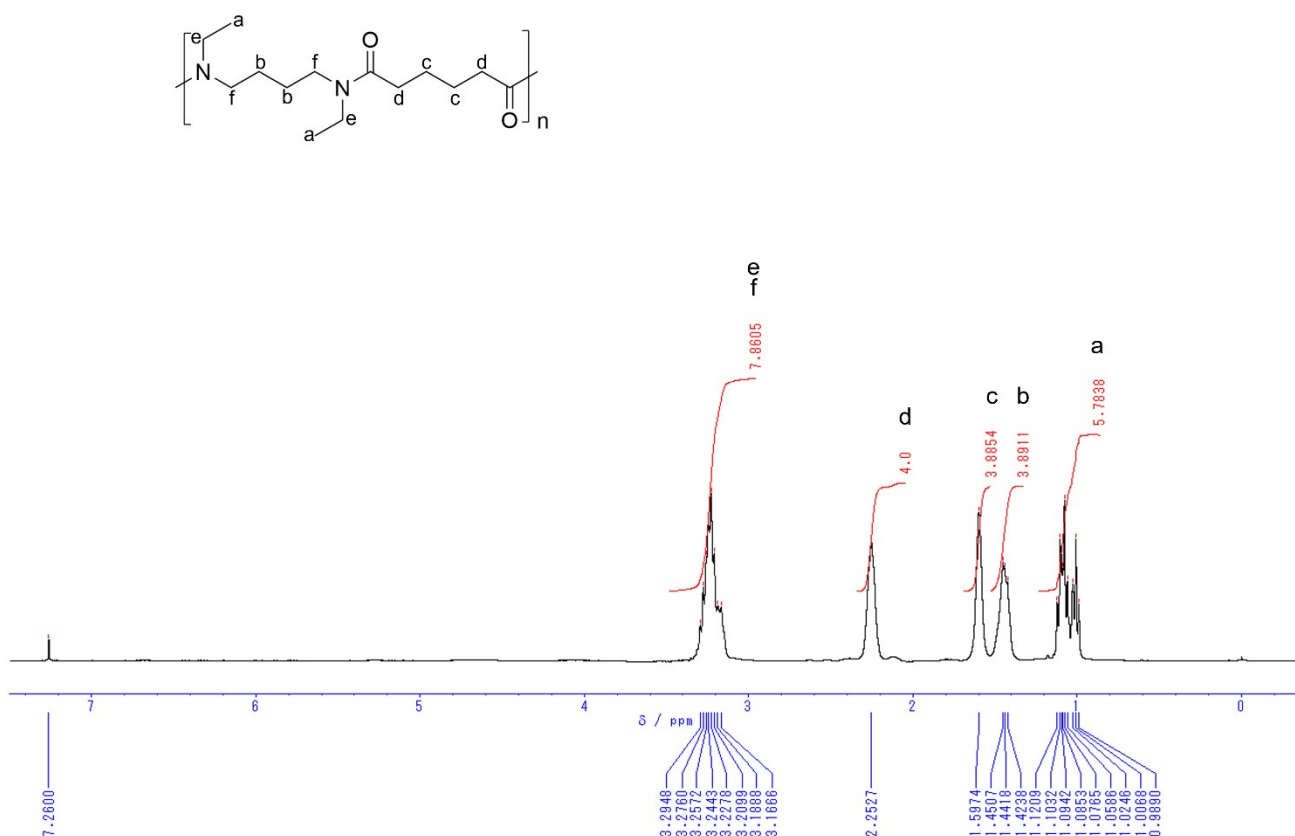


Figure S53. ^1H NMR spectrum of *N*-Et-4,6

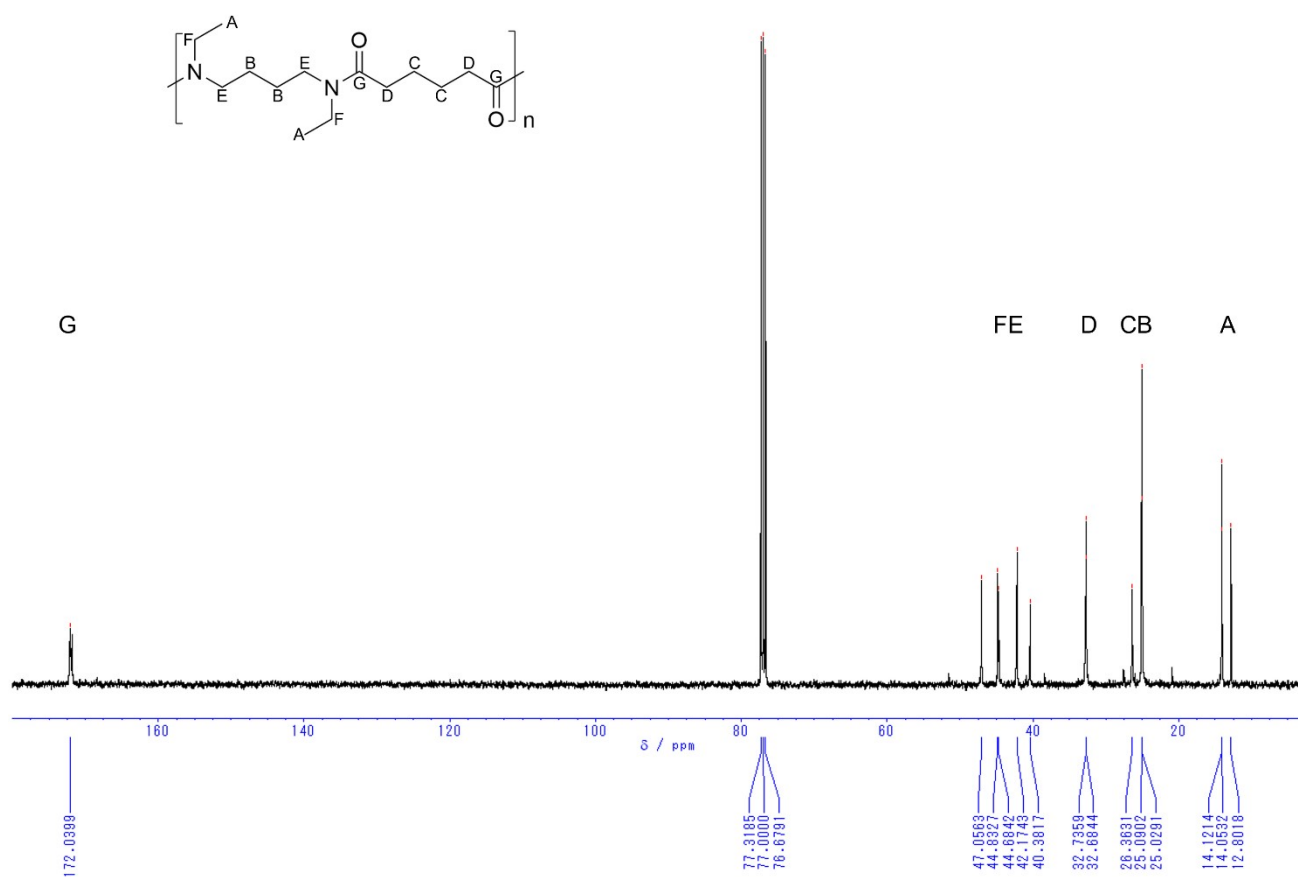


Figure S54. ¹³C NMR spectrum of *N*-Et-4,6

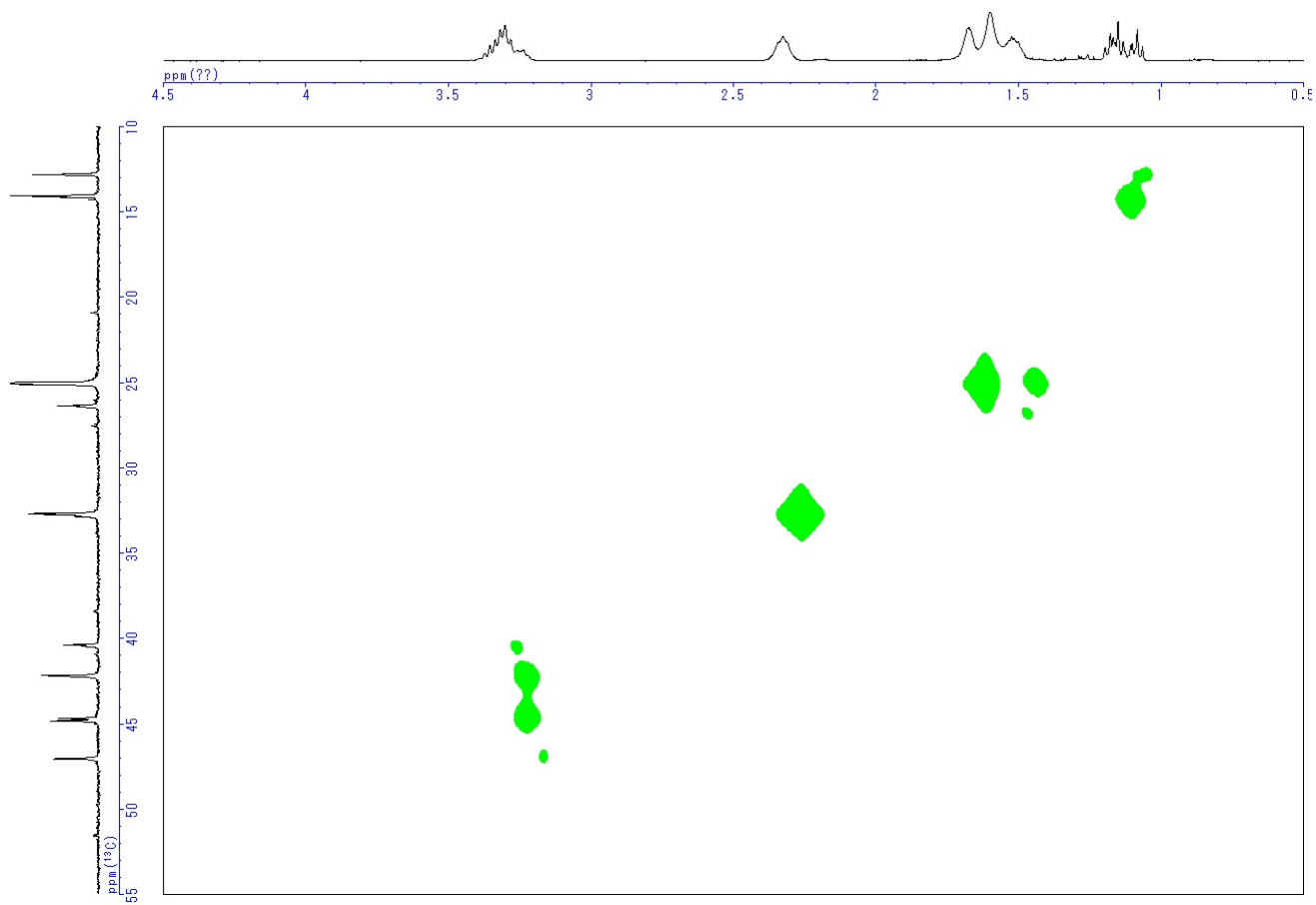


Figure S55. HMQC spectrum of *N*-Et-4,6

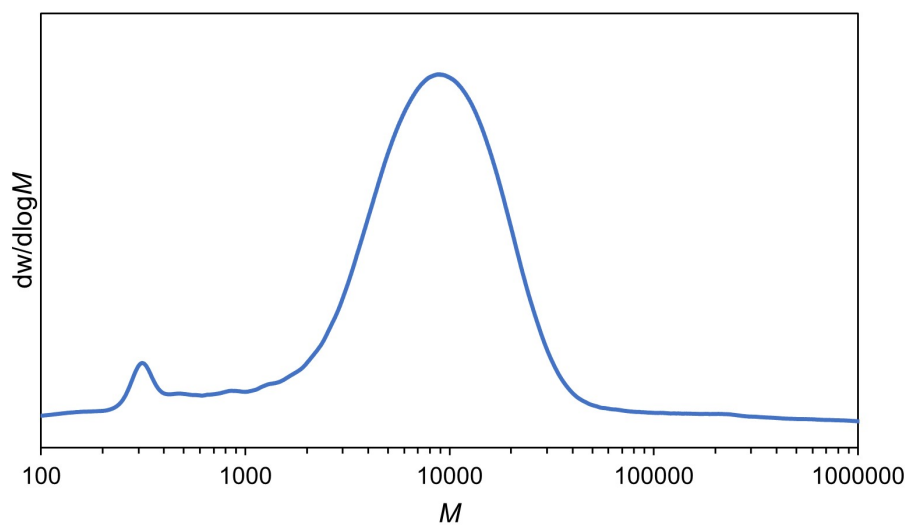


Figure S56. SEC chromatogram of *N*-Et-4,6

N,N'-di-*n*-propylnylon-2,3 (*N-nPr*-2,3)

Polymerization of *N,N'*-di-*n*-propylethylenediamine (356 μ L, 2.00 mmol) and Malonyl chloride (194 μ L, 2.00 mmol) afforded *N-nPr*-2,3 (203 mg, 48% yield) as a brown solid.

^1H NMR (CDCl_3 , 400 MHz) δ = 2.72-4.03 (m, 10 H), 1.41-1.83 (m, 4 H), 0.63-1.08 (m, 6 H).

^{13}C NMR (CDCl_3 , 100 MHz) δ = 167.4, 51.3, 48.0, 47.7, 45.7, 22.4, 21.0, 20.9, 20.7, 11.4, 11.3.

SEC (CHCl_3): M_n = 1.4×10^3 , \mathcal{D} = 1.7.

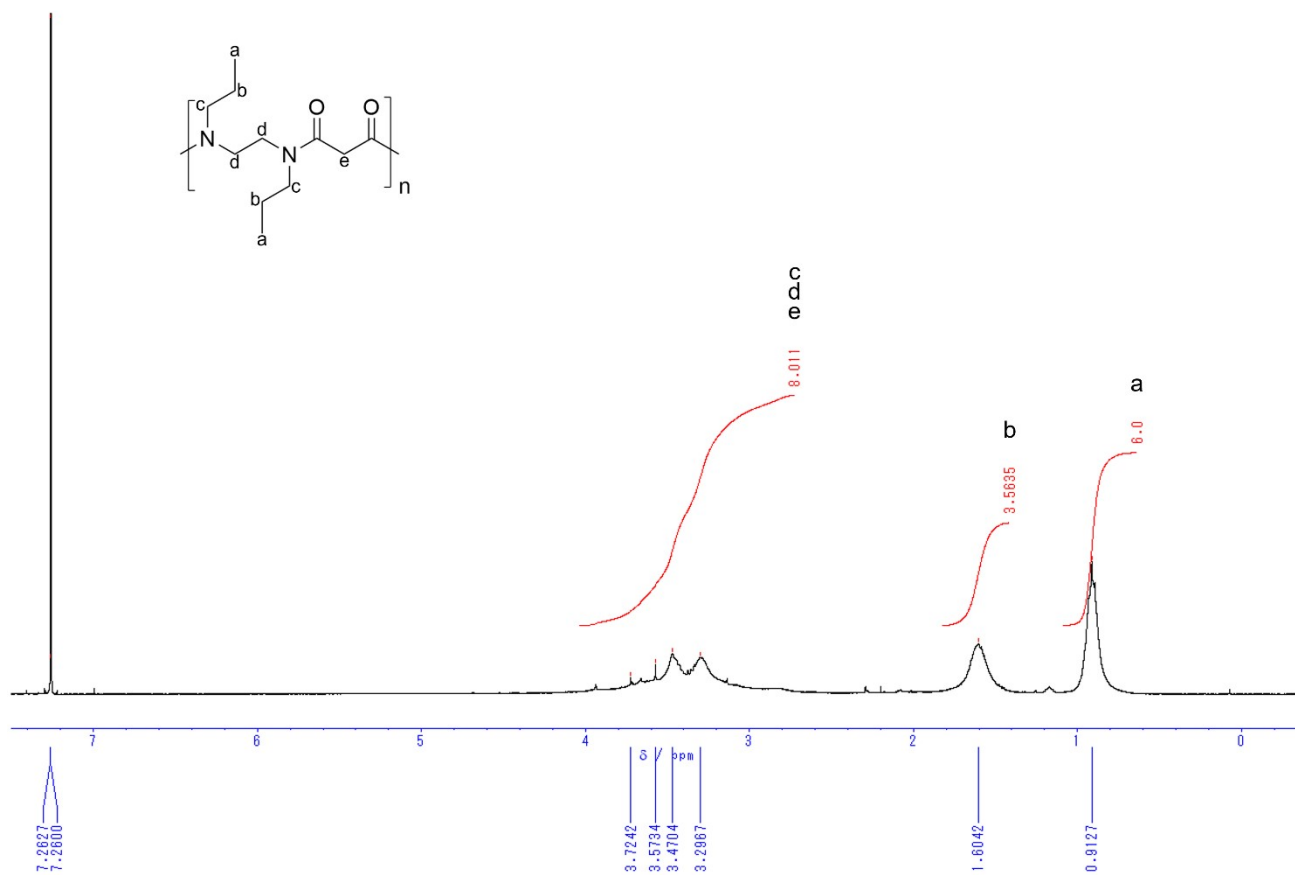


Figure S57. ^1H NMR spectrum of *N-nPr*-2,3

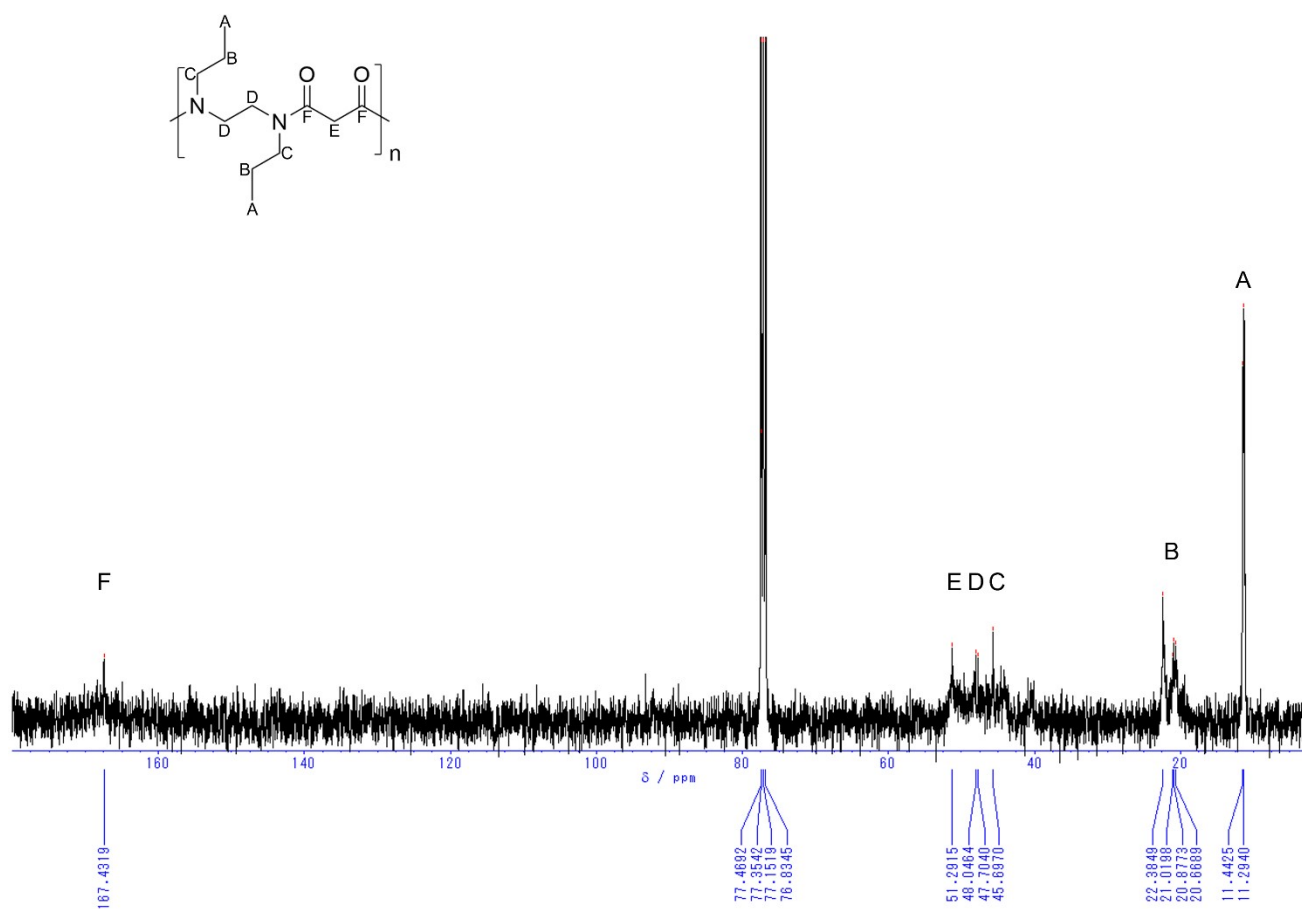


Figure S58. ¹³C NMR spectrum of *N*-*n*Pr-2,3

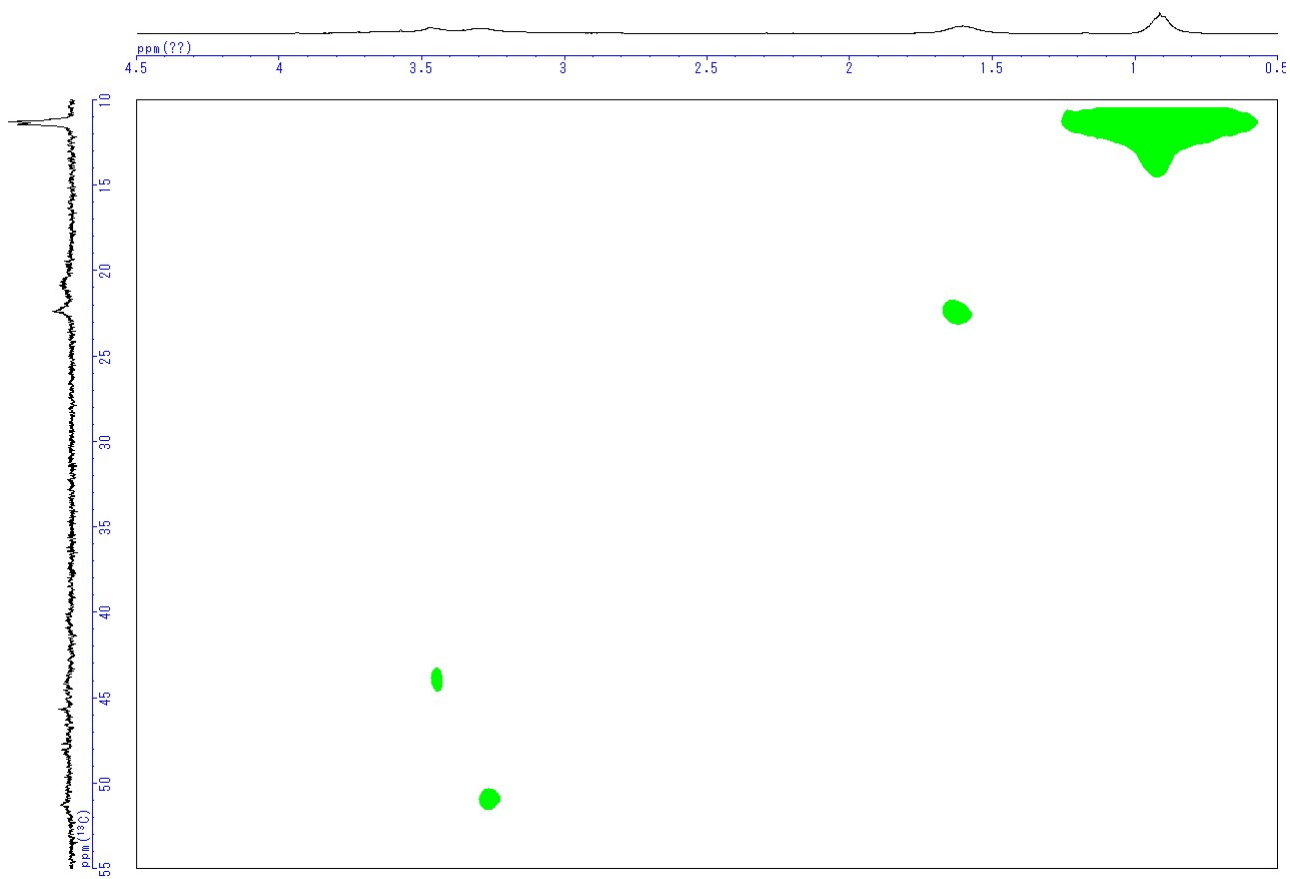


Figure S59. HMQC spectrum of *N-nPr-2,3*

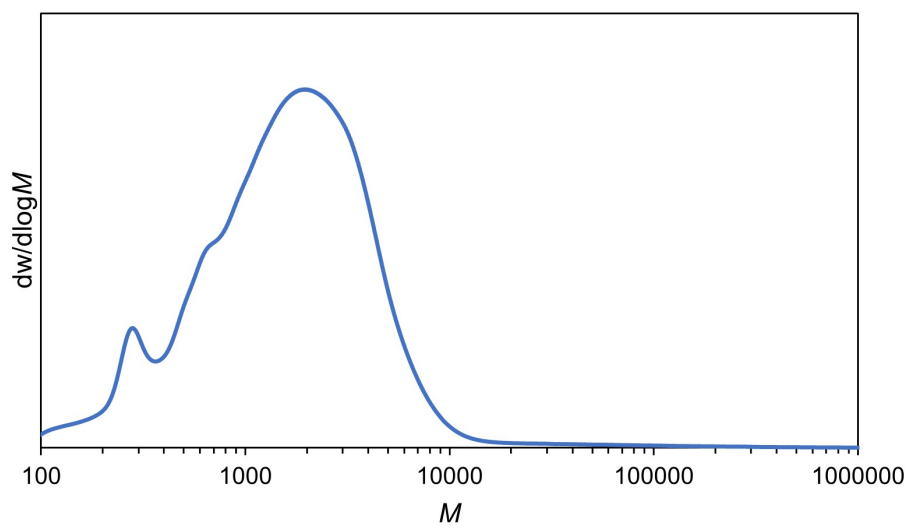


Figure S60. SEC chromatogram of *N-nPr-2,3*

N,N'-di-*n*-propylnylon-2,4 (*N-nPr-2,4*)

Polymerization of *N,N'*-di-*n*-propylethylenediamine (1.41 mL, 7.92 mmol) and Succinyl chloride (895 μ L, 7.91 mmol) afforded *N-nPr-2,4* (187 mg, 10% yield) as a brown solid.

^1H NMR (CDCl_3 , 400 MHz) δ = 3.36-3.66 (m, 4 H), 3.15-3.36 (m, 4 H), 2.43-2.77 (m, 4 H), 1.42-1.79 (m, 4 H), 0.76-1.02 (m, 6 H).

^{13}C NMR (CDCl_3 , 100 MHz) δ = 171.9, 50.5, 44.2, 28.1, 22.2, 21.0, 11.3, 11.2.

SEC (CHCl_3): $M_n = 2.1 \times 10^3$, $\text{Đ} = 1.1$.

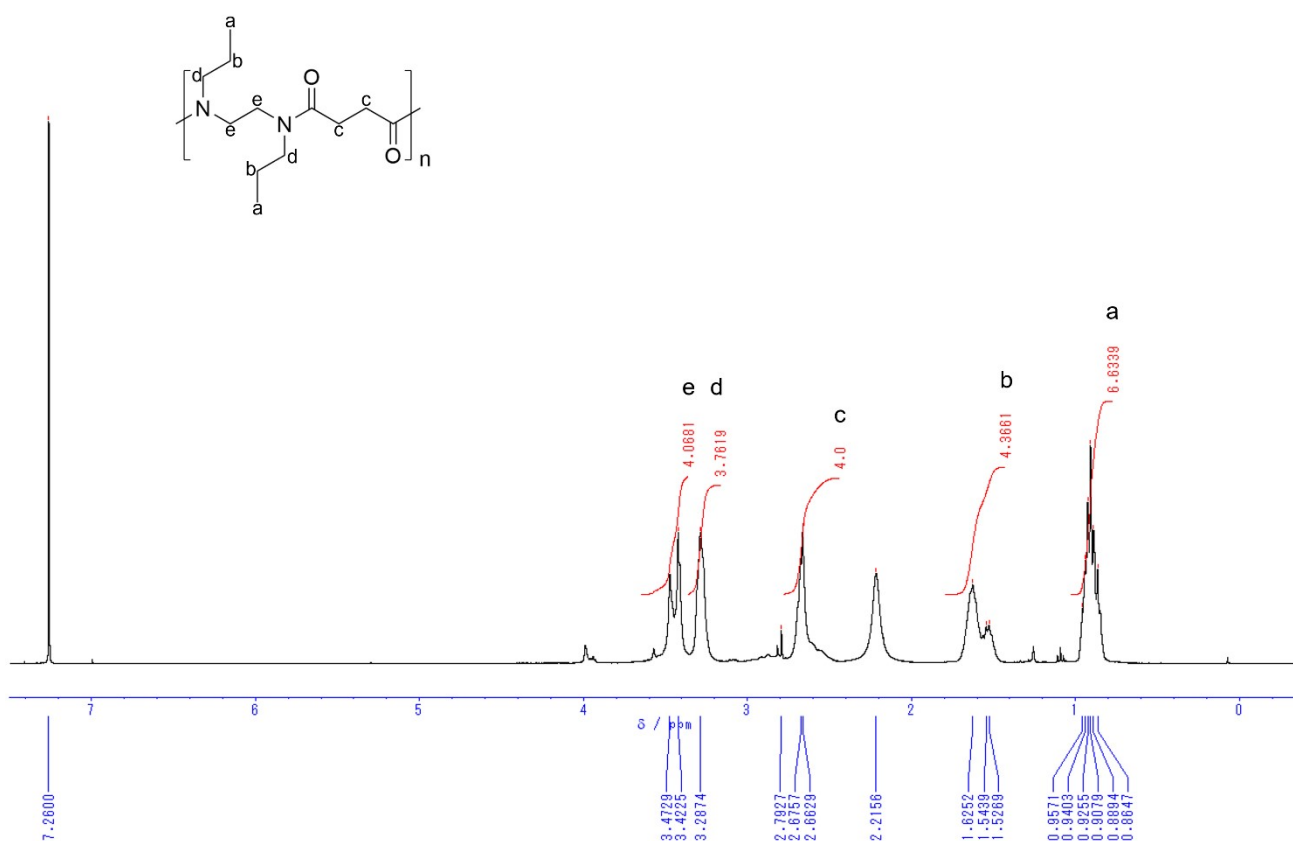


Figure S61. ^1H NMR spectrum of *N-nPr-2,4*

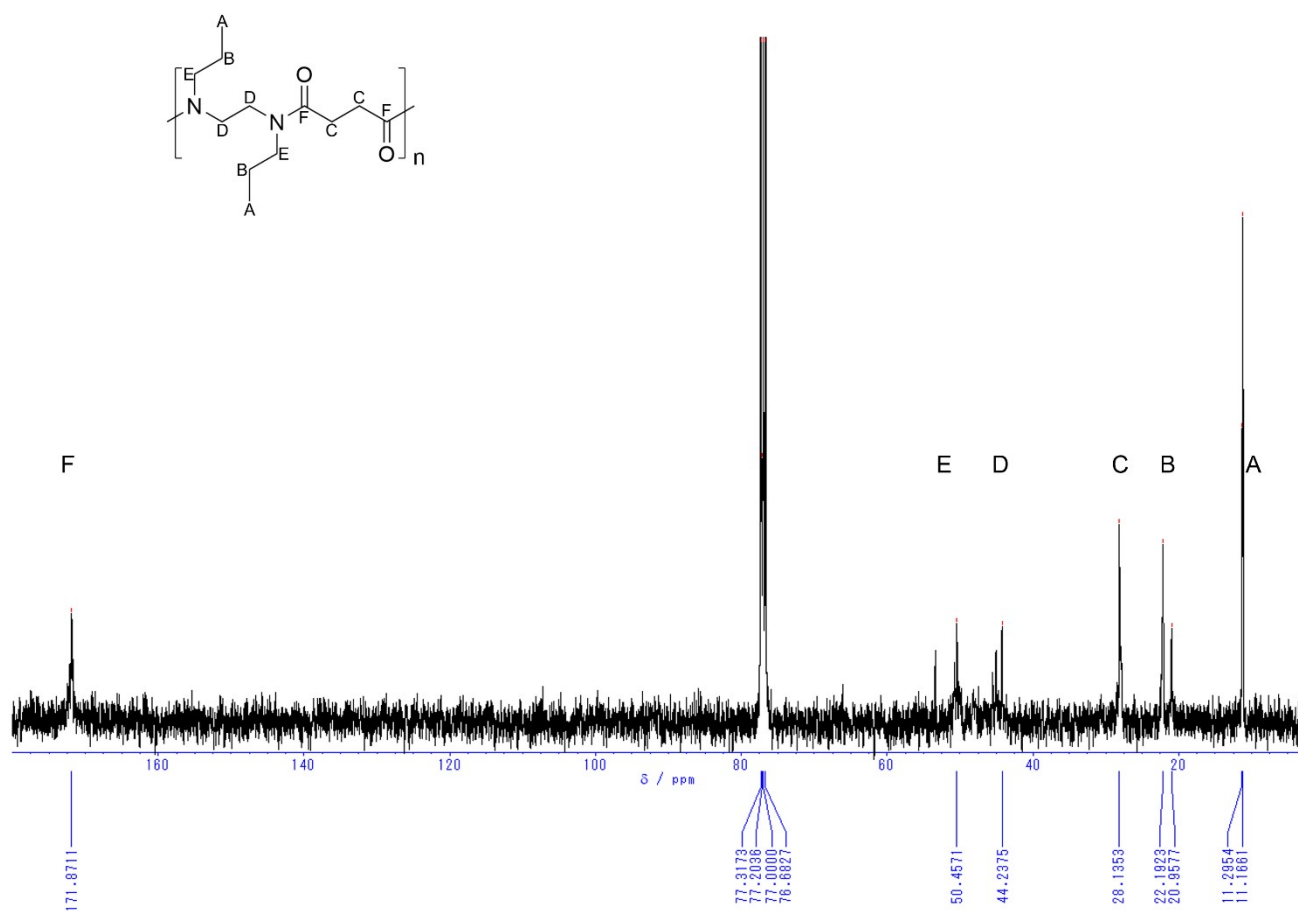


Figure S62. ^{13}C NMR spectrum of *N-nPr-2,4*

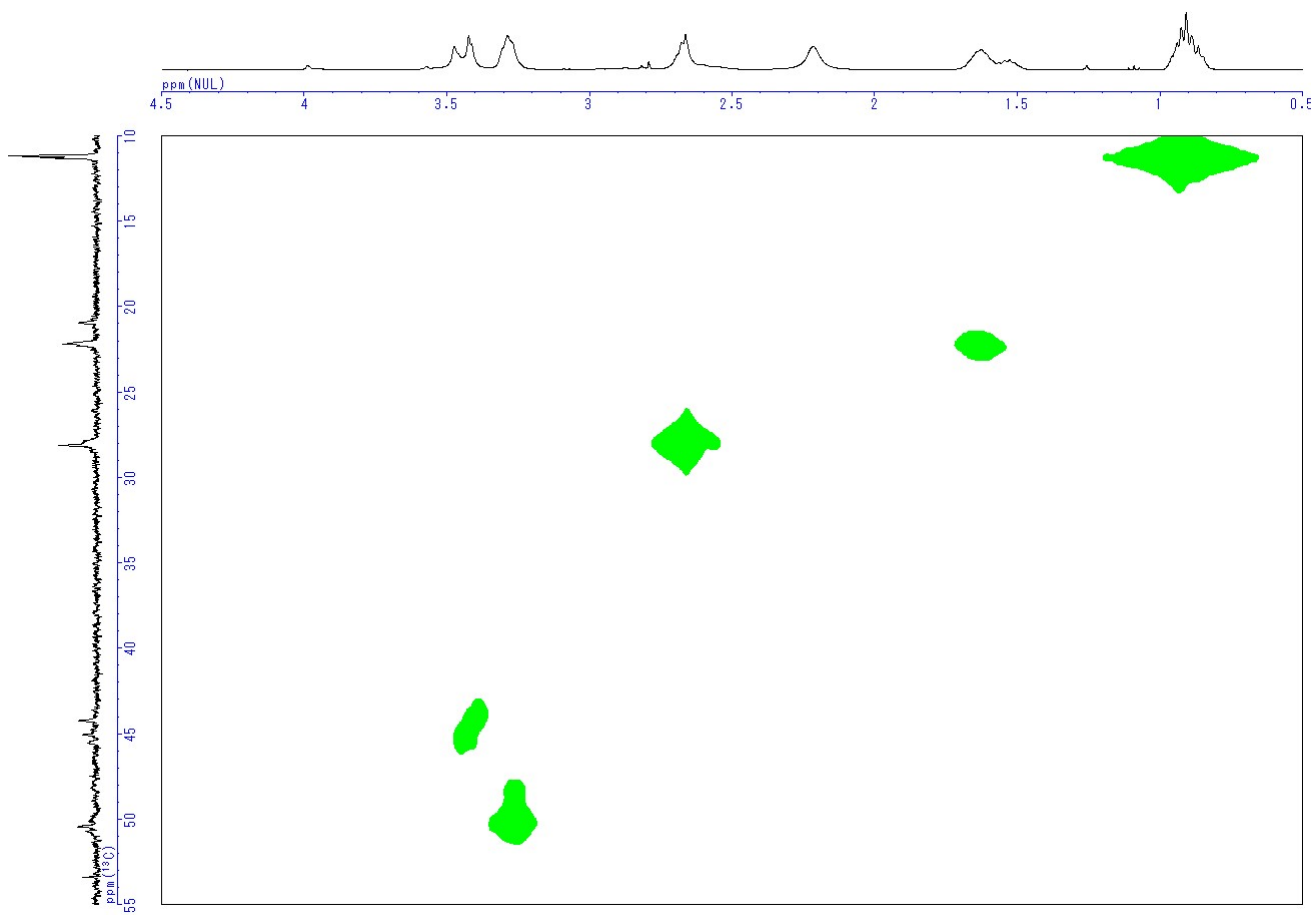


Figure S63. HMQC spectrum of *N-nPr-2,4*

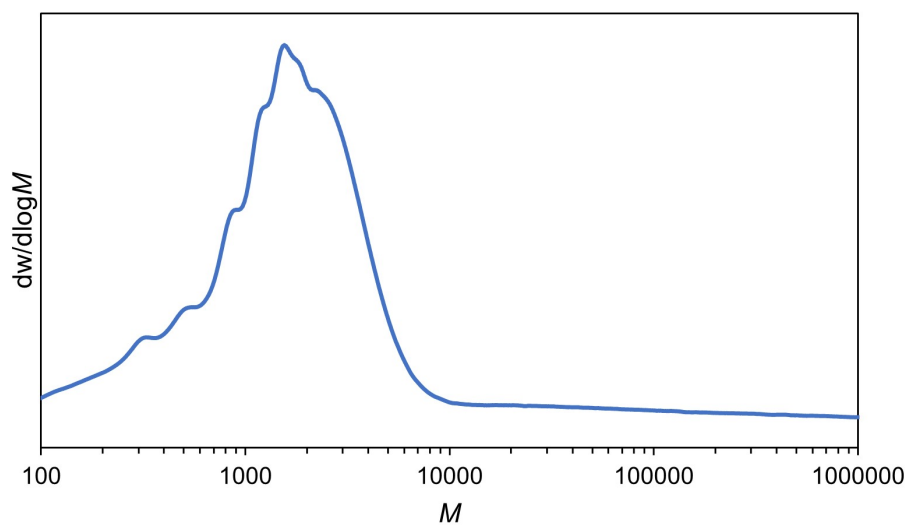


Figure S64. SEC chromatogram of *N-nPr-2,4*

N,N'-di-*n*-propylnylon-2,5 (*N-nPr-2,5*)

Polymerization of *N,N'*-di-*n*-propylethylenediamine (356 μL , 2.00 mmol) and Glutaryl chloride (258 μL , 2.00 mmol) afforded *N-nPr-2,5* (217 mg, 45% yield) as a yellow solid.

^1H NMR (CDCl_3 , 400 MHz) δ = 3.33-3.56 (m, 4 H), 3.13-3.33 (m, 4 H), 2.32-2.50 (m, 4 H), 1.86-2.04 (m, 2 H), 1.45-1.65 (m, 4 H), 0.81-0.99 (m, 6 H).

^{13}C NMR (CDCl_3 , 100 MHz) δ = 172.2, 50.1, 47.6, 44.8, 43.7, 31.8, 22.2, 22.1, 20.8, 20.5, 11.1, 10.9.

SEC (CHCl_3): $M_n = 5.7 \times 10^3$, $\bar{D} = 1.7$.

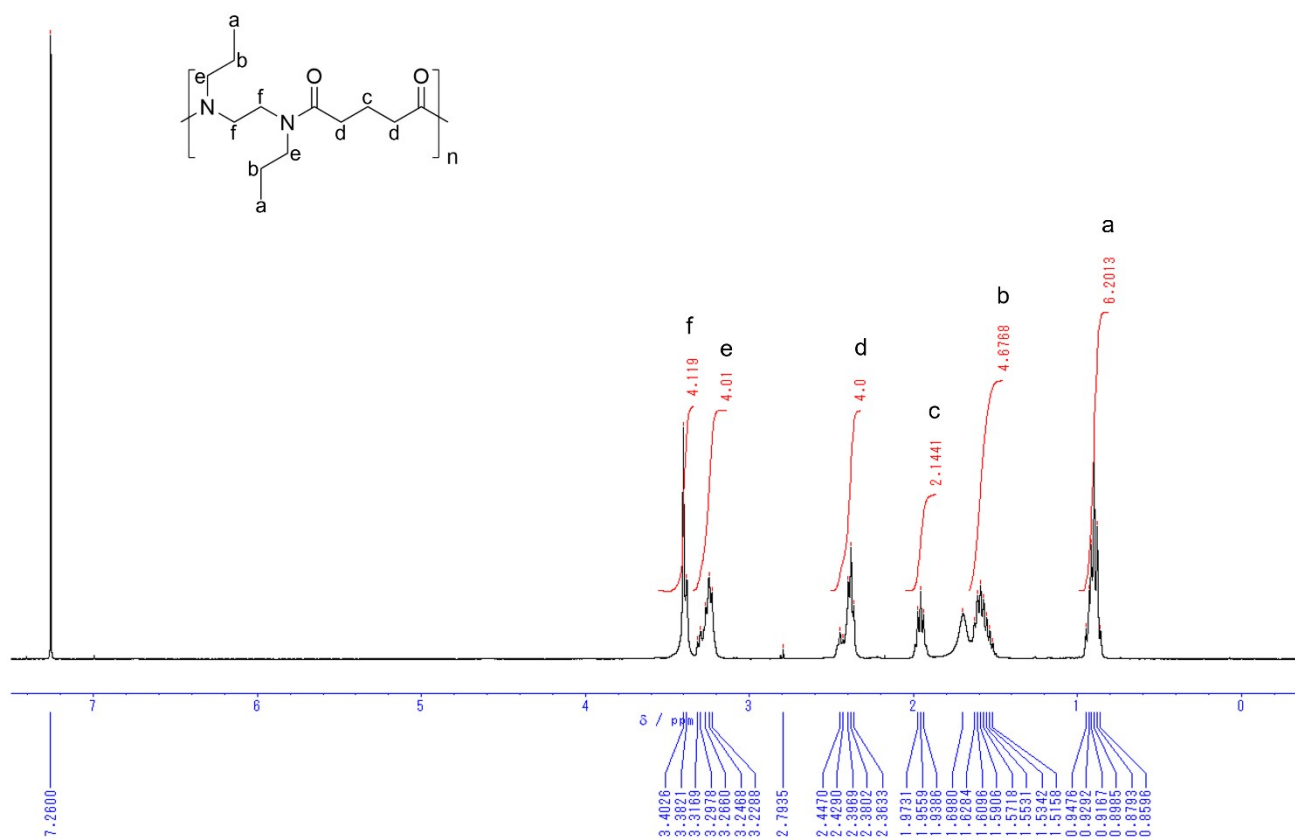


Figure S65. ^1H NMR spectrum of *N-nPr-2,5*

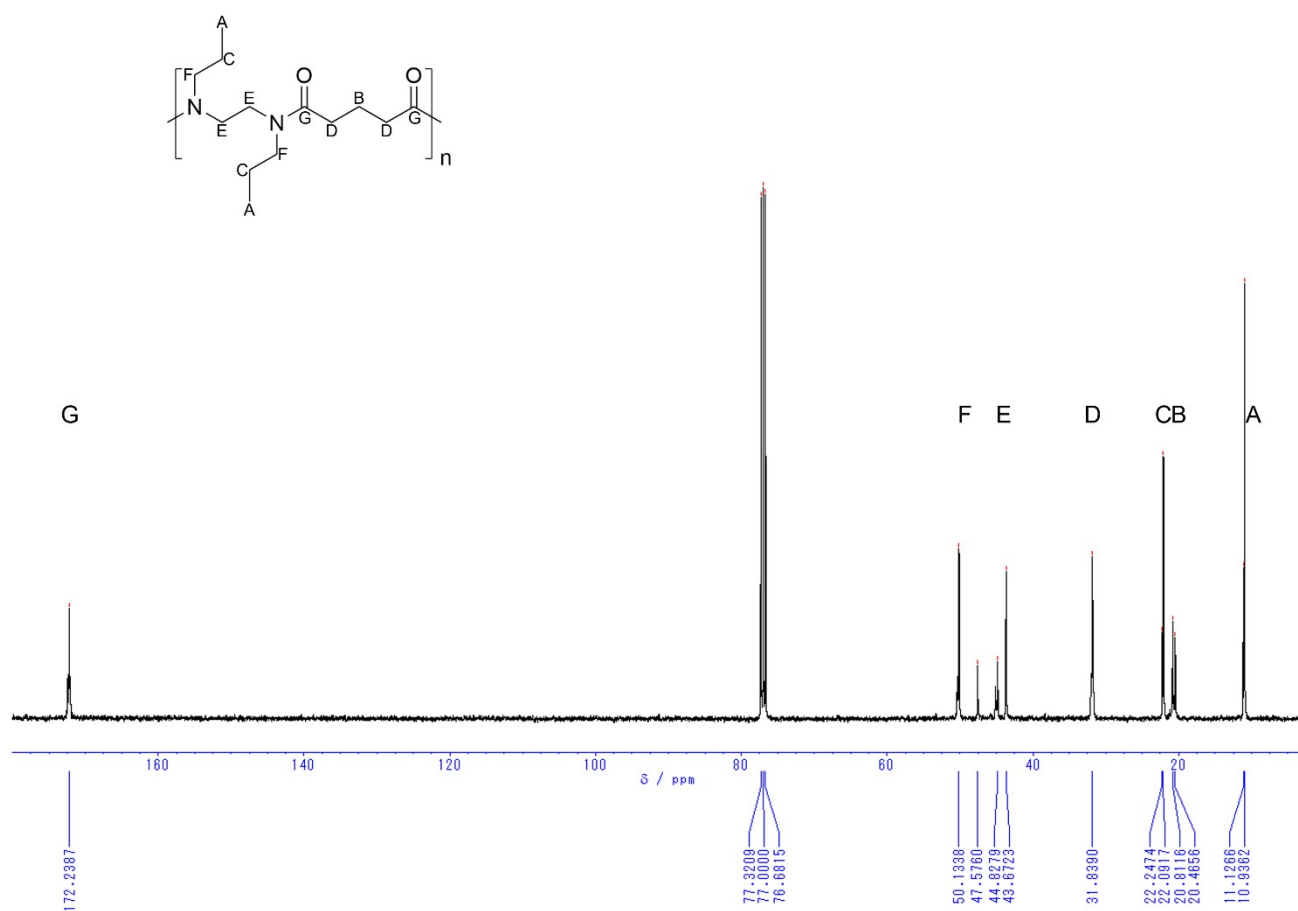


Figure S66. ^{13}C NMR spectrum of *N*-*n*Pr-2,5

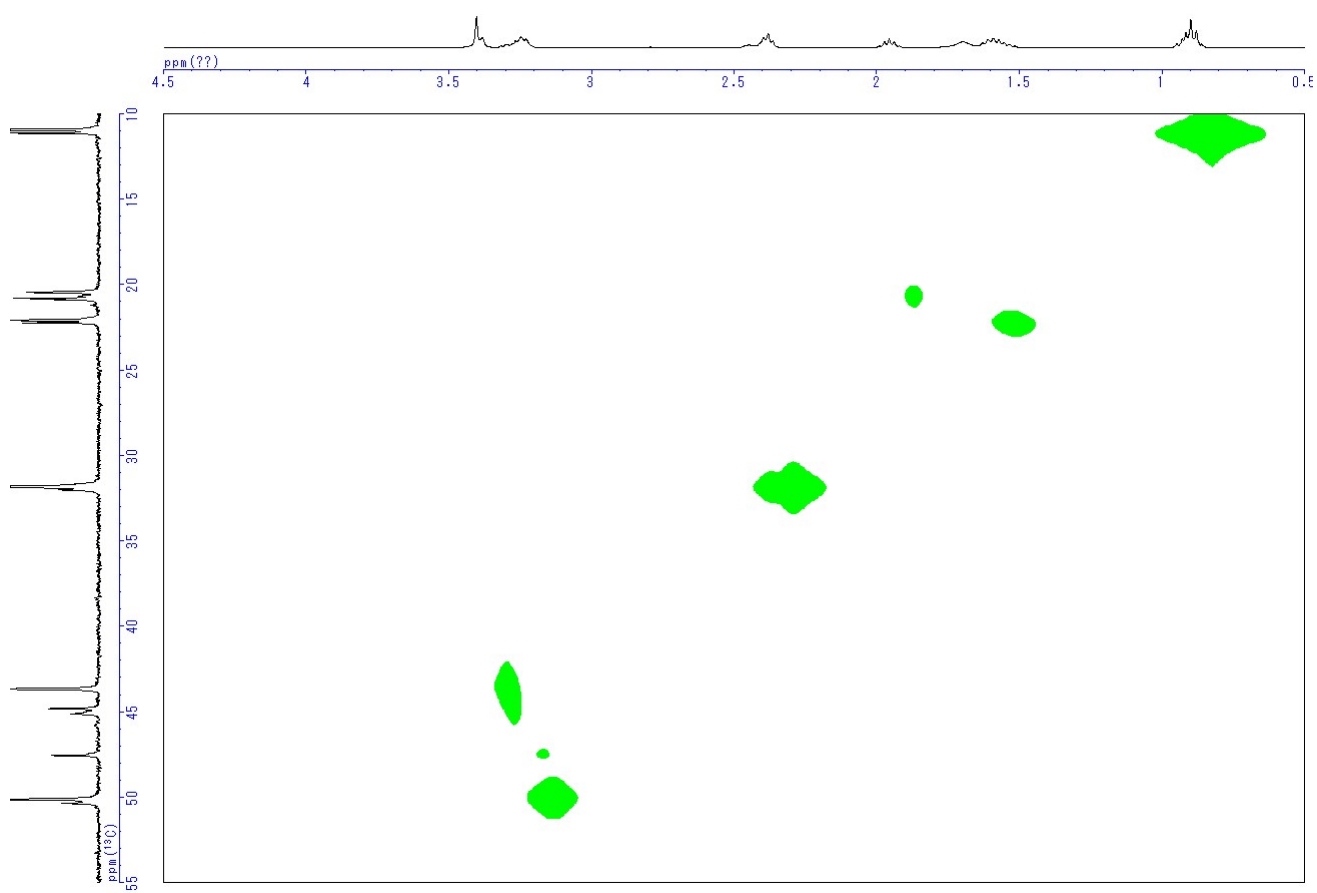


Figure S67. HMQC spectrum of *N-nPr-2,5*

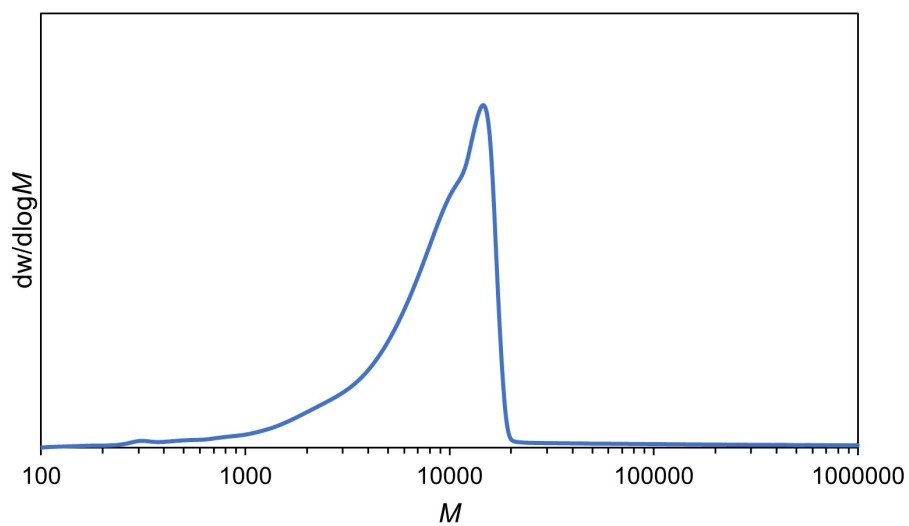


Figure S68. SEC chromatogram of *N-nPr-2,5*

N,N'-di-*n*-propylnylon-2,6 (*N-nPr-2,6*)

Polymerization of *N,N'*-di-*n*-propylethylenediamine (356 μL , 2.00 mmol) and Adipoyl chloride (291 μL , 2.00 mmol) afforded *N-nPr-2,6* (195 mg, 38% yield) as a brown solid.

^1H NMR (CDCl_3 , 400 MHz) δ = 3.32-3.54 (m, 4 H), 3.09-3.33 (m, 4 H), 2.26-2.51 (m, 4 H), 1.43-1.69 (m, 8 H), 0.81-0.99 (m, 6 H).

^{13}C NMR (CDCl_3 , 100 MHz) δ = 172.6, 50.4, 43.9, 32.8, 25.0, 22.3, 11.3, 11.1.

SEC (CHCl_3): M_n = 7.4×10^3 , \mathcal{D} = 1.7.

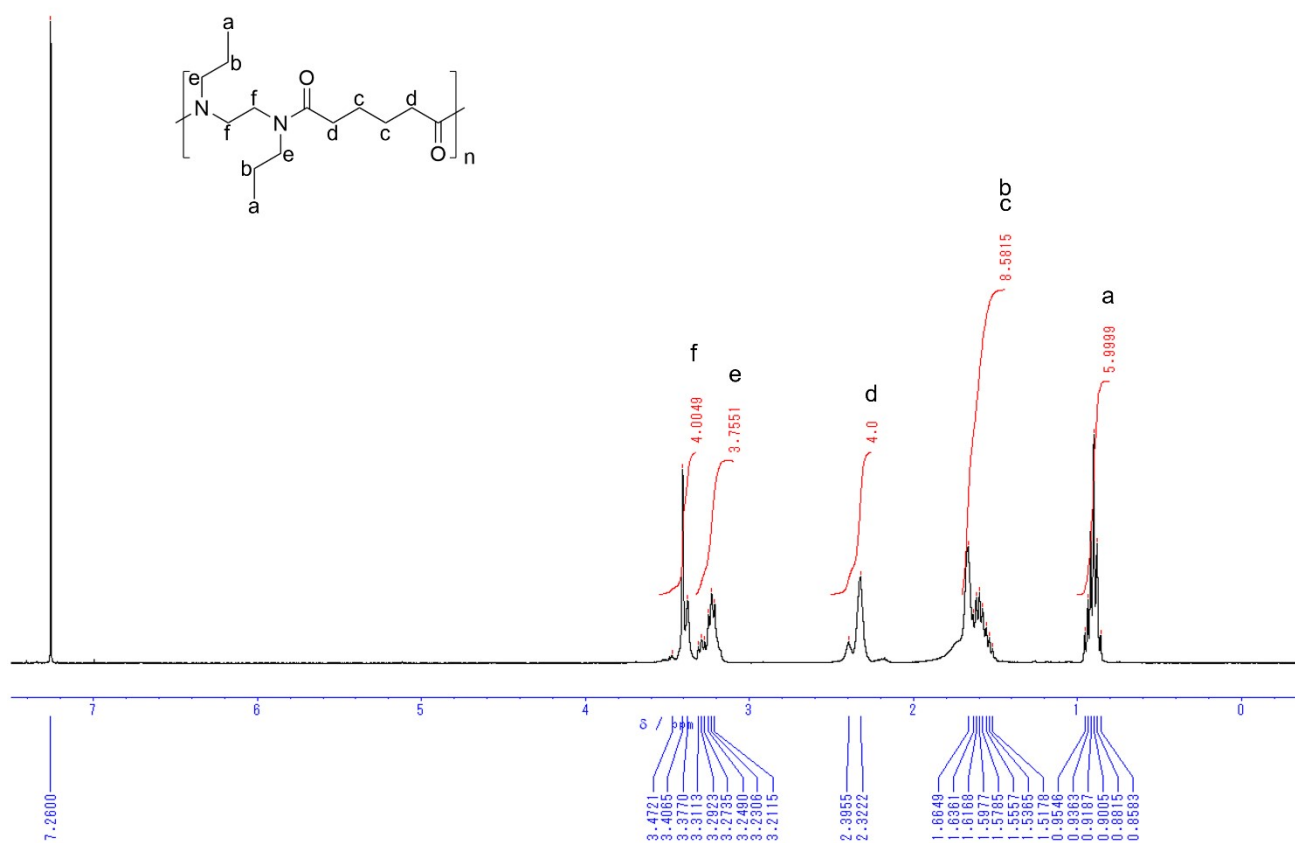


Figure S69. ^1H NMR spectrum of *N-nPr-2,6*

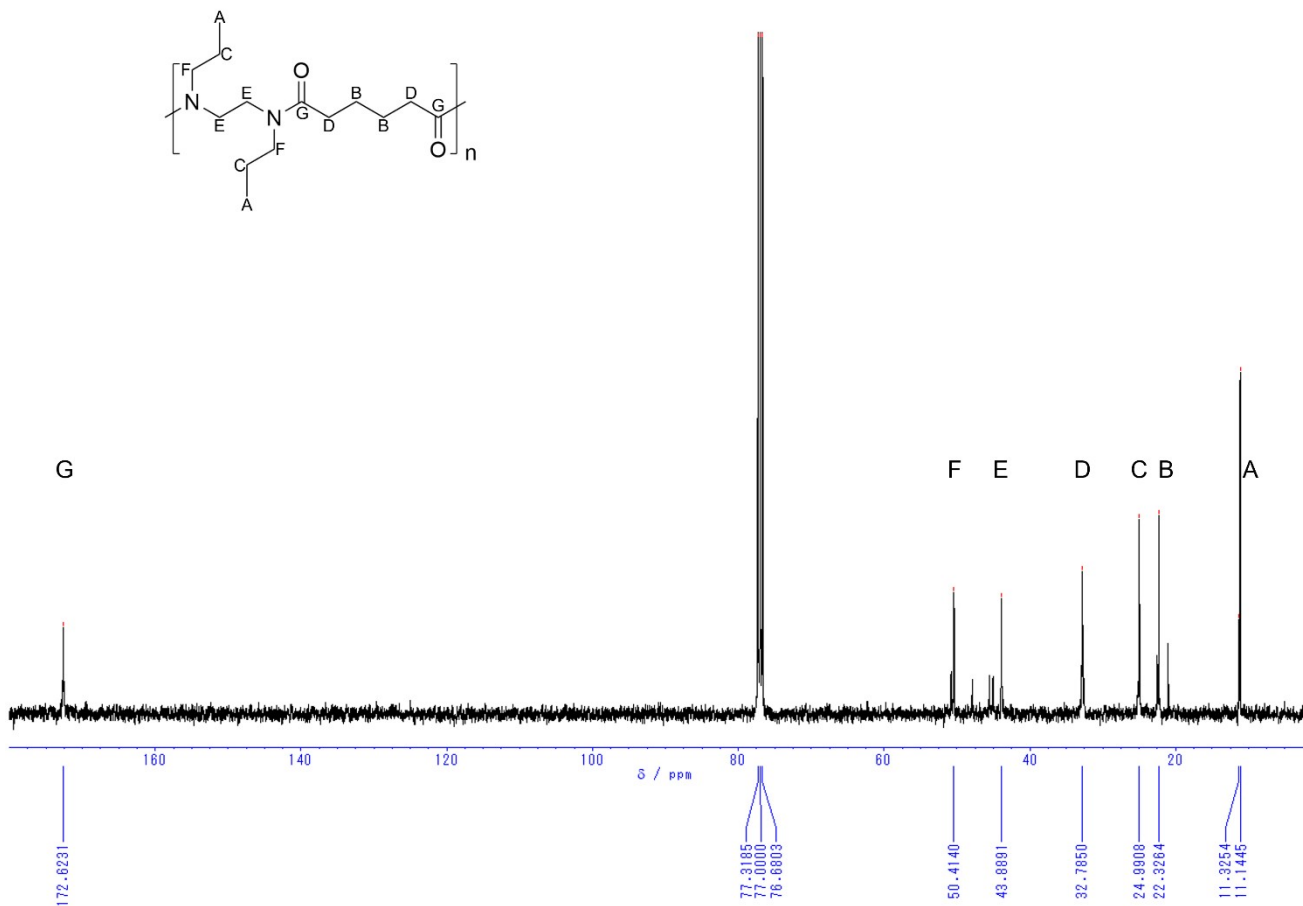


Figure S70. ¹³C NMR spectrum of *N-nPr-2,6*

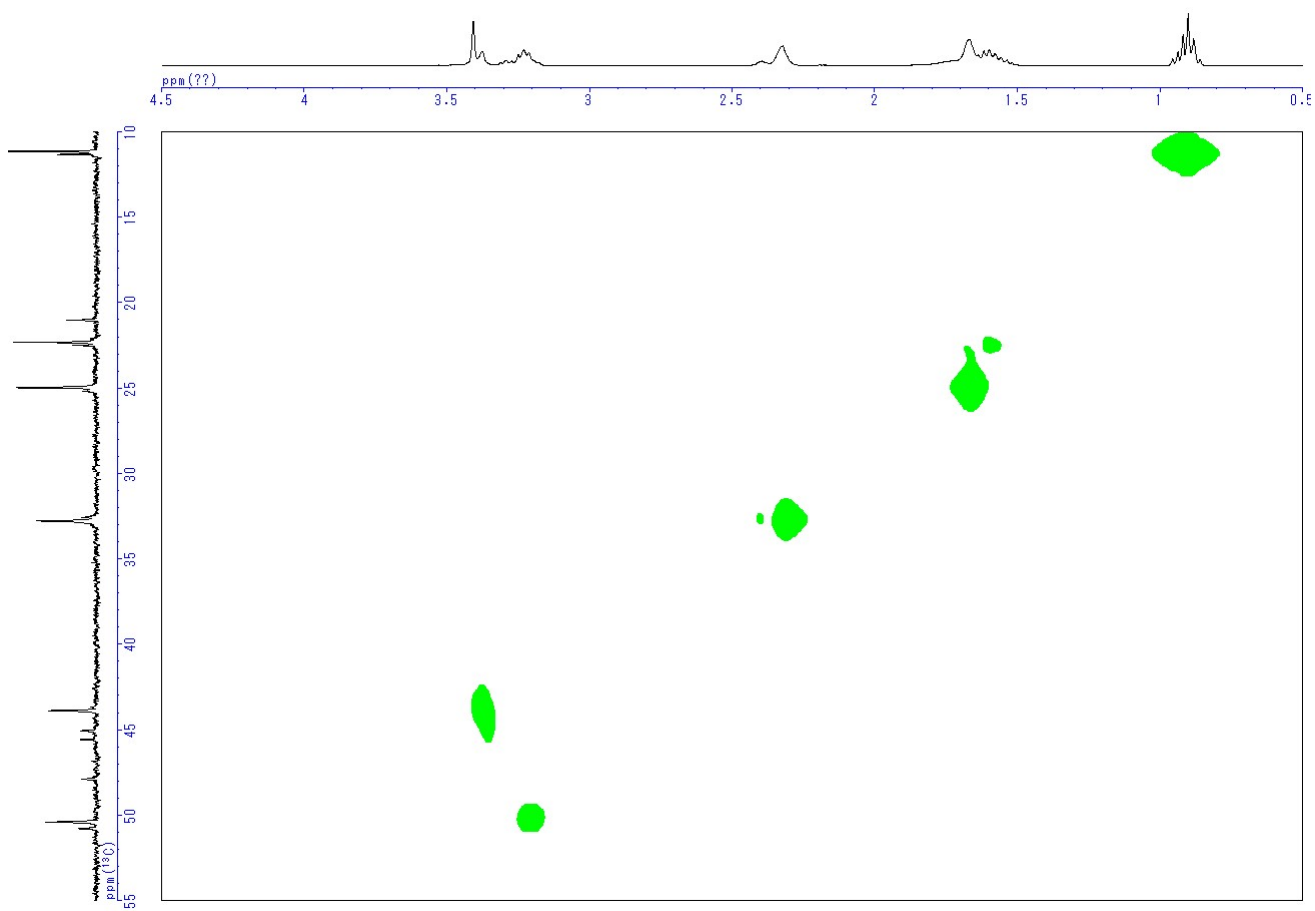


Figure S71. HMQC spectrum of *N-nPr-2,6*

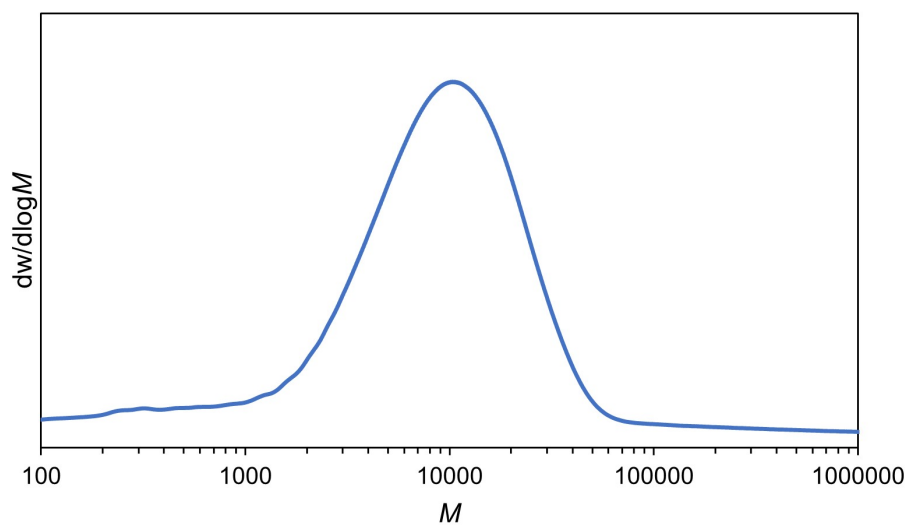


Figure S72. SEC chromatogram of *N-nPr-2,6*

N,N'-di-isopropylnylon-2,3 (*N-iPr-2,3*)

Polymerization of *N,N'*-di-isopropylethylenediamine (361 μL , 2.00 mmol) and Malonyl chloride (194 μL , 2.00 mmol) afforded *N-iPr-2,3* (255 mg, 60% yield) as a yellow solid.

^1H NMR (CDCl_3 , 400 MHz) δ = 3.55-4.41 (m, 4 H), 2.68-3.55 (m, 4 H), 0.92-1.49 (m, 12 H).

^{13}C NMR (CDCl_3 , 100 MHz) δ = 166.8, 49.6, 49.1, 41.7, 39.5, 29.8, 21.4, 21.0, 20.3, 20.1, 19.9, 19.2.

SEC (CHCl_3): M_n = 1.2×10^3 , \mathcal{D} = 1.4.

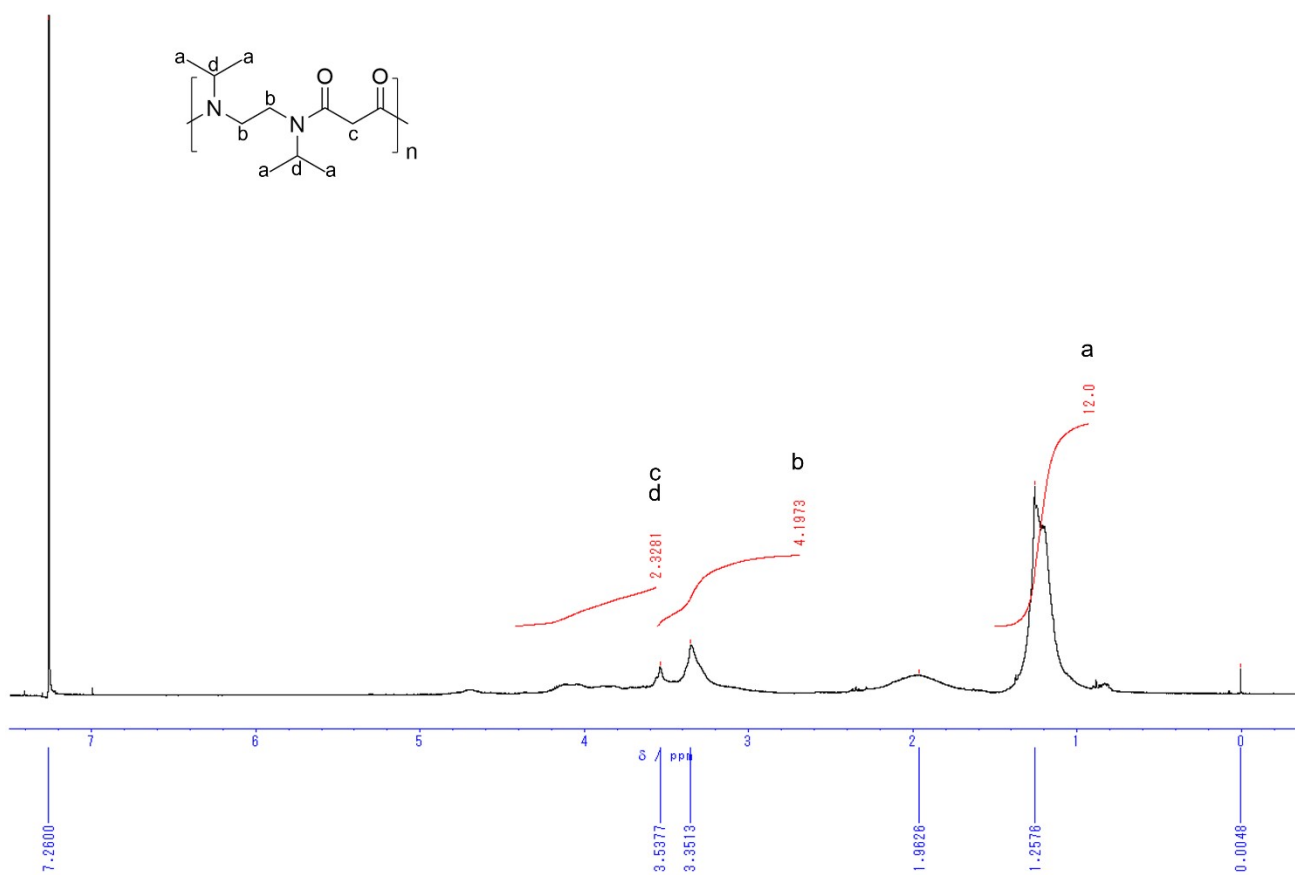


Figure S73. ^1H NMR spectrum of *N-iPr-2,3*

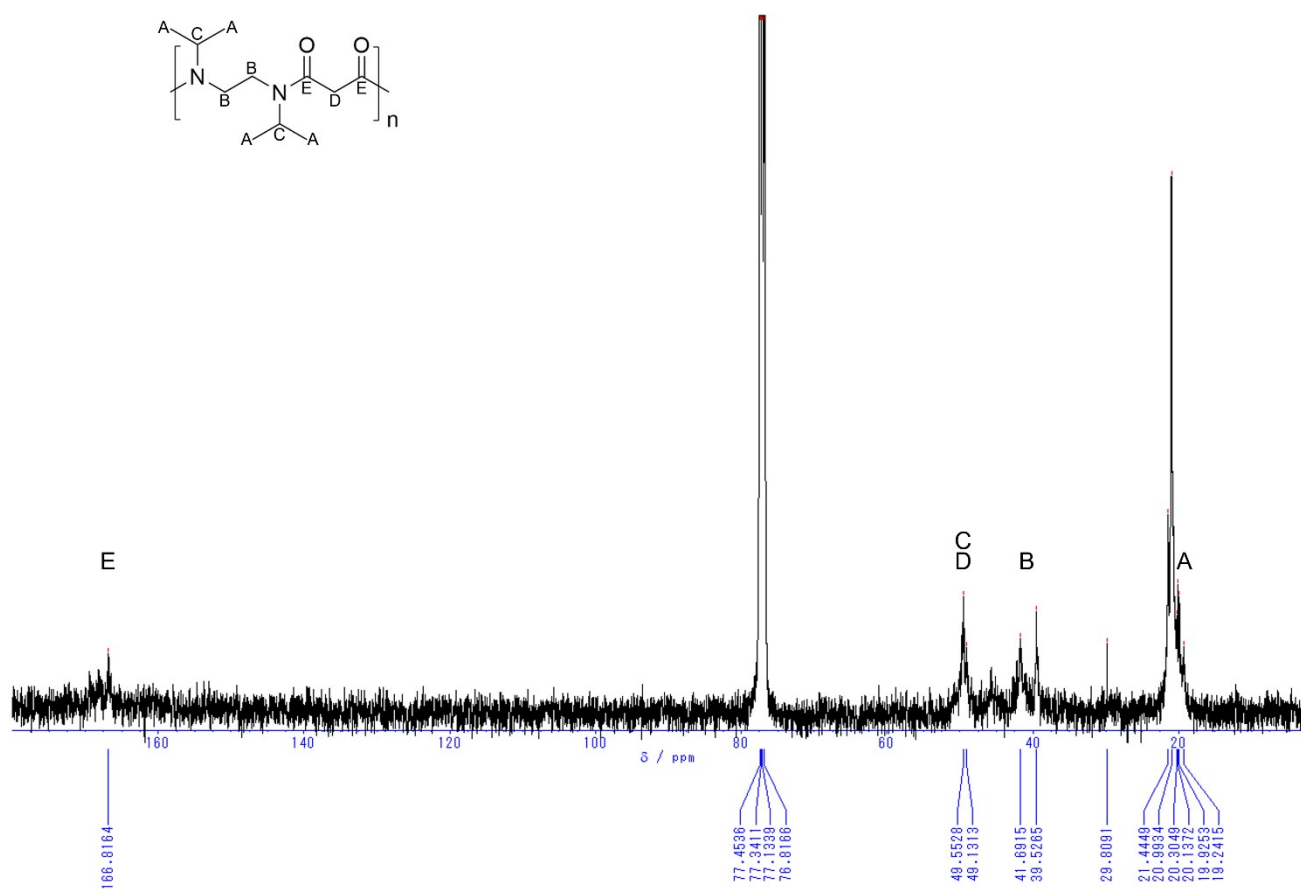


Figure S74. ^{13}C NMR spectrum of *N*-iPr-2,3

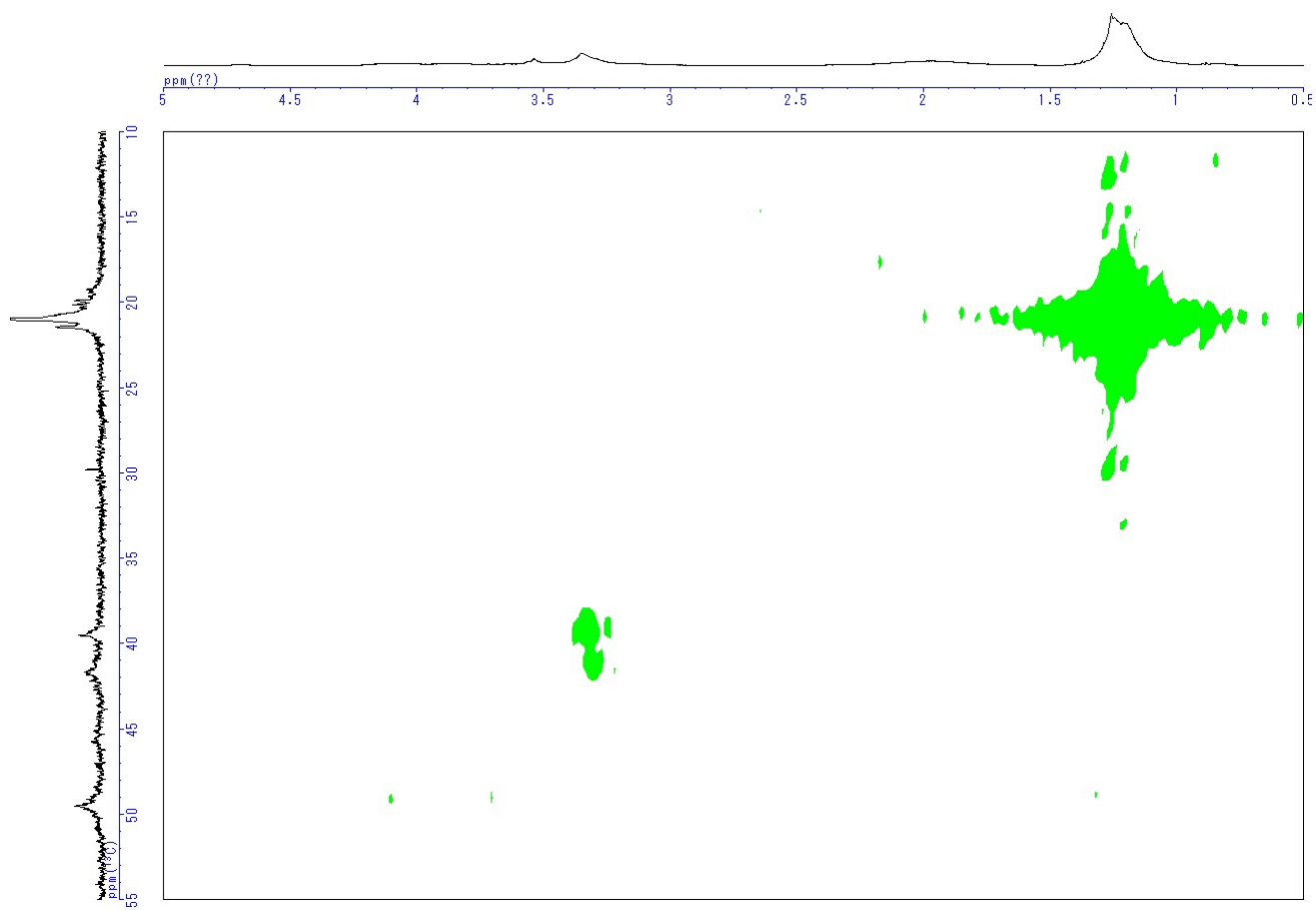


Figure S75. HMQC spectrum of *N-iPr-2,3*

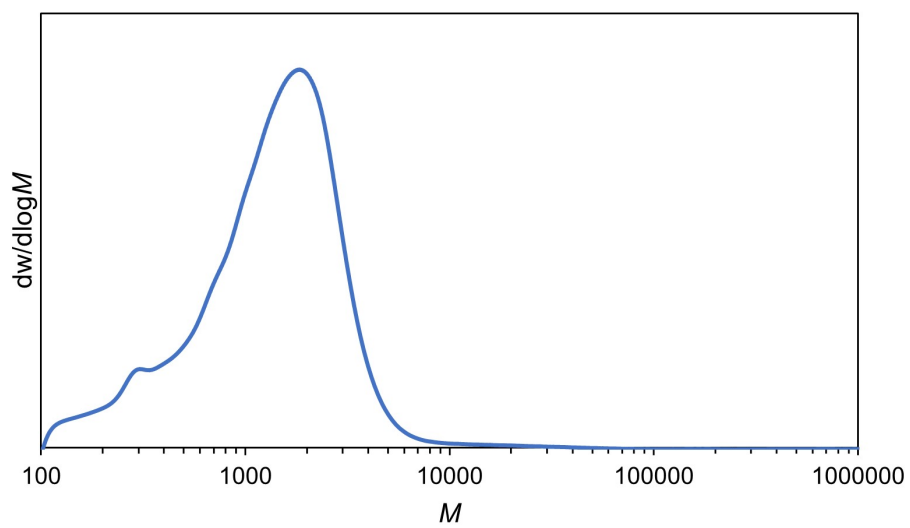


Figure S76. SEC chromatogram of *N-iPr-2,3*

N,N'-di-isopropylnylon-2,4 (*N-iPr-2,4*)

Polymerization of *N,N'*-di-isopropylethylenediamine (361 μL , 2.00 mmol) and Succinyl chloride (226 μL , 2.00 mmol) afforded *N-iPr-2,4* (61.0 mg, 14% yield) as a brown solid.

^1H NMR (CDCl_3 , 400 MHz) δ = 3.93-4.31 (m, 2 H), 3.22-3.45 (m, 4 H), 2.61-2.89 (m, 4 H), 1.12-1.33 (m, 12 H).

^{13}C NMR (CDCl_3 , 100 MHz) δ = 171.7, 48.1, 39.4, 29.0, 21.3, 20.9, 20.5.

SEC (CHCl_3): M_n = 1.3×10^3 , Đ = 1.5.

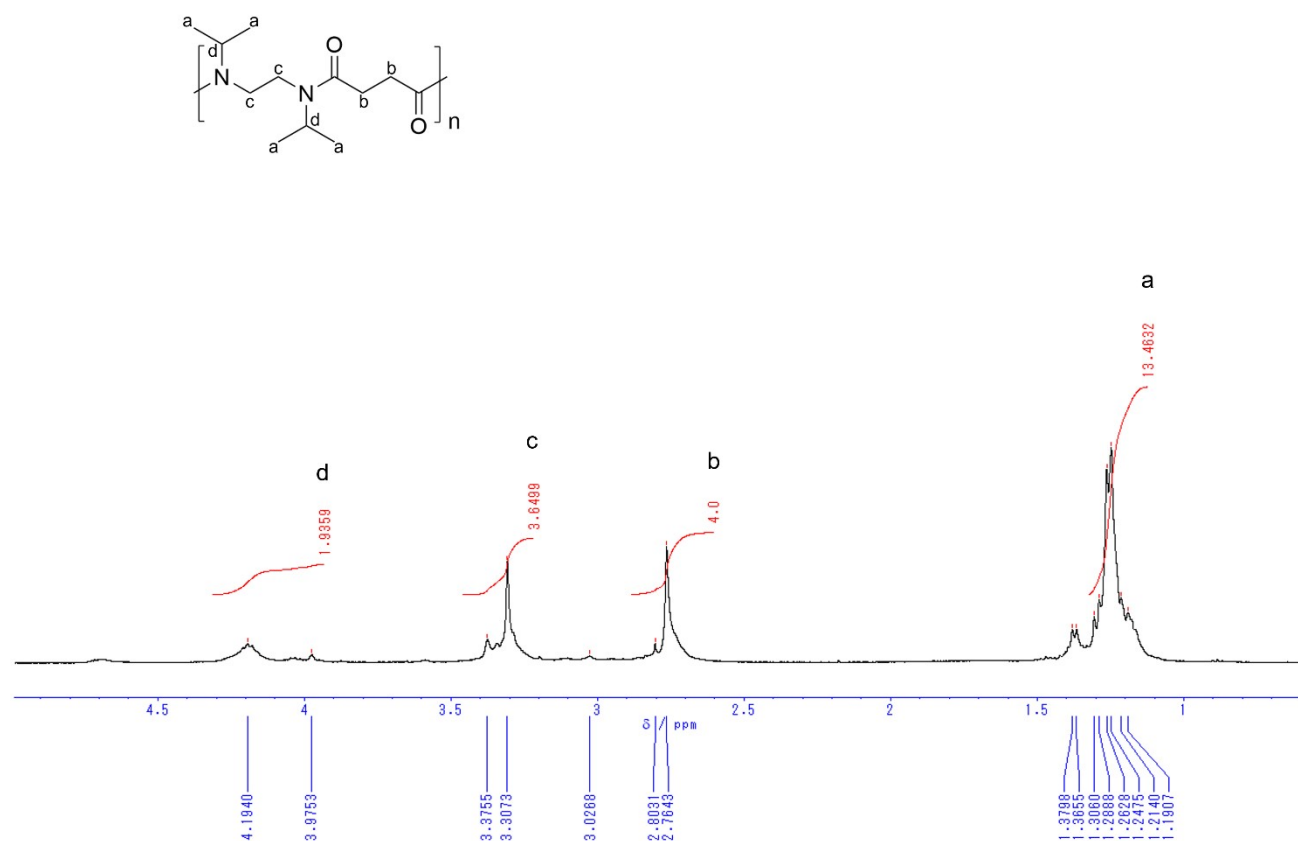


Figure S77. ^1H NMR spectrum of *N-iPr-2,4*

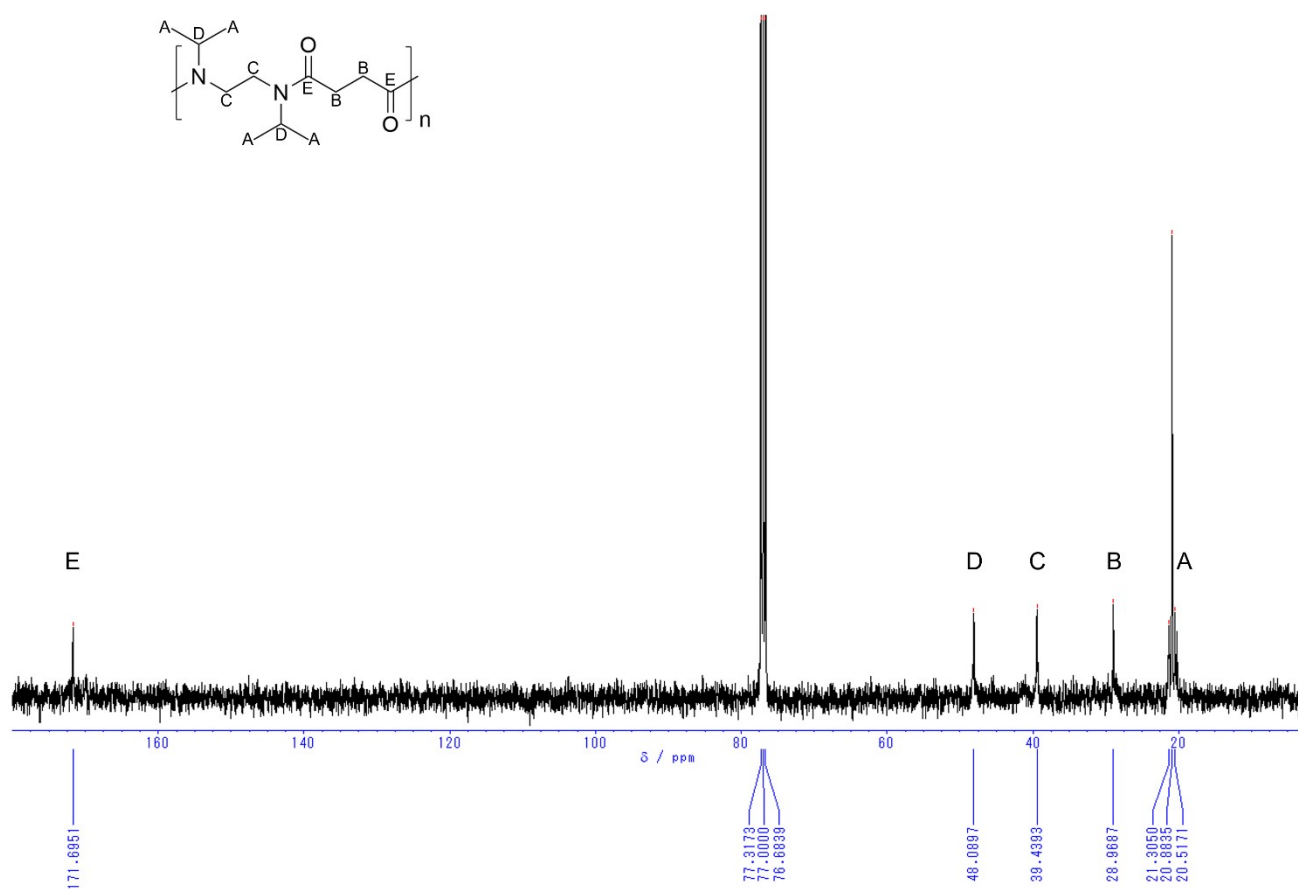


Figure S78. ¹³C NMR spectrum of *N*-iPr-2,4

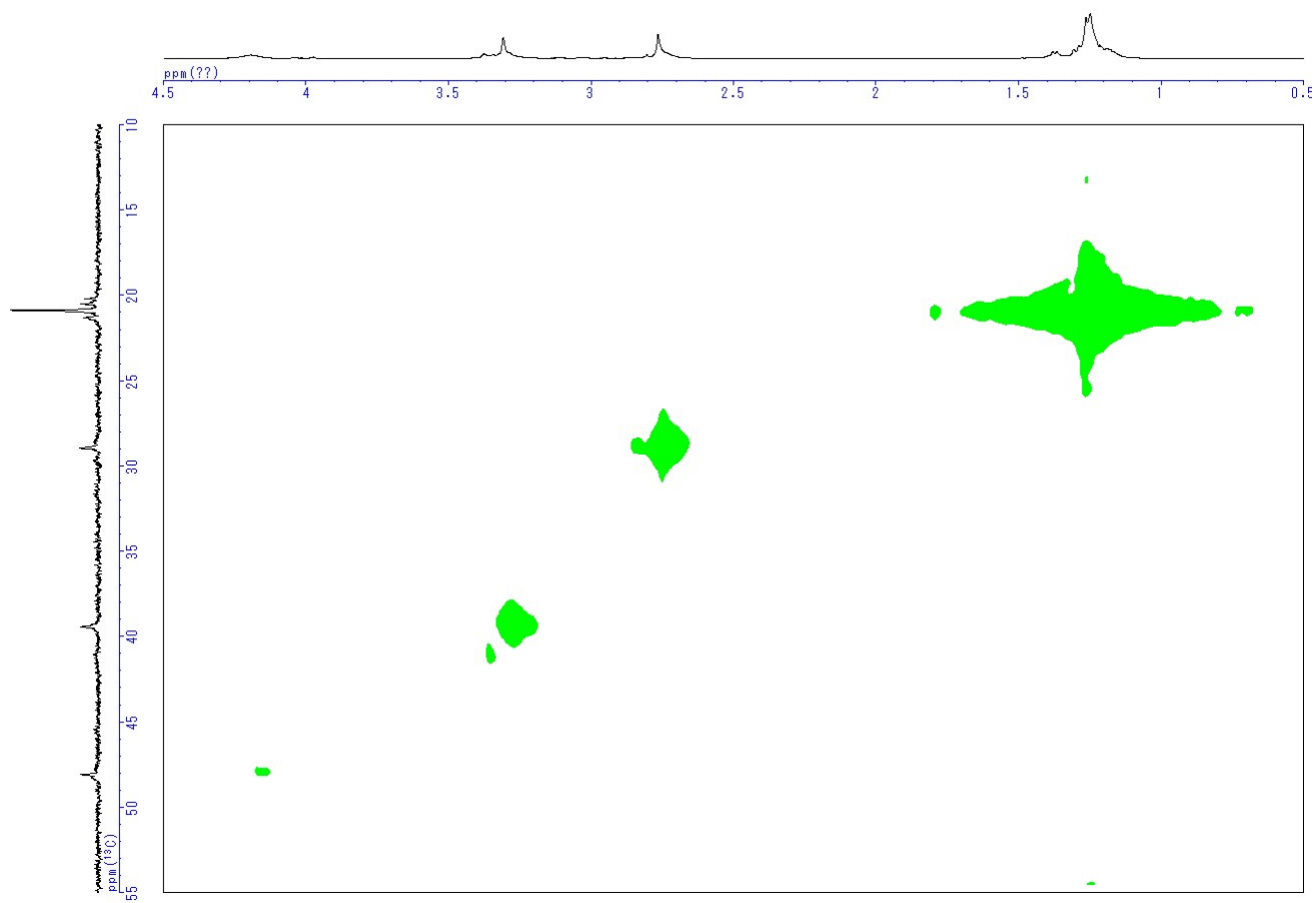


Figure S79. HMQC spectrum of *N-iPr-2,4*

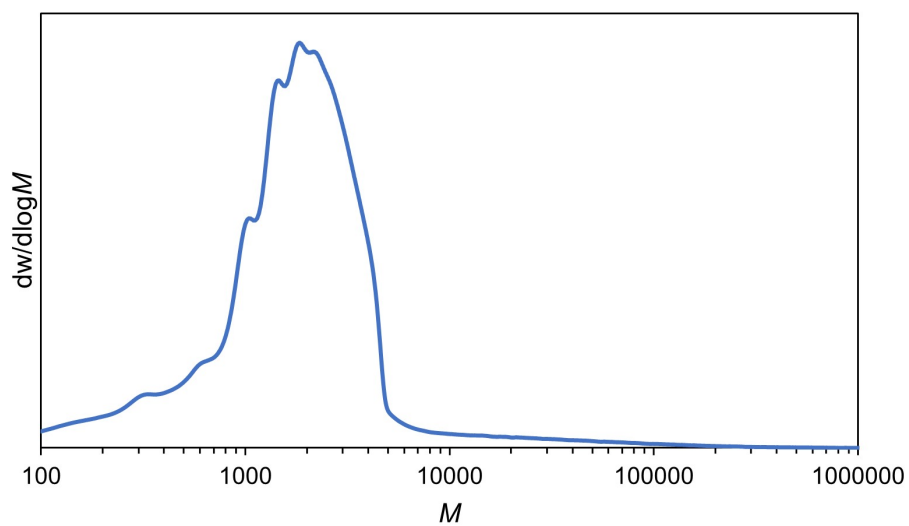


Figure S80. SEC chromatogram of *N-iPr-2,4*

N,N'-di-isopropylnylon-2,5 (*N-iPr-2,5*)

Polymerization of *N,N'*-di-isopropylethylenediamine (361 μL , 2.00 mmol) and Glutaryl chloride (258 μL , 2.00 mmol) afforded *N-iPr-2,5* (324 mg, 67% yield) as a yellow solid.

^1H NMR (CDCl_3 , 400 MHz) δ = 3.99-4.21 (m, 2 H), 3.21-3.37 (m, 4 H), 2.35-2.72 (m, 4 H), 1.91-2.09 (m, 2 H), 1.06-1.33 (m, 12 H).

^{13}C NMR (CDCl_3 , 100 MHz) δ = 172.2, 49.3, 39.3, 33.0, 21.0.

SEC (CHCl_3): M_n = 4.9×10^3 , \mathcal{D} = 1.5.

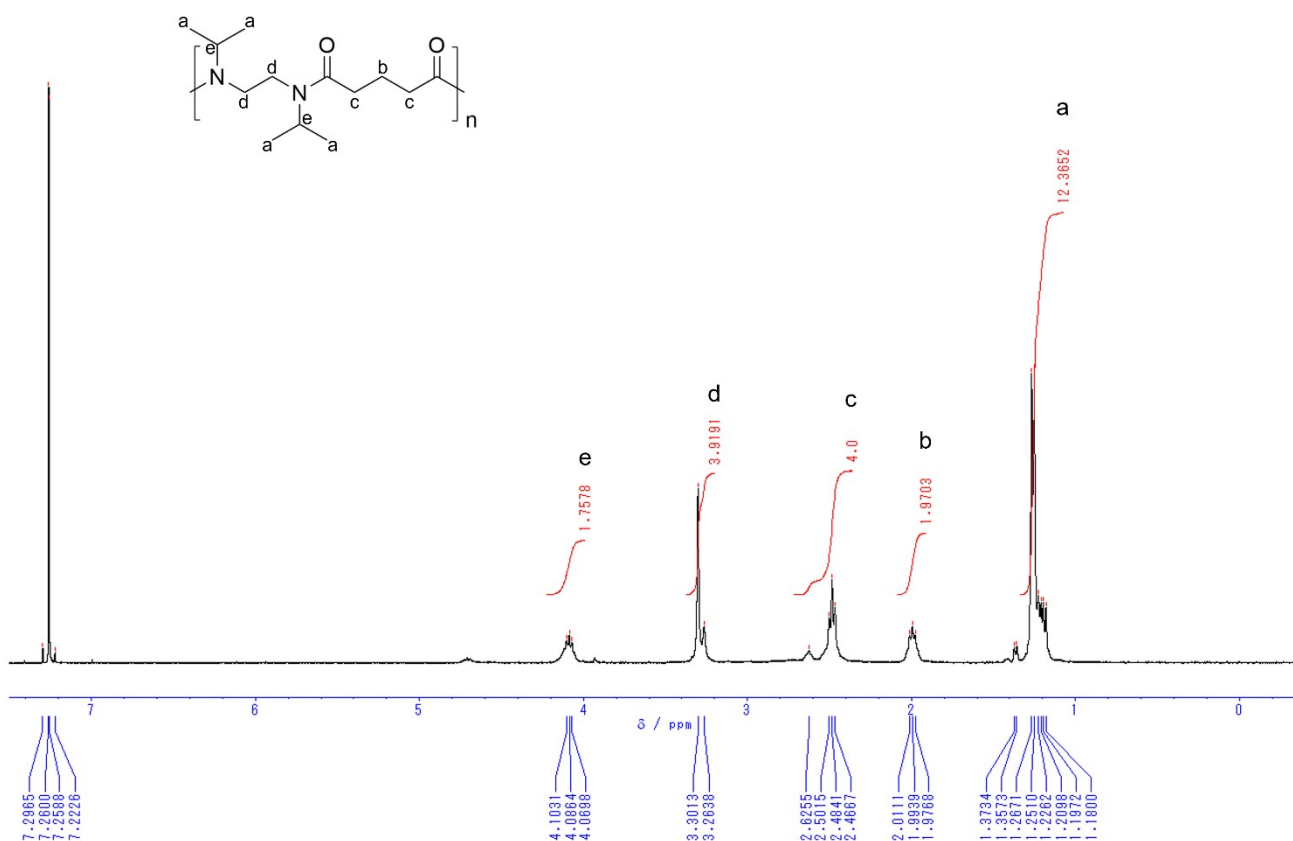


Figure S81. ^1H NMR spectrum of *N-iPr-2,5*

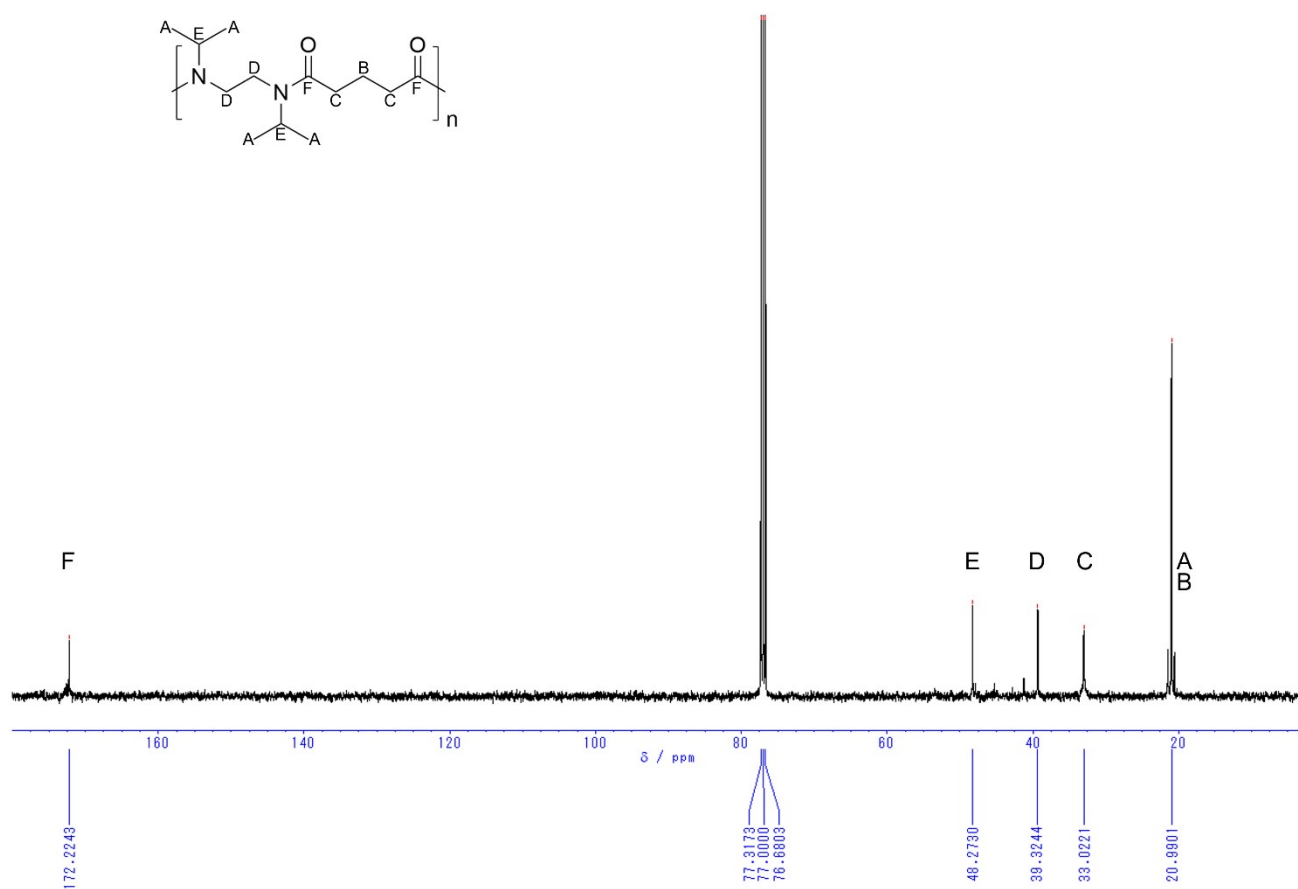


Figure S82. ¹³C NMR spectrum of *N*-iPr-2,5

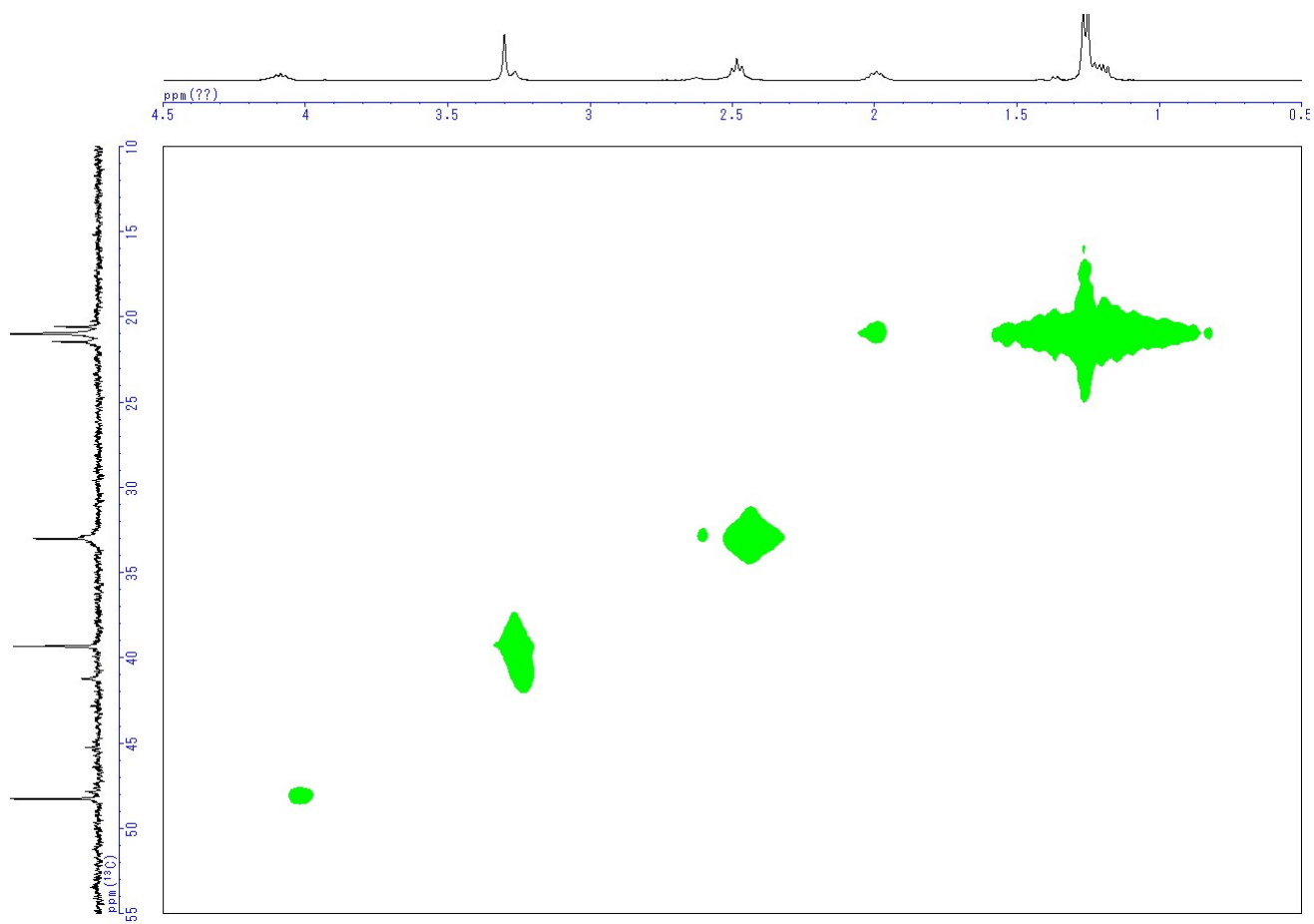


Figure S83. HMQC spectrum of *N-iPr-2,5*

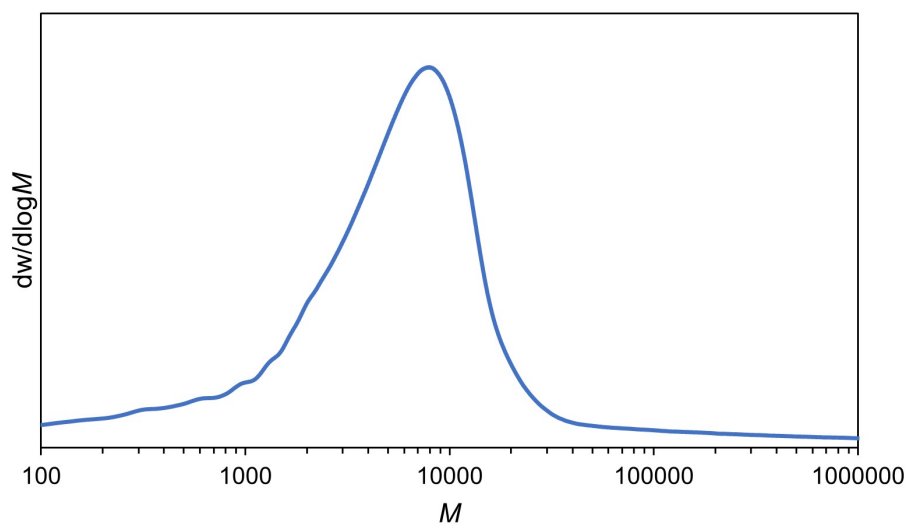


Figure S84. SEC chromatogram of *N-iPr-2,5*

N,N'-di-isopropylnylon-2,6 (*N-iPr-2,6*)

Polymerization of *N,N'*-di-isopropylethylenediamine (361 μL , 2.00 mmol) and Adipoyl chloride (291 μL , 2.00 mmol) afforded *N-iPr-2,6* (445 mg, 88% yield) as a white solid.

^1H NMR (CDCl_3 , 400 MHz) δ = 3.92-4.16 (m, 2 H), 3.17-3.39 (m, 4 H), 2.26-2.61 (m, 4 H), 1.54-1.82 (m, 4 H), 1.13-1.32 (m, 12 H).

^{13}C NMR (CDCl_3 , 100 MHz) δ = 172.4, 48.3, 39.4, 33.5, 25.1, 21.4, 20.9.

SEC (CHCl_3): M_n = 3.8×10^3 , \bar{D} = 2.4.

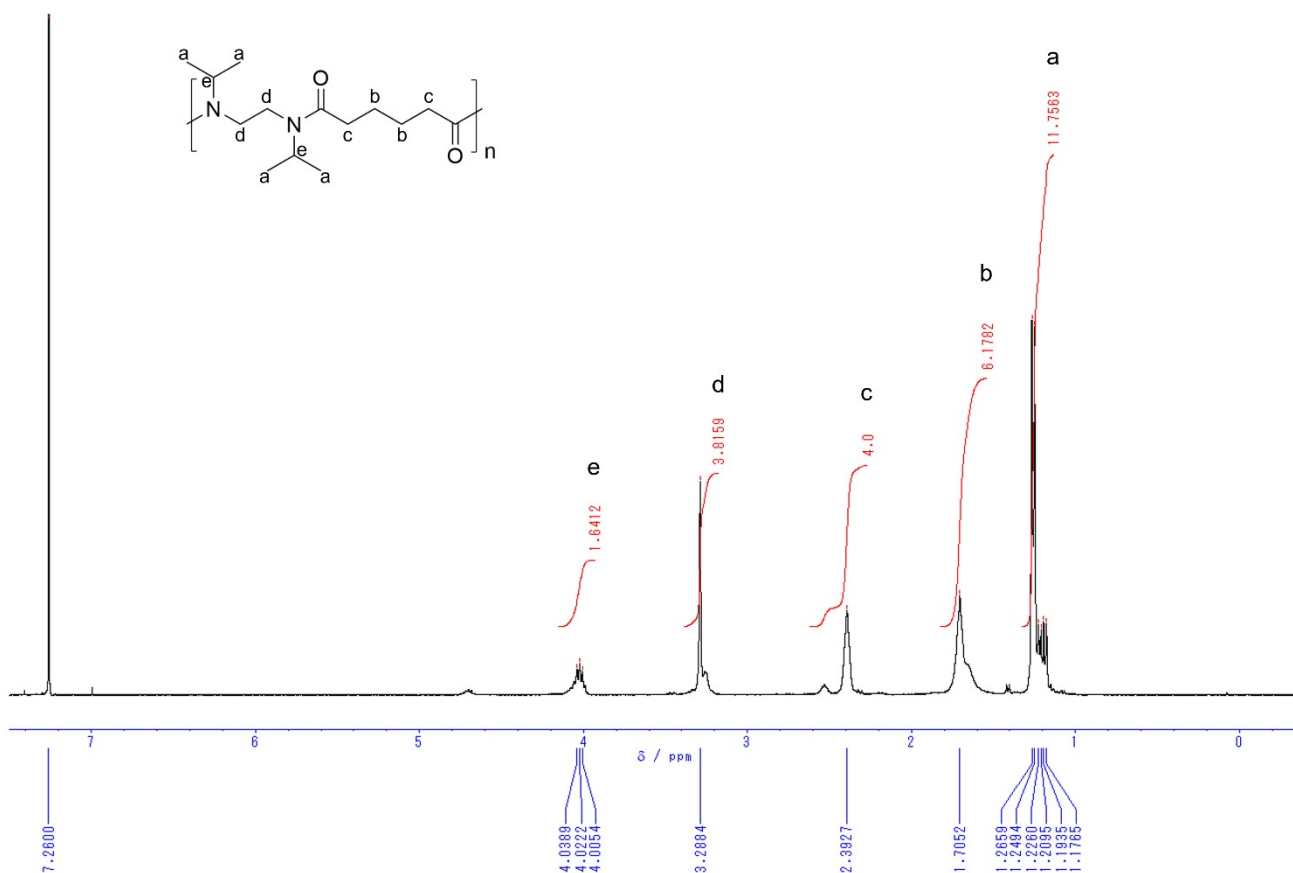


Figure S85. ^1H NMR spectrum of *N-iPr-2,6*

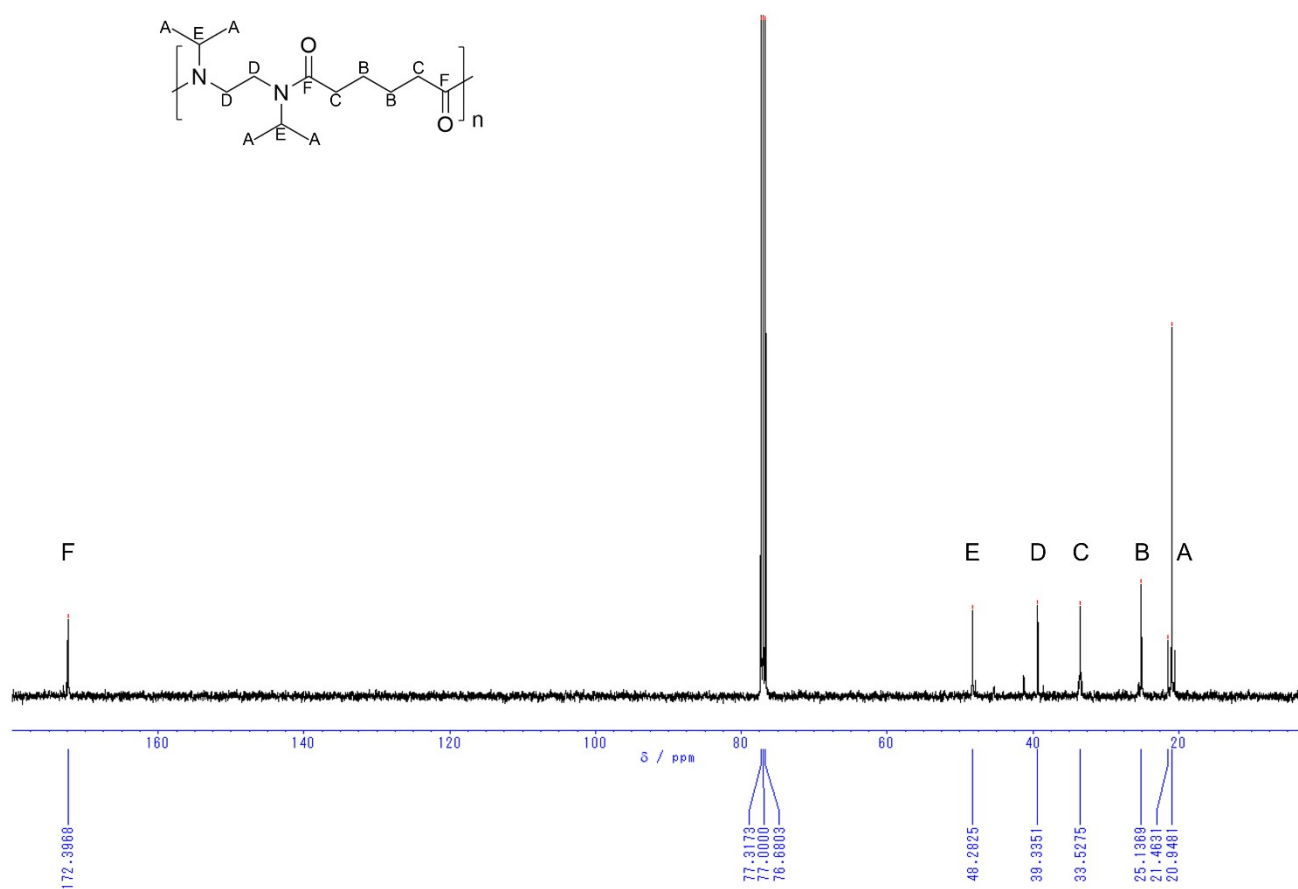


Figure S86. ¹³C NMR spectrum of *N*-iPr-2,6

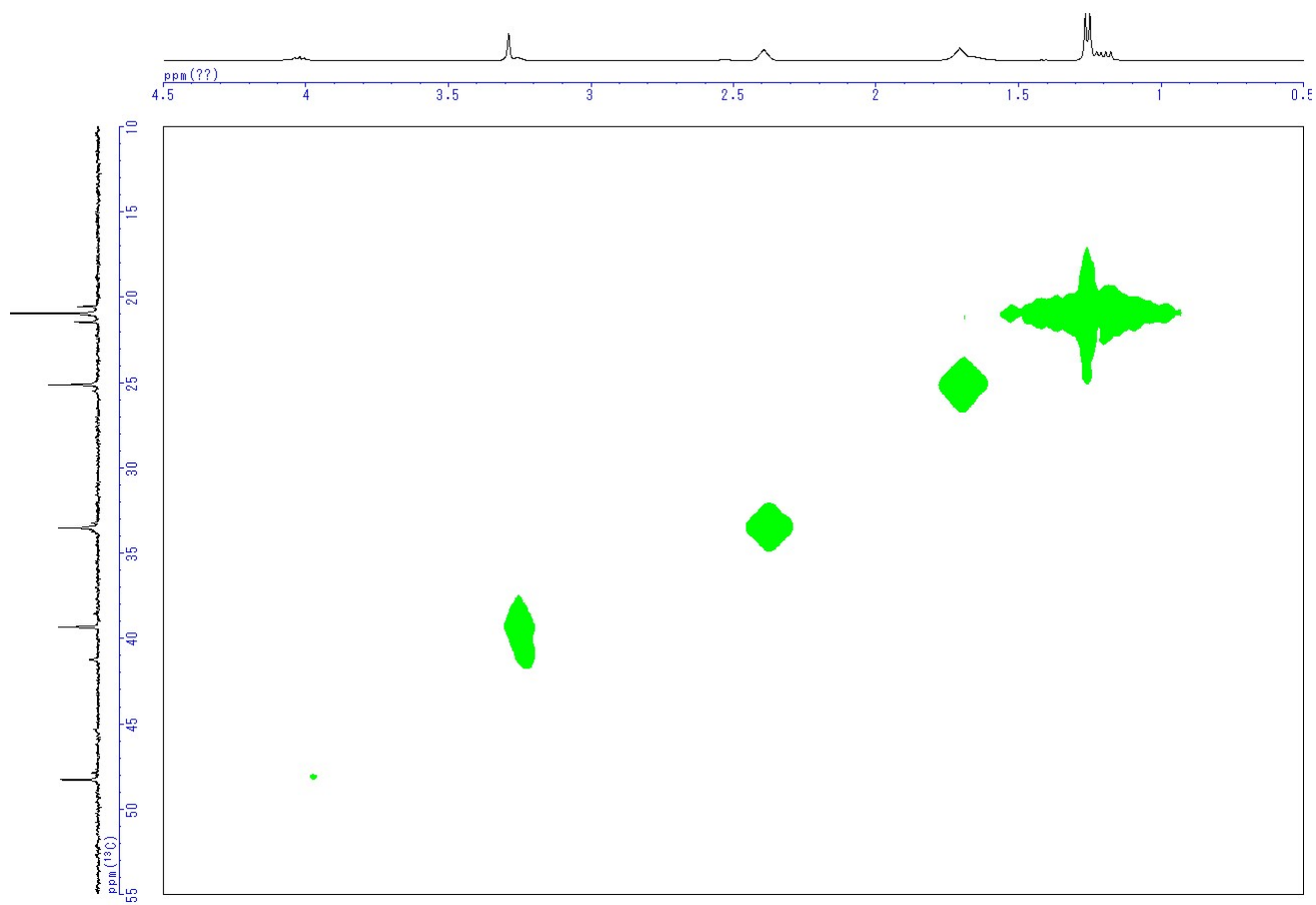


Figure S87. HMQC spectrum of *N-iPr-2,6*

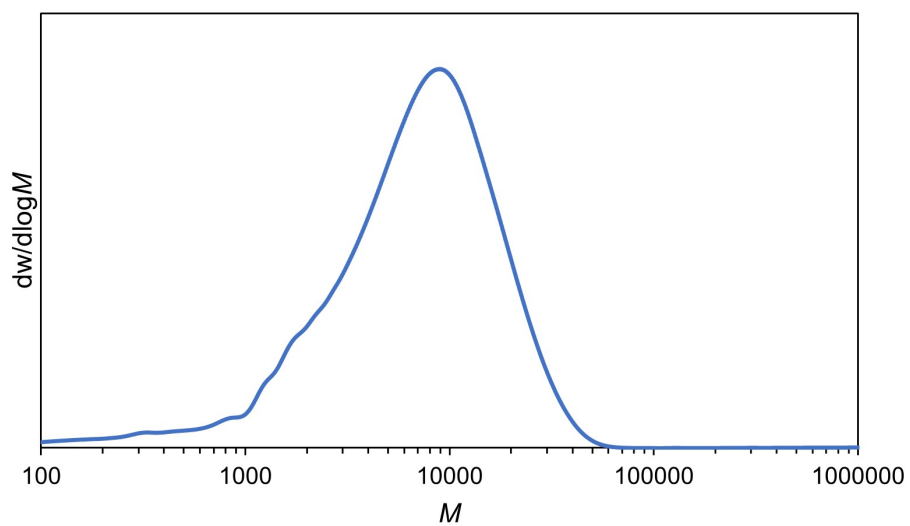


Figure S88. SEC chromatogram of *N-iPr-2,6*

N,N'-dimethylnylon-4,Me-5 (*N*-Me-4,Me-5)

Polymerization of *N,N'*-dimethyl-1,4-butanediamine (265 μ L, 1.82 mmol) and 3-Methyl-glutaryl chloride (264 μ L, 1.82 mmol) afforded *N*-Me-4,Me-5 (276 mg, 67% yield) as a yellow solid.

^1H NMR (CDCl_3 , 400 MHz) δ = 3.20-3.57 (m, 4 H), 2.80-3.11 (m, 6 H), 1.99-2.61 (m, 5 H), 1.33-1.74 (m, 4 H), 0.93-1.17 (m, 3 H).

^{13}C NMR (CDCl_3 , 100 MHz) δ = 171.9, 49.7, 47.4, 40.7, 35.6, 25.8, 24.6, 24.5, 20.4, 20.4.

SEC (CHCl_3): M_n = 6.4×10^3 , \mathcal{D} = 1.8.

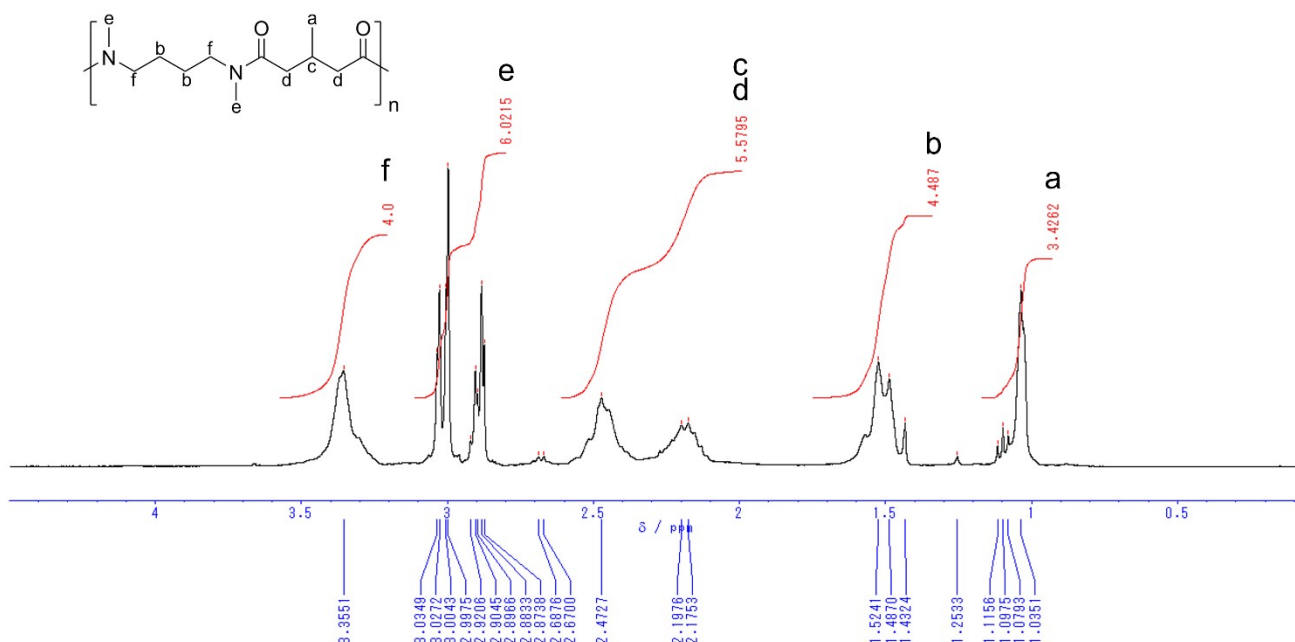


Figure S89. ^1H NMR spectrum of *N*-Me-4,Me-5

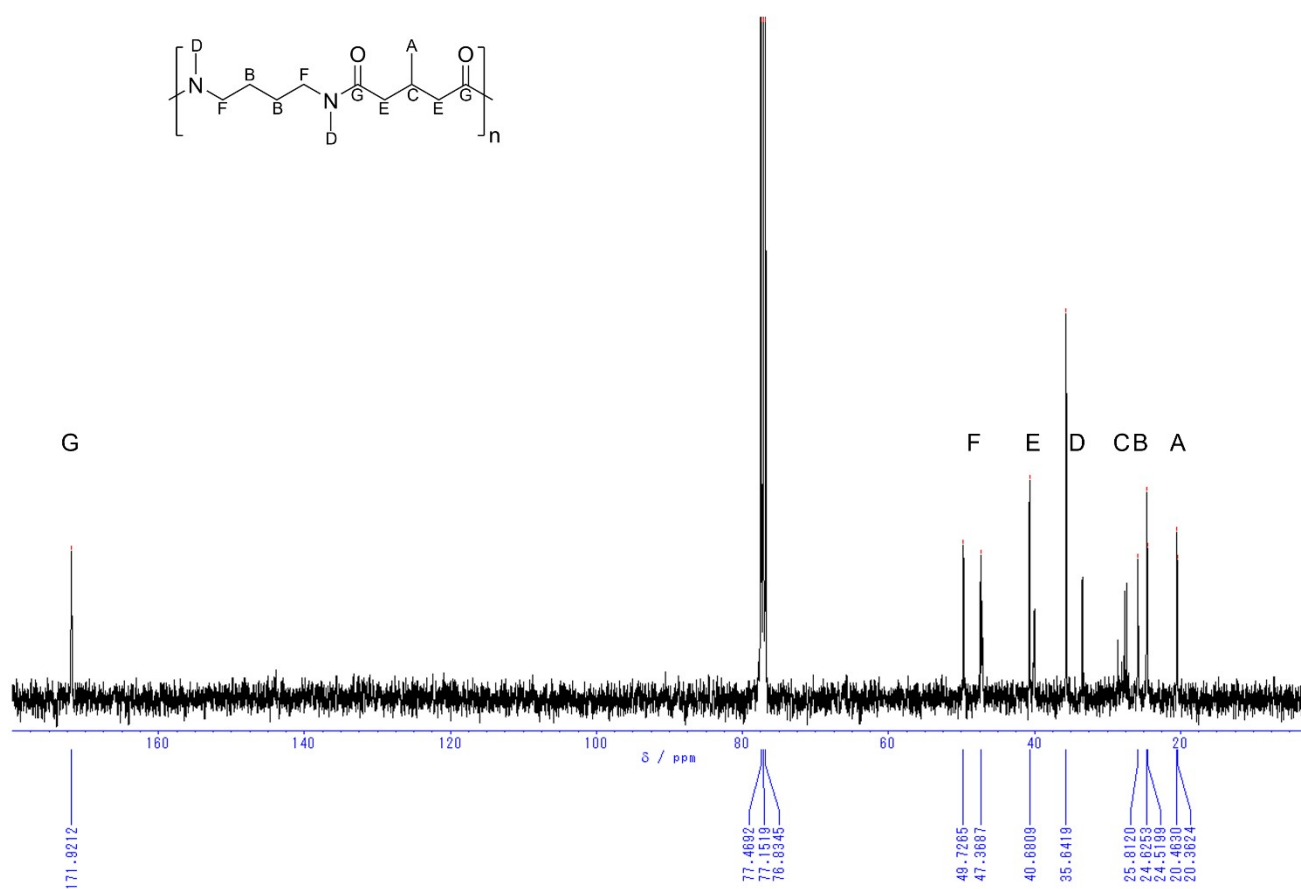


Figure S90. ¹³C NMR spectrum of N-Me-4,Me-5

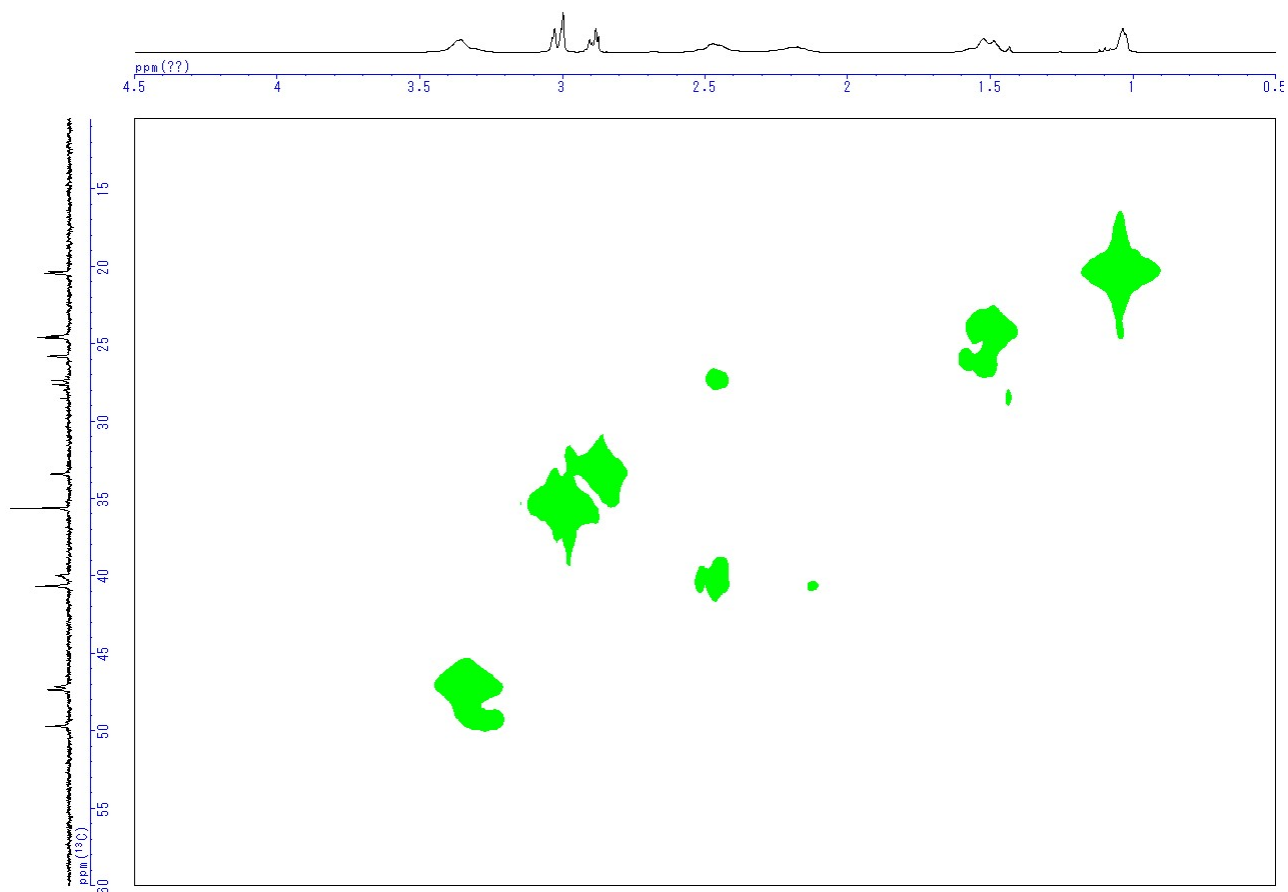


Figure S91. HMQC spectrum of *N*-Me-4,Me-5

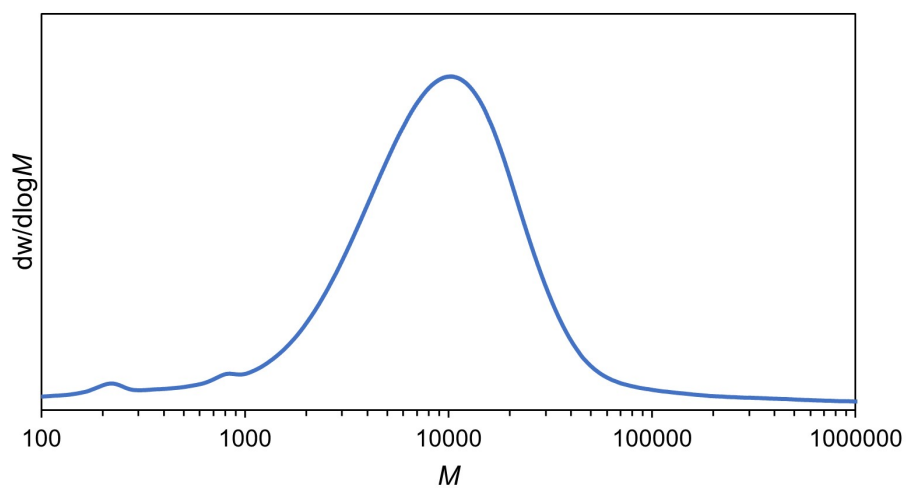


Figure S92. SEC chromatogram of *N*-Me-4,Me-5

N,N'-diethylnylon-2,Me-5 (*N*-Et-2,Me-5)

Polymerization of *N,N'*-diethylethylenediamine (287 μ L, 2.00 mmol) and 3-Methyl Glutaryl chloride (291 μ L, 2.00 mmol) afforded *N*-Et-2,Me-5 (295 mg, 65% yield) as a yellow solid.

^1H NMR (CDCl_3 , 400 MHz) δ = 3.21-3.73 (m, 8 H), 1.87-2.58 (m, 5 H), 1.07-1.23 (m, 6 H), 0.93-1.87 (m, 3 H).

^{13}C NMR (CDCl_3 , 100 MHz) δ = 171.8, 45.0, 43.7, 43.5, 39.8, 27.8, 20.4, 14.5, 13.2.

SEC (CHCl_3): M_n = 6.1×10^3 , D = 1.6.

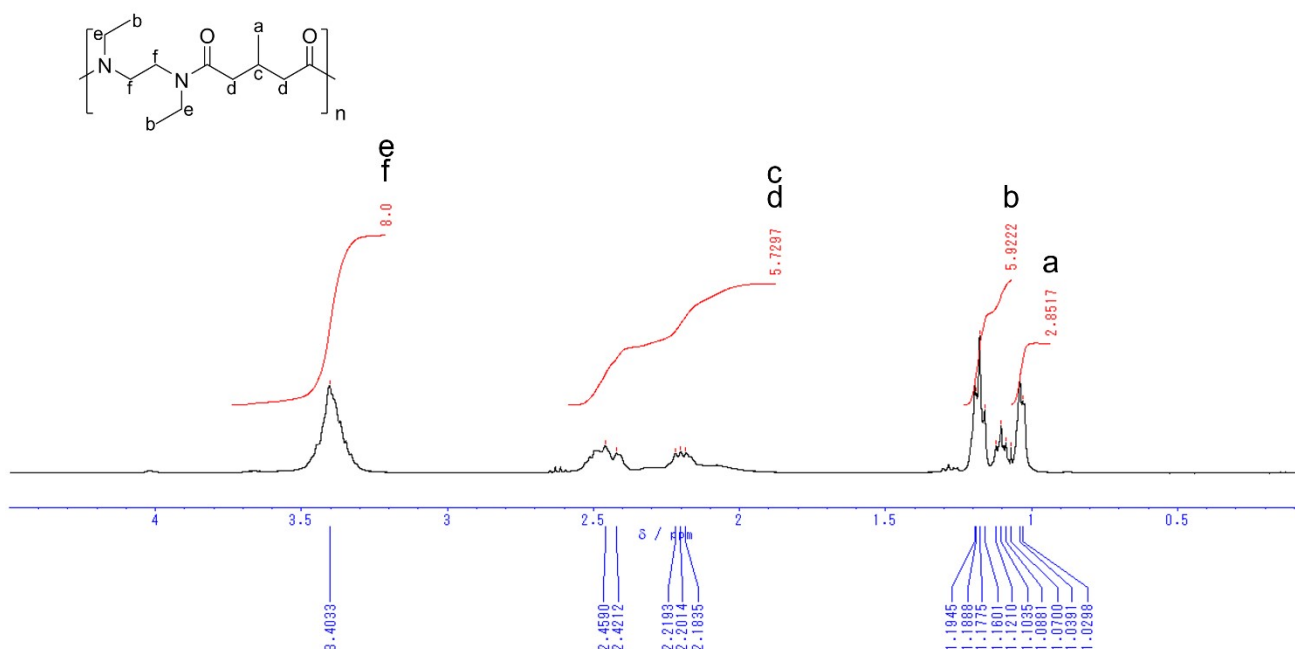


Figure S93. ^1H NMR spectrum of *N*-Et-2,Me-5

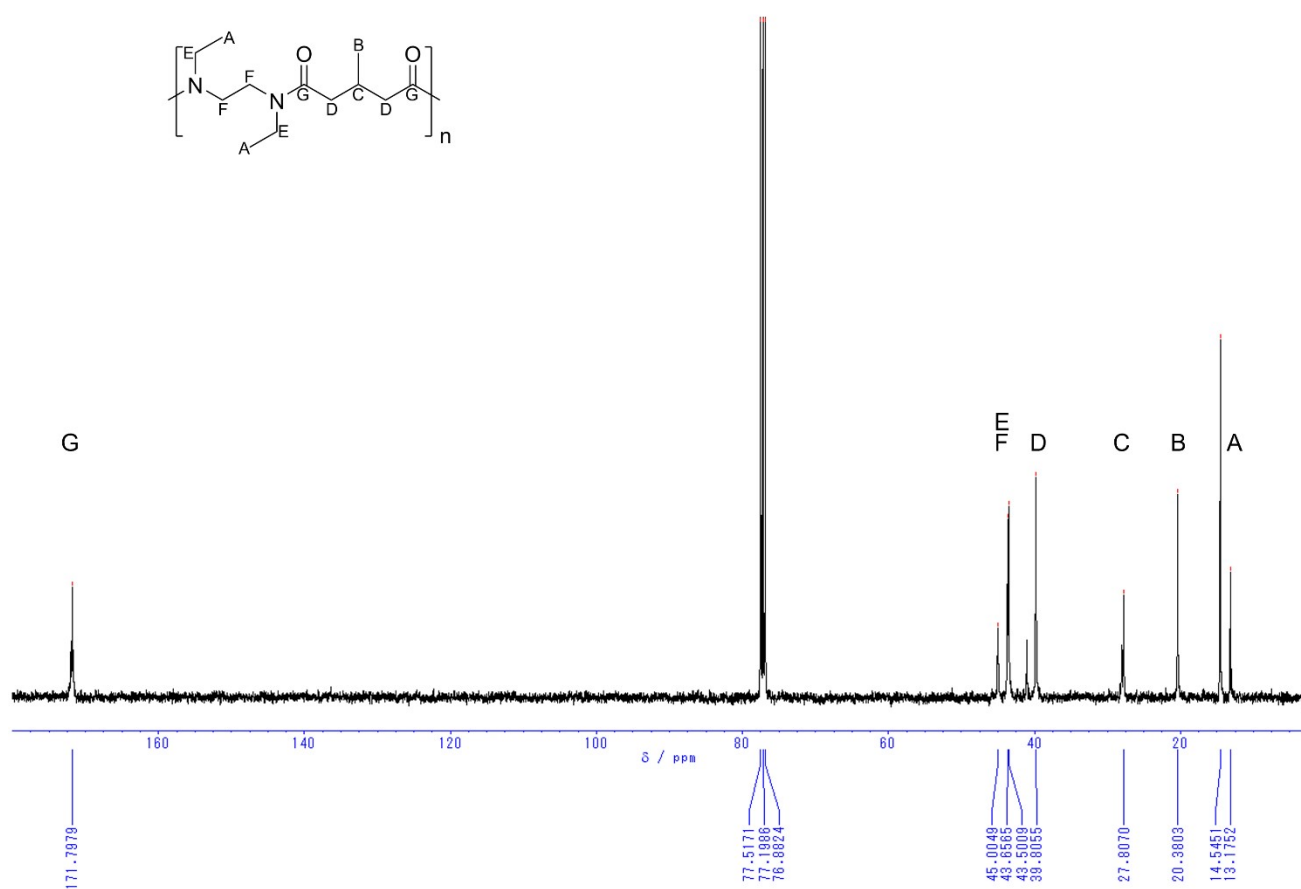


Figure S94. ^{13}C NMR spectrum of *N*-Et-2,Me-5

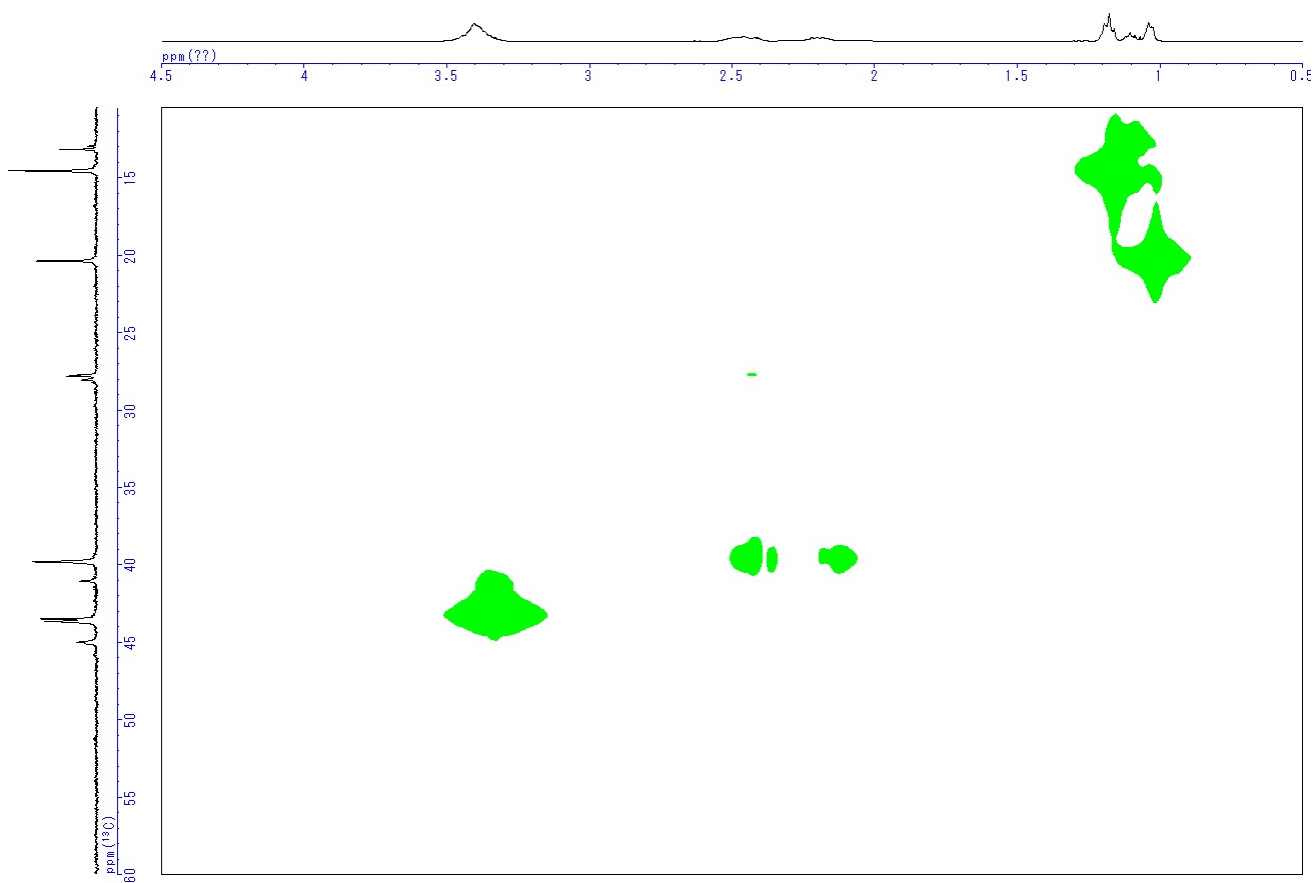


Figure S95. HMQC spectrum of *N*-Et-2,Me-5

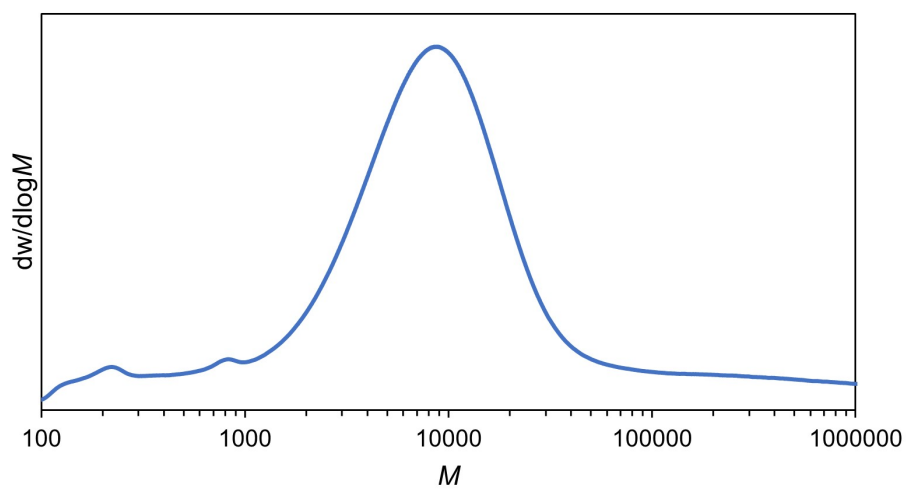


Figure S96. SEC chromatogram of *N*-Me-4,Me-5

***N,N'*-dimethylnylon-2,6-*ran*-*N,N'*-dimethylnylon-2,10 (*N*-Me-2,6-*ran*-*N*-Me-2,10)**

Polymerization of *N,N'*-dimethylethylenediamine (215 μ L, 2.00 mmol), Adipoyl chloride (145 μ L, 1.00 mmol) and Sebacoyl chloride (214 μ L, 1.00 mmol) afforded *N*-Me-2,6-*ran*-*N*-Me-2,10 (121mg, 27% yield) as a yellow solid.

^1H NMR (CDCl_3 , 400 MHz) δ = 3.31-3.66 (m, 4 H), 2.78-3.16 (m, 6 H), 2.09-2.48 (m, 4 H), 1.41-1.86 (m, 4 H), 1.13-1.41 (m, 4 H).

^{13}C NMR (CDCl_3 , 100 MHz) δ = 173.1, 172.7, 46.8, 46.6, 44.4, 44.3, 36.5, 35.5, 33.5, 32.9, 32.3, 29.1, 29.0, 25.2, 24.6, 24.5, 24.4.

SEC (CHCl_3): M_n = 1.9×10^4 , Đ = 1.6.

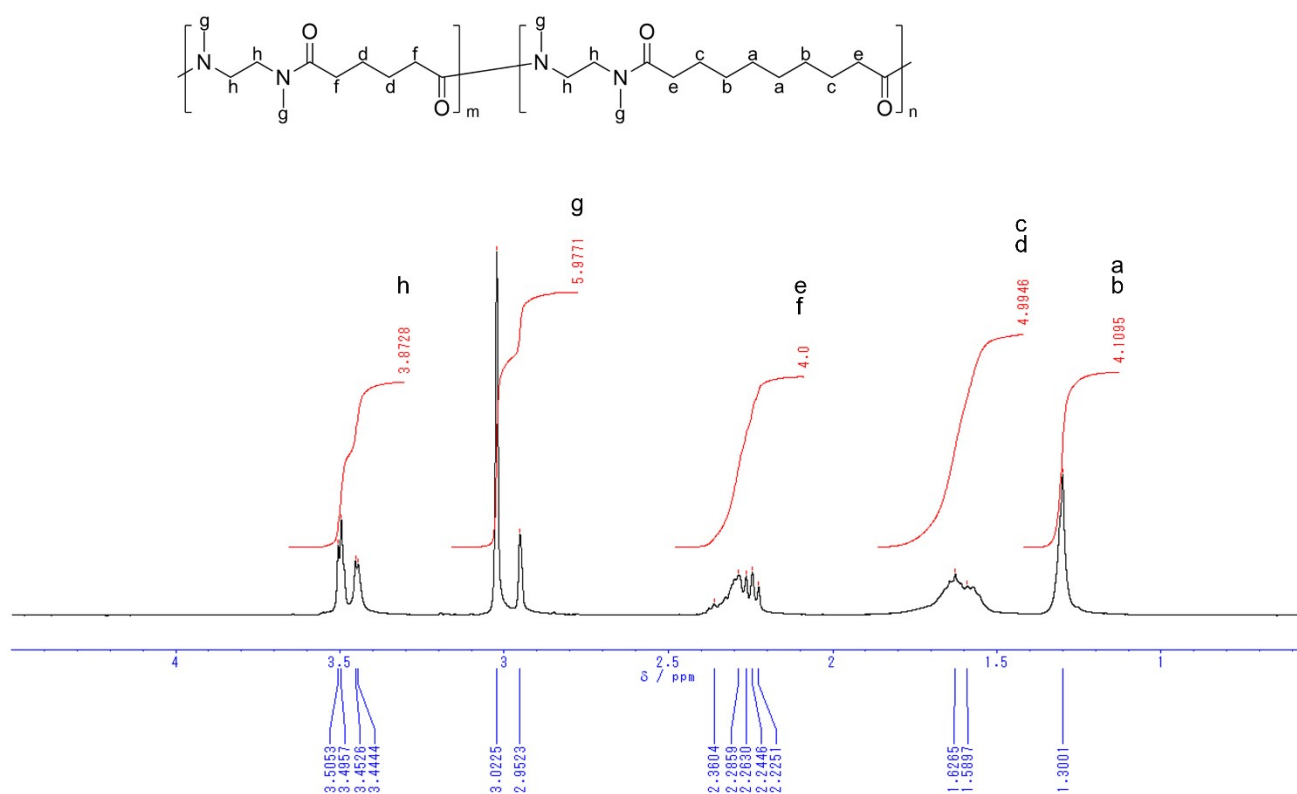


Figure S97. ^1H NMR spectrum of *N*-Me-2,6-*ran*-*N*-Me-2,10

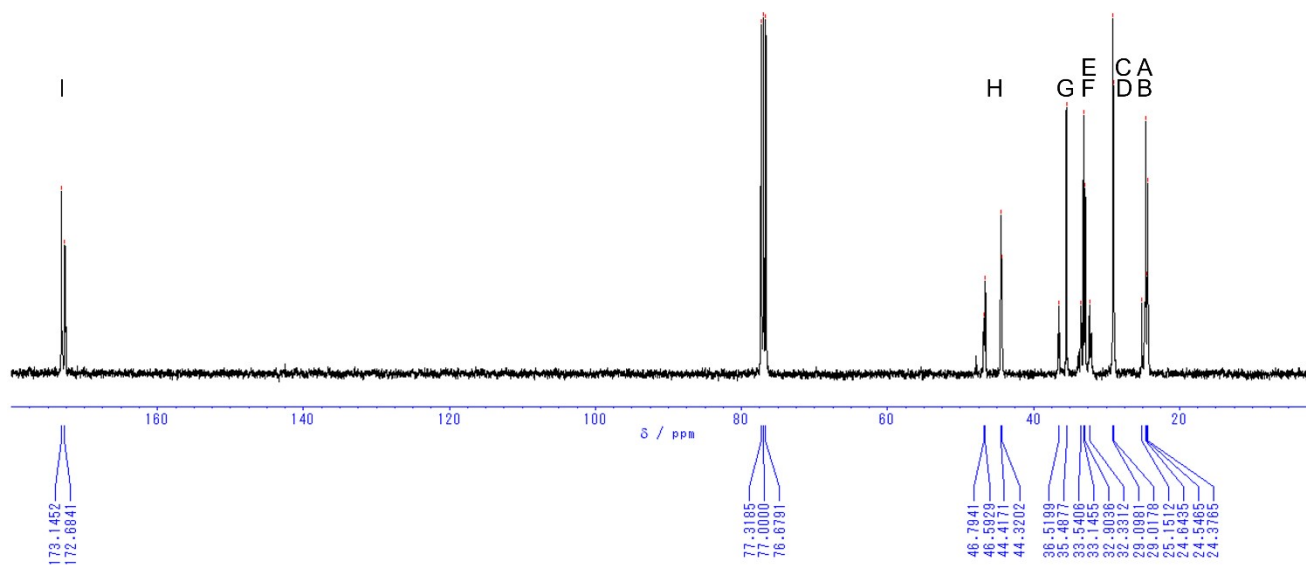
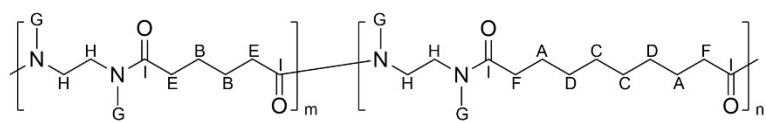


Figure S98. ^{13}C NMR spectrum of *N*-Me-2,6-*ran*-*N*-Me-2,10

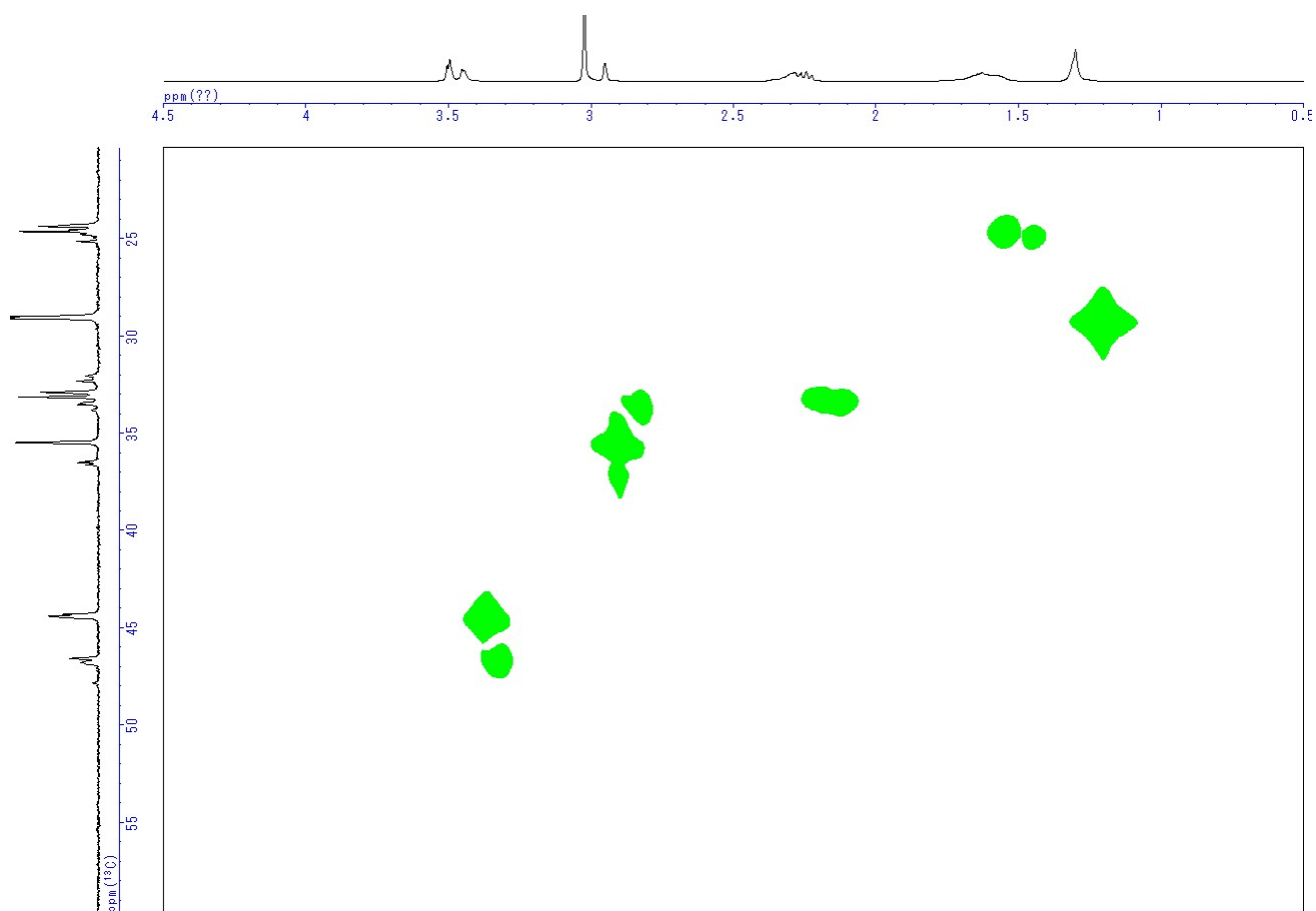


Figure S99. HMQC spectrum of *N*-Me-2,6-*ran*-*N*-Me-2,10

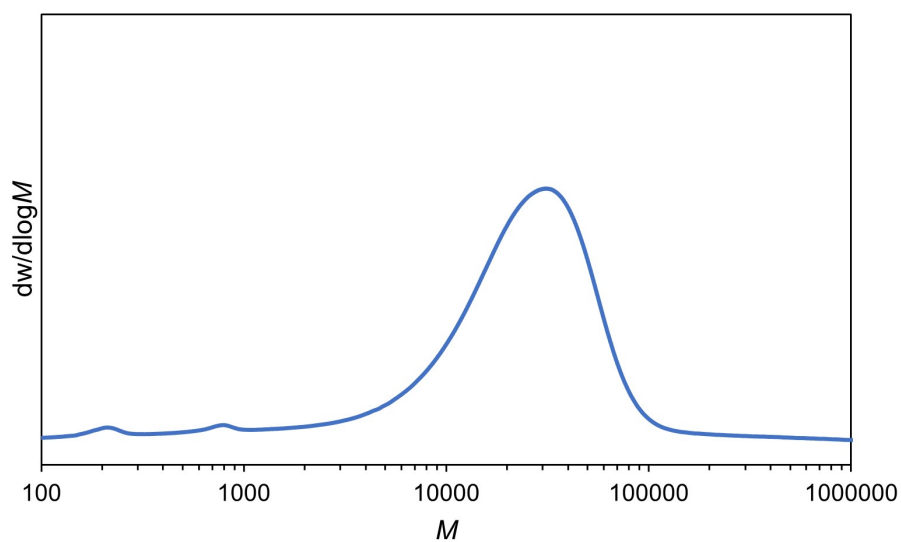


Figure S100. SEC chromatogram of *N*-Me-2,6-*ran*-*N*-Me-2,10

***N,N'*-diethylnylon-2,4-*ran*-*N,N'*-diethylnylon-2,8 (*N*-Et-2,4-*ran*-*N*-Et-2,8)**

Polymerization of *N,N'*-diethylethylenediamine (287 μ L, 2.00 mmol), Succinyl chloride (113 μ L, 1.00 mmol) and Suberoyl chloride (180 μ L, 1.00 mmol) afforded *N*-Et-2,4-*ran*-*N*-Et-2,8 (89.2 mg, 20% yield) as a brown solid.

^1H NMR (CDCl_3 , 400 MHz) δ = 3.25-3.55 (m, 4 H), 2.59-2.77 (m, 6 H), 2.21-2.41 (m, 4 H), 1.51-1.75 (m, 4 H), 1.29-1.44 (m, 4 H), 0.97-1.29 (m, 4 H).

^{13}C NMR (CDCl_3 , 100 MHz) δ = 173.0, 171.8, 45.0, 43.9, 43.4, 33.0, 29.5, 28.1, 25.3, 14.5, 14.3, 13.2.

SEC (CHCl_3): M_n = 5.5×10^3 , D = 1.5.

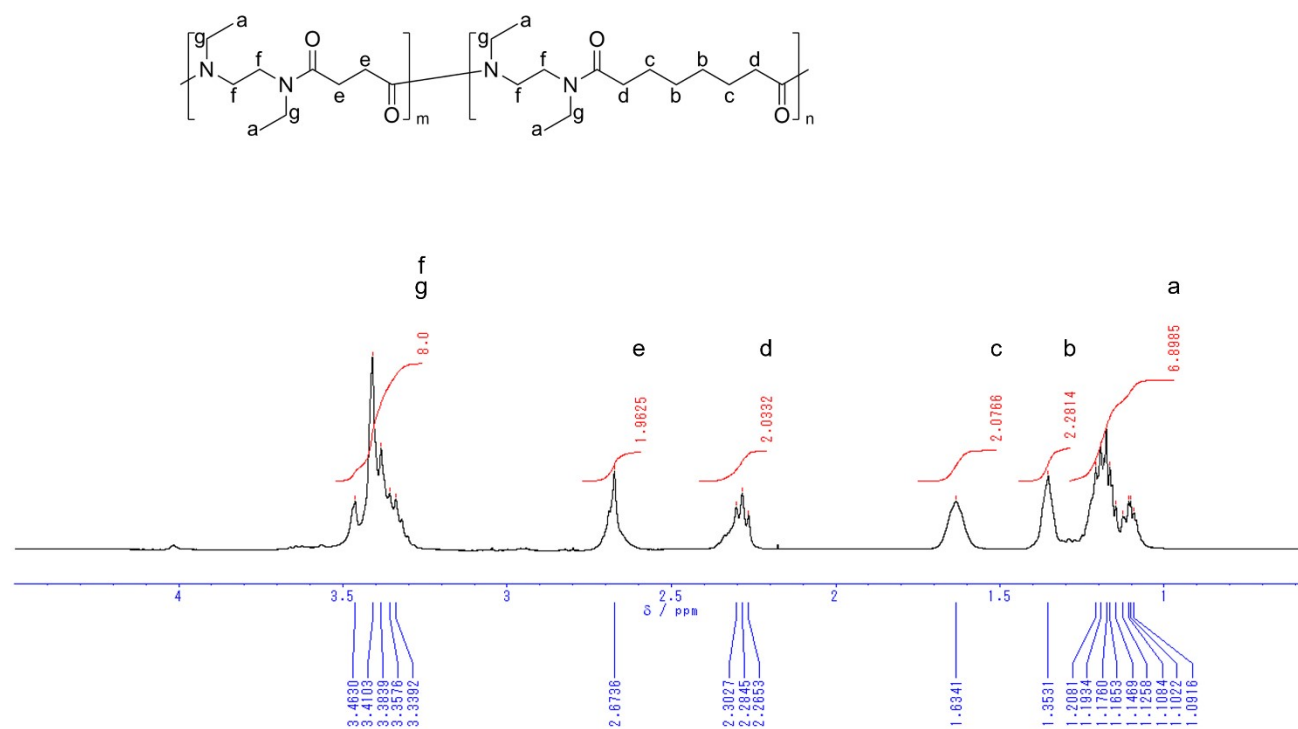


Figure S101. ^1H NMR spectrum of *N*-Et-2,4-*ran*-*N*-Et-2,8

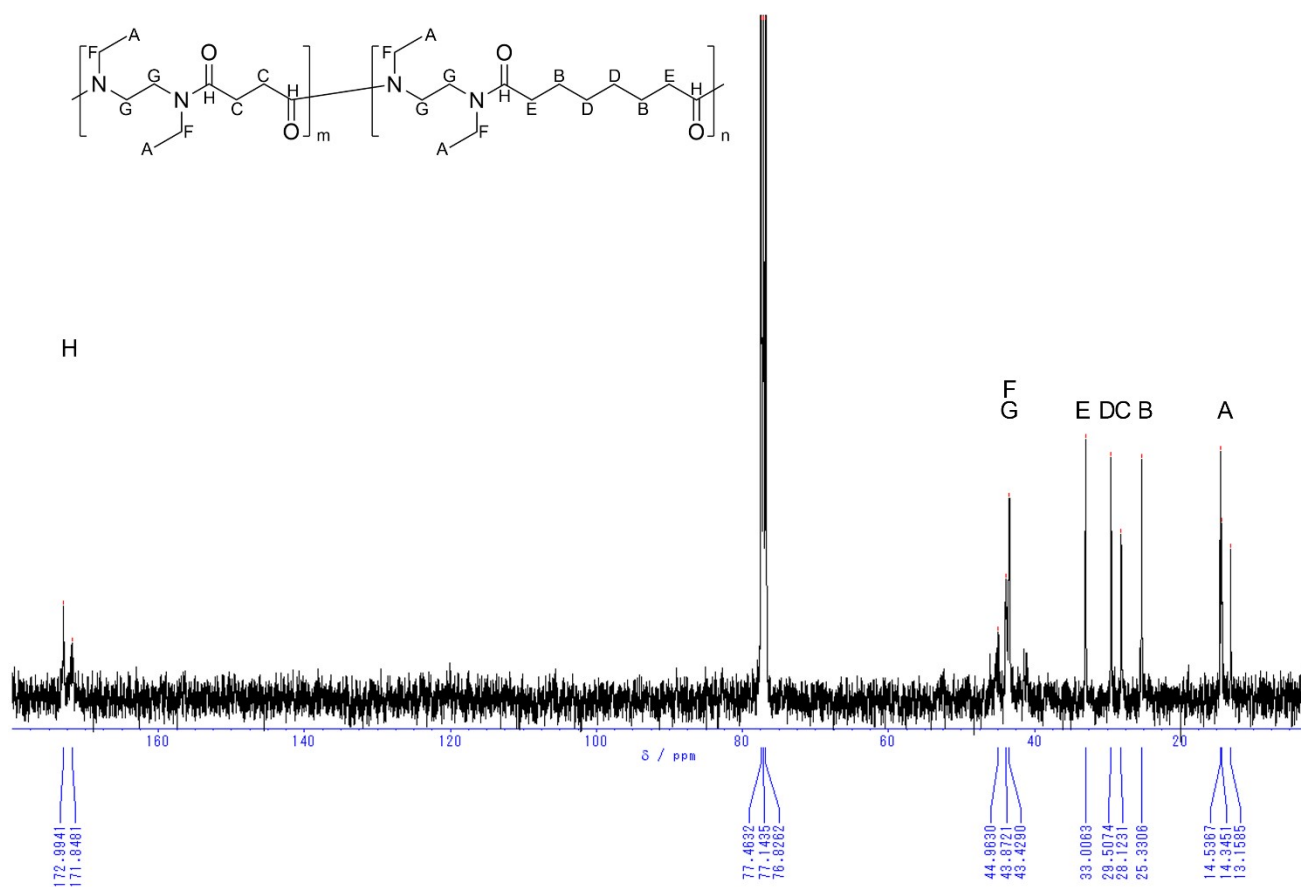


Figure S102. ^{13}C NMR spectrum of N -Et-2,4-*ran*- N -Et-2,8

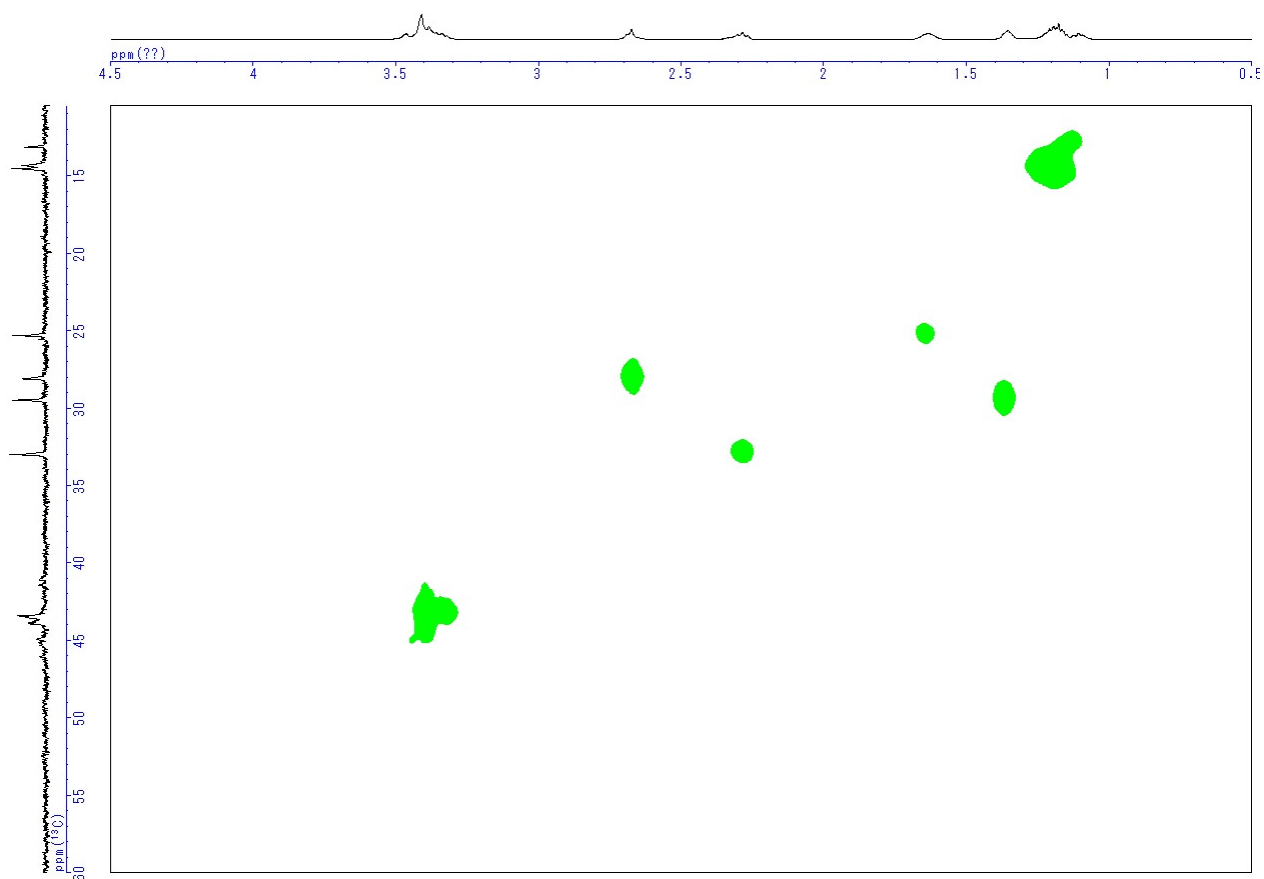


Figure S103. HMQC spectrum of *N*-Et-2,4-*ran*-*N*-Et-2,8

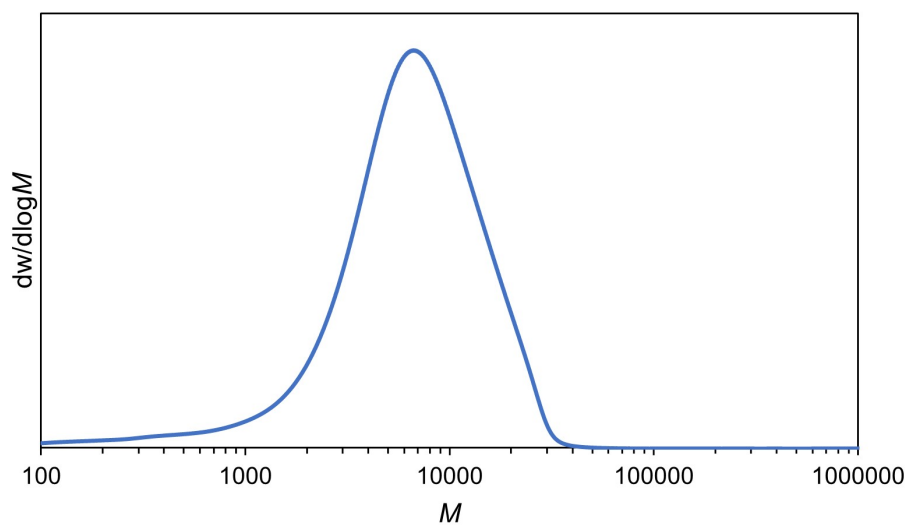
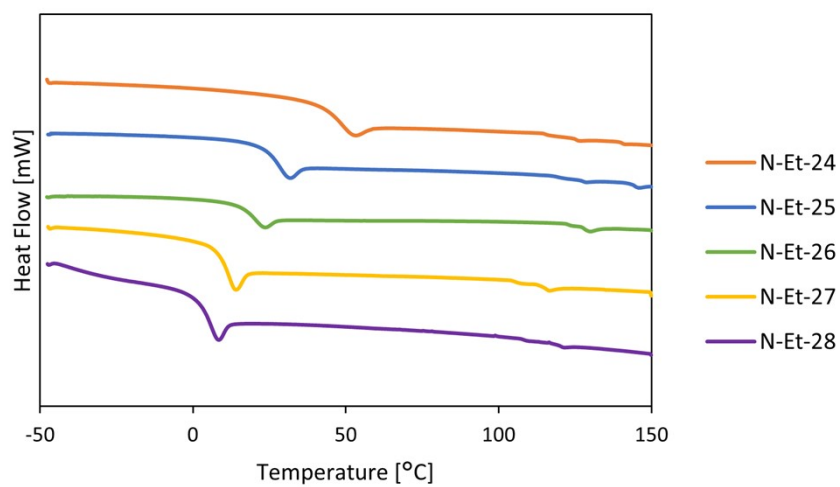


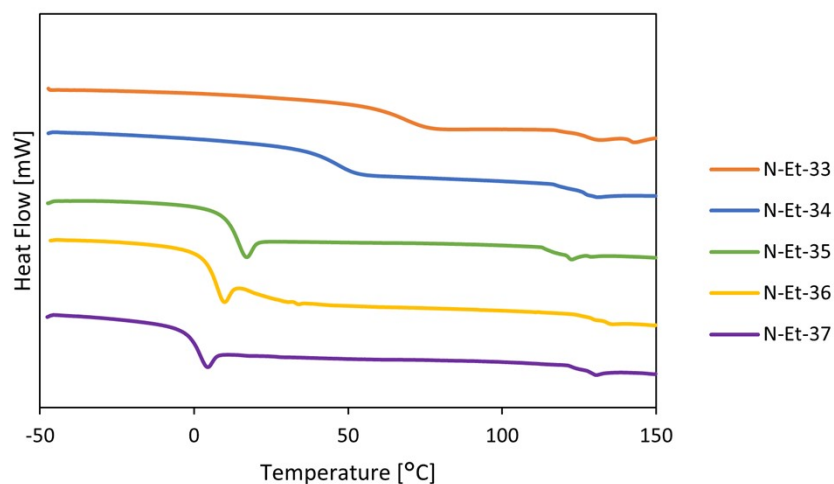
Figure S104. SEC chromatogram of *N*-Et-2,4-*ran*-*N*-Et-2,8

4 Thermal properties of *N*-alkylated nylons analyzed by DSC



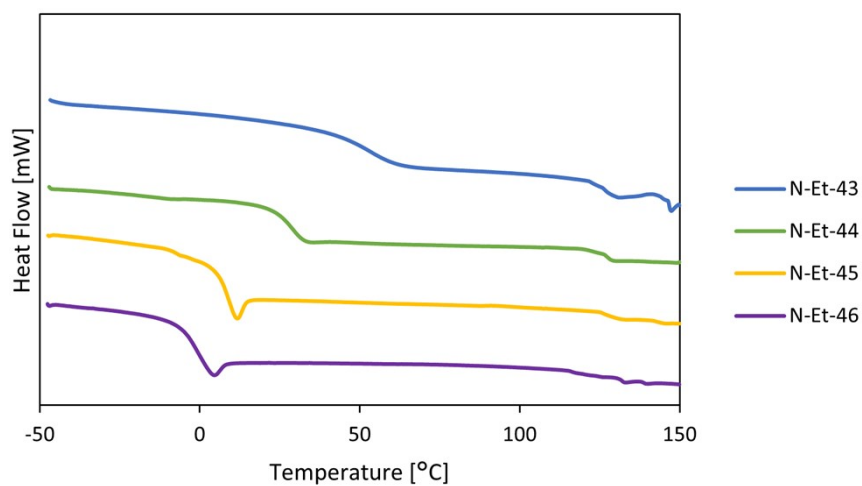
<i>N</i> -Et-2, <i>q</i>	T_g
<i>N</i> -Et-2,4	45 °C
<i>N</i> -Et-2,5	25 °C
<i>N</i> -Et-2,6	18 °C
<i>N</i> -Et-2,7	9 °C
<i>N</i> -Et-2,8	3 °C

Figure S105. DSC thermogram of *N*-Et-2,*q* (*q* = 4-8).



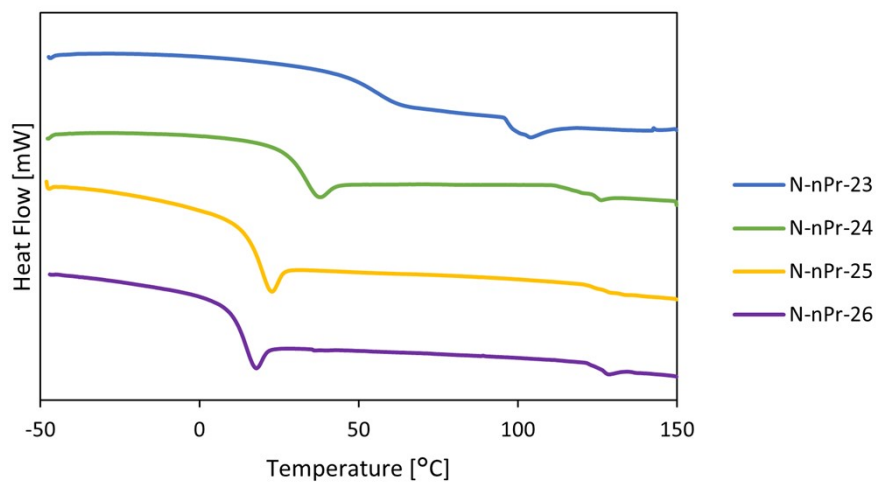
<i>N-Et-3,q</i>	T_g
<i>N-Et-3,3</i>	68 °C
<i>N-Et-3,4</i>	46 °C
<i>N-Et-3,5</i>	12 °C
<i>N-Et-3,6</i>	6 °C
<i>N-Et-3,7</i>	0 °C

Figure S106. DSC thermogram of *N-Et-3,q* ($q = 3-7$).



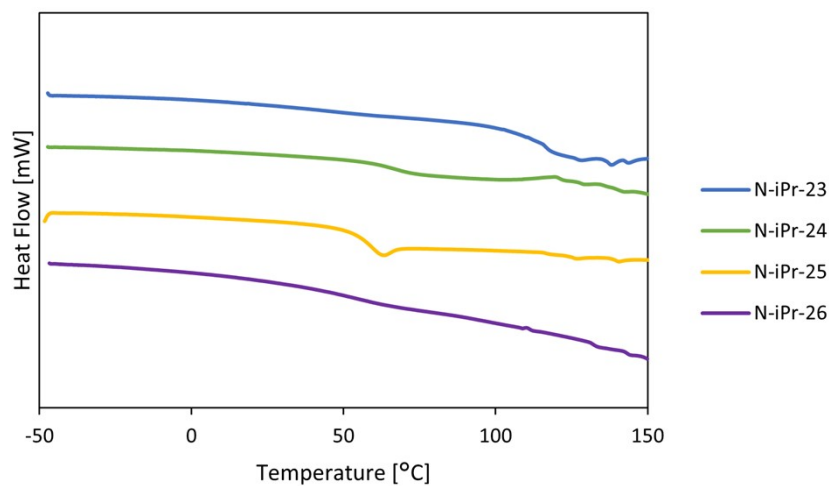
<i>N-Et-4,q</i>	T_g
<i>N-Et-4,3</i>	56 °C
<i>N-Et-4,4</i>	27 °C
<i>N-Et-4,5</i>	6 °C
<i>N-Et-4,6</i>	-2 °C

Figure S107. DSC thermogram of *N-Et-4,q* ($q = 3-6$).



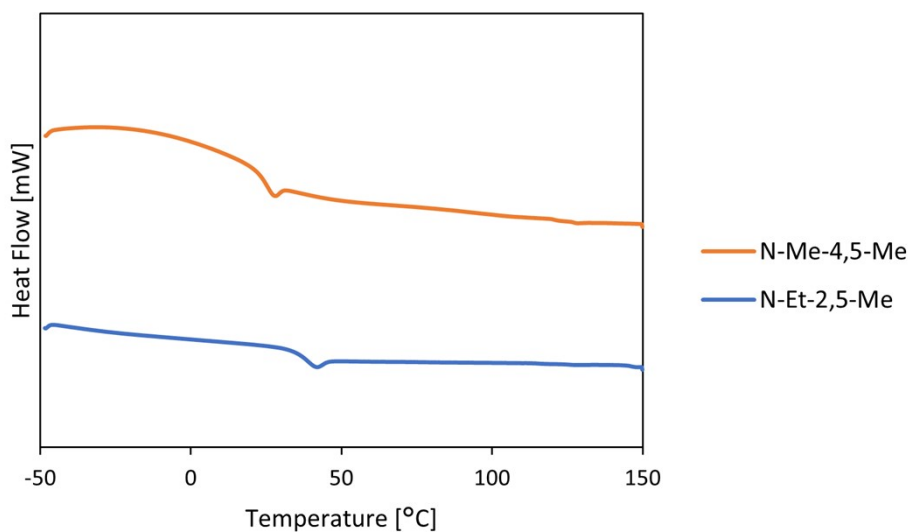
<i>N-nPr-2,q</i>	T_g
<i>N-nPr-2,3</i>	55 °C
<i>N-nPr-2,4</i>	29 °C
<i>N-nPr-2,5</i>	17 °C
<i>N-nPr-2,6</i>	12 °C

Figure S108. DSC thermogram of *N-nPr-2,q* ($q = 3-6$).



<i>N-iPr-2,q</i>	T_g
<i>N-iPr-2,3</i>	119 °C
<i>N-iPr-2,4</i>	80 °C
<i>N-iPr-2,5</i>	55 °C
<i>N-iPr-2,6</i>	51 °C

Figure S109. DSC thermogram of *N-iPr-2,q* ($q = 3-6$).



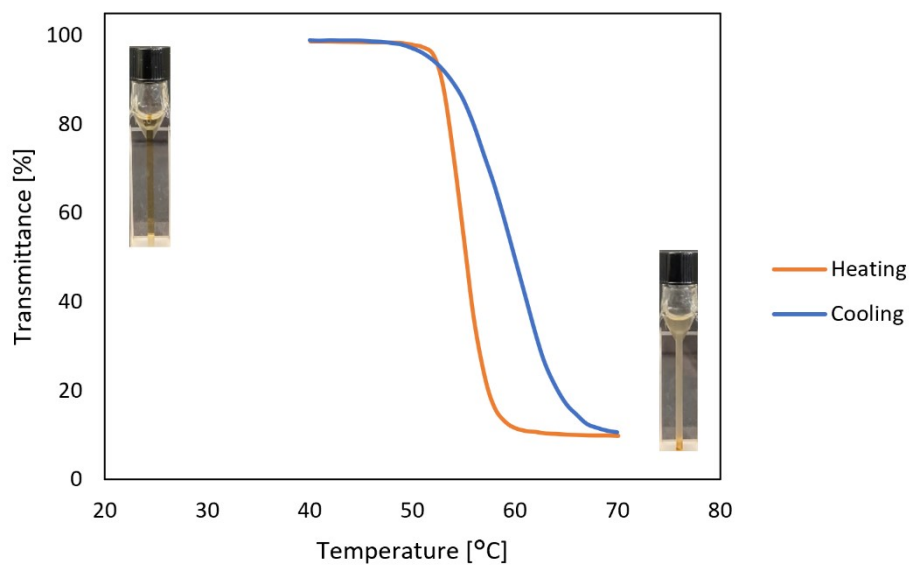
<i>N-R-p,5-Me</i>	T_g
<i>N-Me-4,5-Me</i>	23 °C
<i>N-Et-2,5-Me</i>	36 °C

Figure S110. DSC thermogram of *N-R-p,5-Me* ($R = \text{Me}, p = 4$), ($R = \text{Et}, p = 2$).

DSC 2nd heating curves of *N-Et-2,q* ($q = 4-8$), *N-Et-3,q* ($q = 3-7$), *N-Et-4,q* ($q = 3-6$), *N-nPr-2,q* ($q = 3-6$), and *N-iPr-2,q* ($q = 3-6$), *N-R-p,5-Me* ($R = \text{Me}, p = 4$), ($R = \text{Et}, p = 2$) are shown in Figure S105, S106 S107, S108, S109 and S110, respectively.

5 Thermo-responsiveness of *N*-alkylated nylons

(a)



(b)

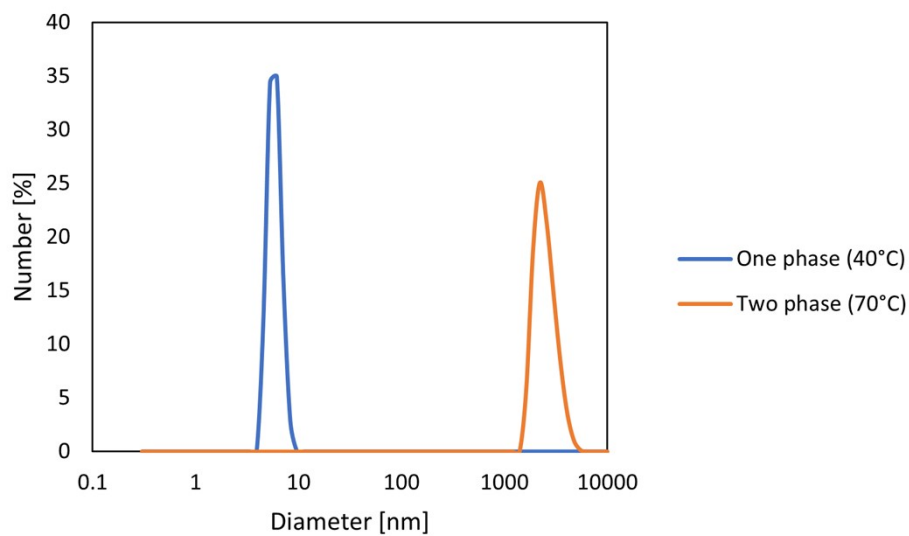
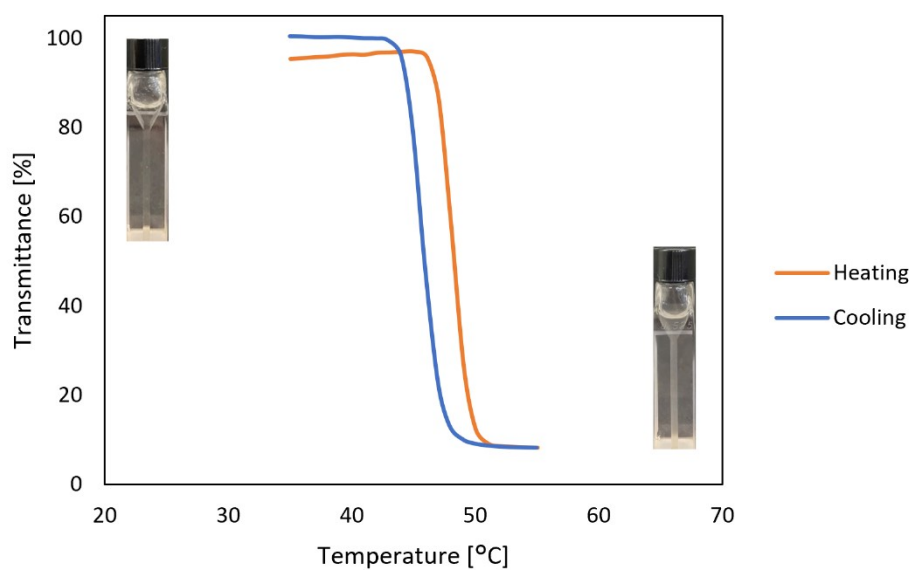


Figure S111. (a) Transmittance change at 800 nm of *N*-Et-2,5 in water (10 mg/mL) by the temperature changes; the orange and blue lines represent the heating and cooling processes, respectively. (b) Dynamic light scattering

(a)



(b)

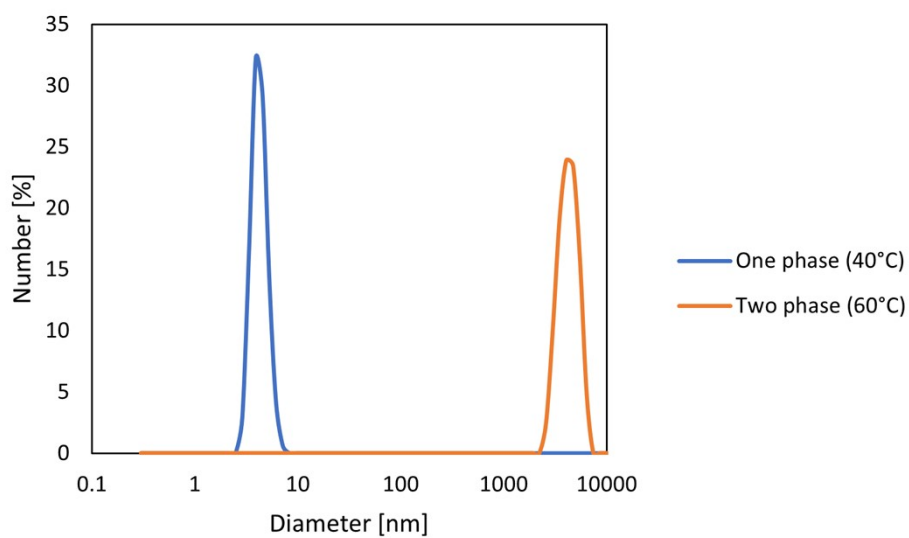
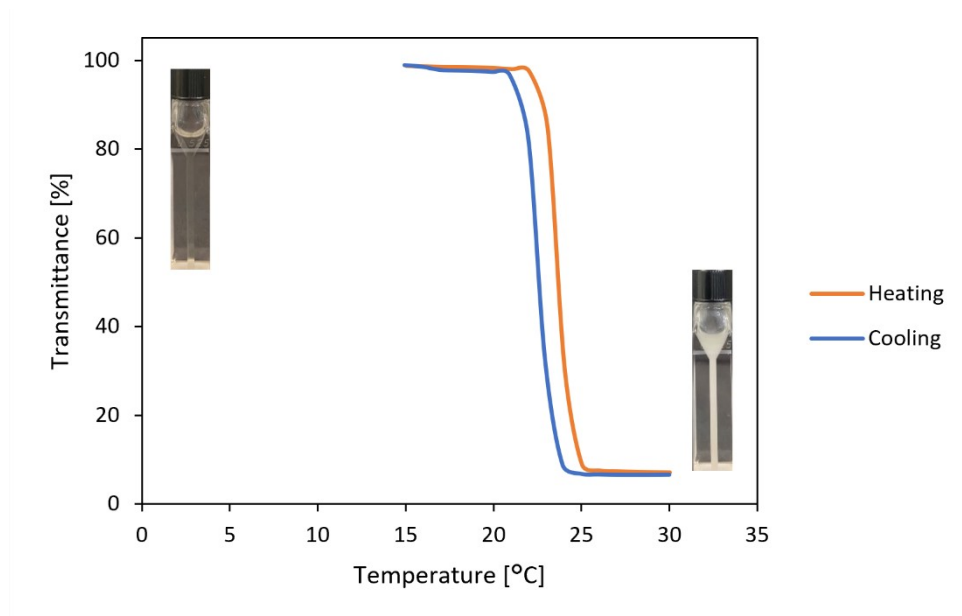


Figure S112. (a) Transmittance change at 800 nm of *N-Et-2,6* in water (10 mg/mL) by the temperature changes; the orange and blue lines represent the heating and cooling processes, respectively. (b) Dynamic light scattering

(a)



(b)

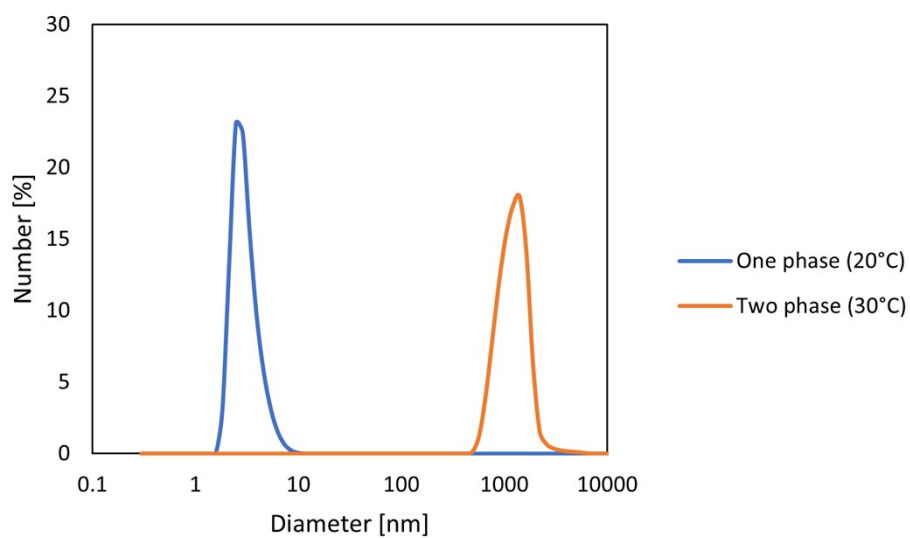
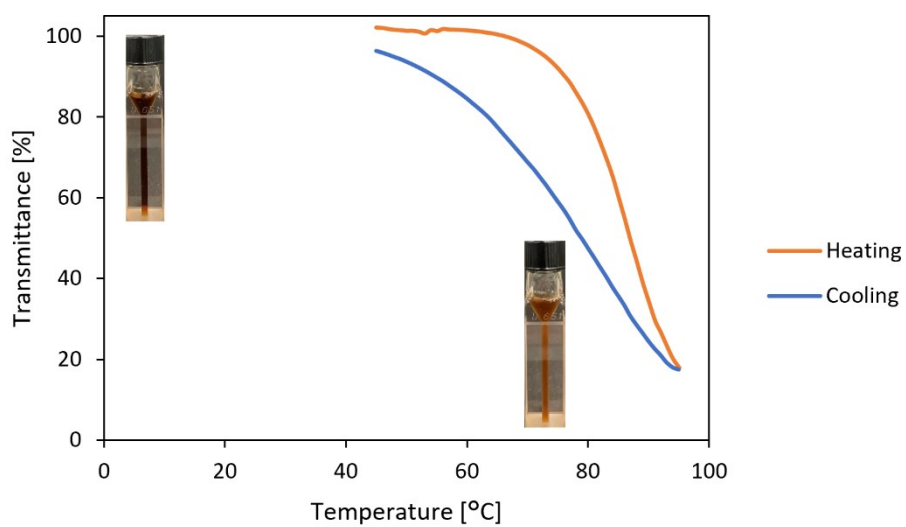


Figure S113. (a) Transmittance change at 800 nm of *N-Et-2,7* in water (10 mg/mL) by the temperature changes; the orange and blue lines represent the heating and cooling processes, respectively. (b) Dynamic light scattering

(a)



(b)

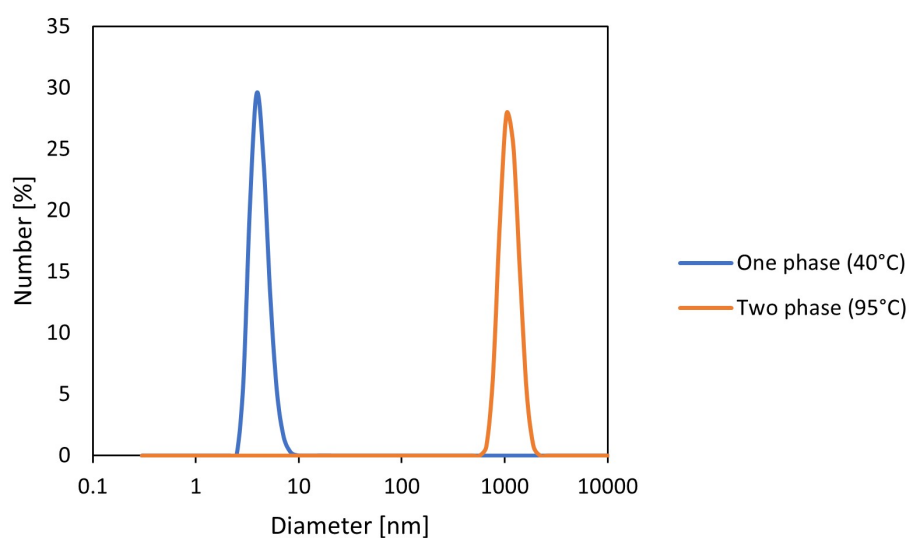
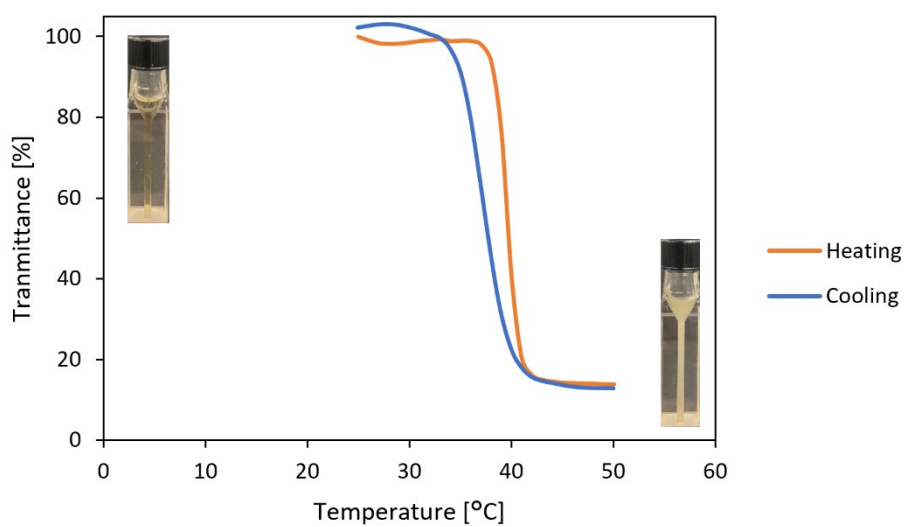


Figure S114. (a) Transmittance change at 800 nm of *N-Et-3,4* in water (10 mg/mL) by the temperature changes; the orange and blue lines represent the heating and cooling processes, respectively. (b) Dynamic light scattering

(a)



(b)

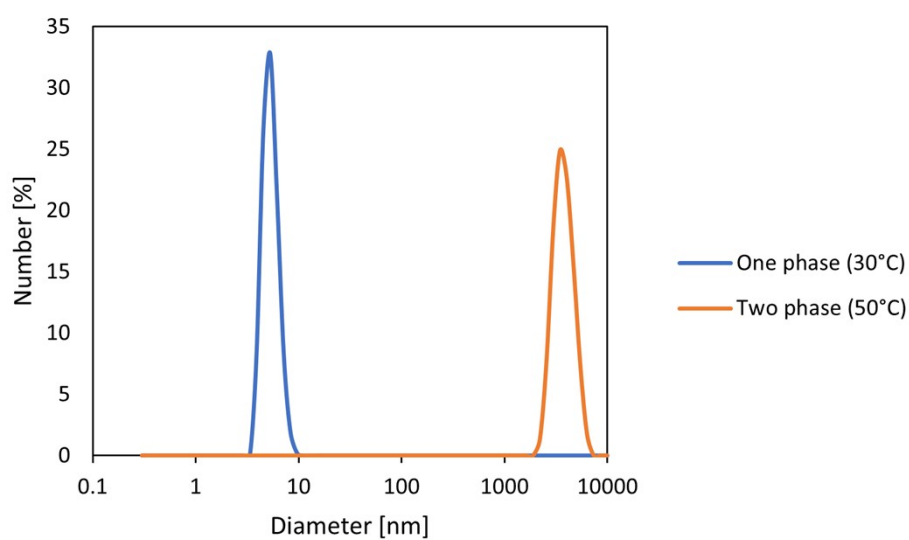
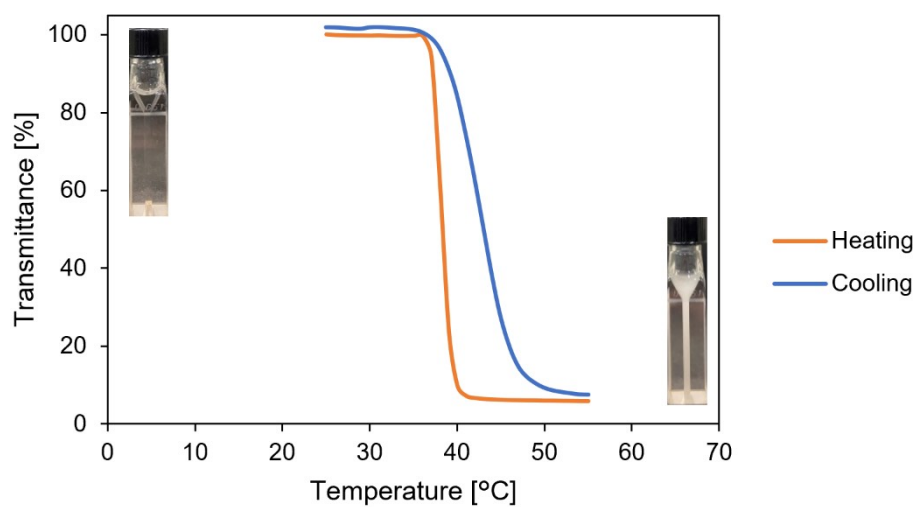


Figure S115. (a) Transmittance change at 800 nm of *N-Et-3,5* in water (10 mg/mL) by the temperature changes; the orange and blue lines represent the heating and cooling processes, respectively. (b) Dynamic light scattering

(a)



(b)

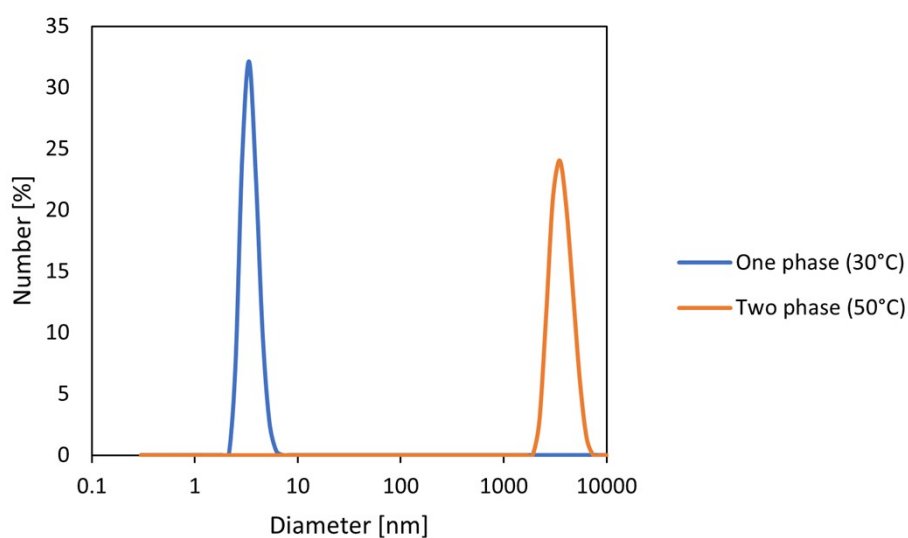
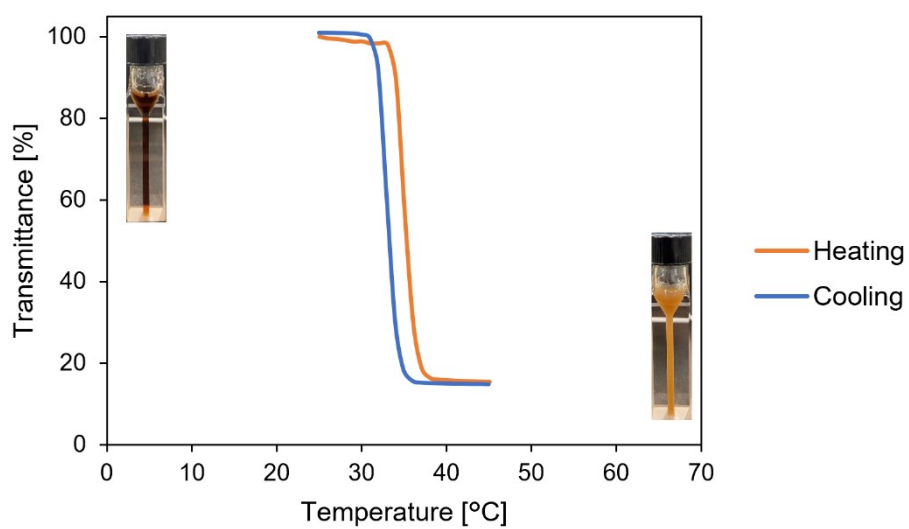


Figure S116. (a) Transmittance change at 800 nm of *N-Et-3,6* in water (10 mg/mL) by the temperature changes; the orange and blue lines represent the heating and cooling processes, respectively. (b) Dynamic light scattering

(a)



(b)

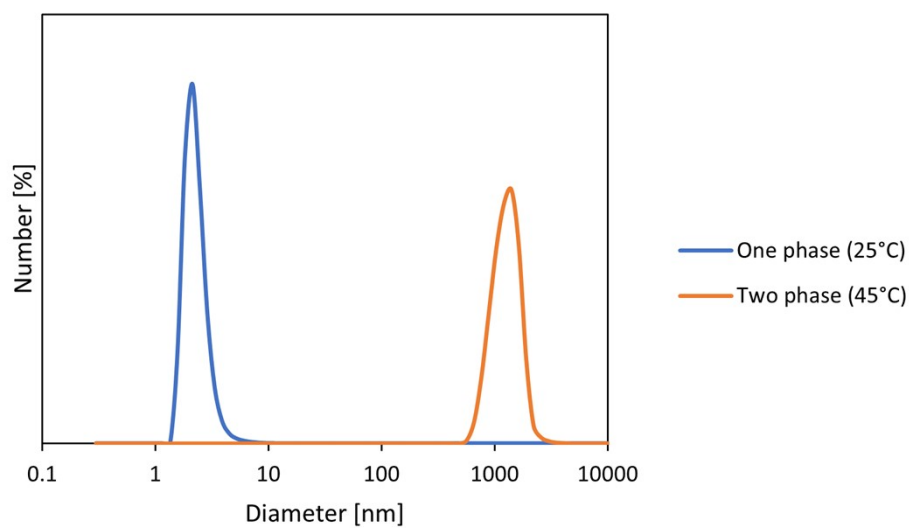
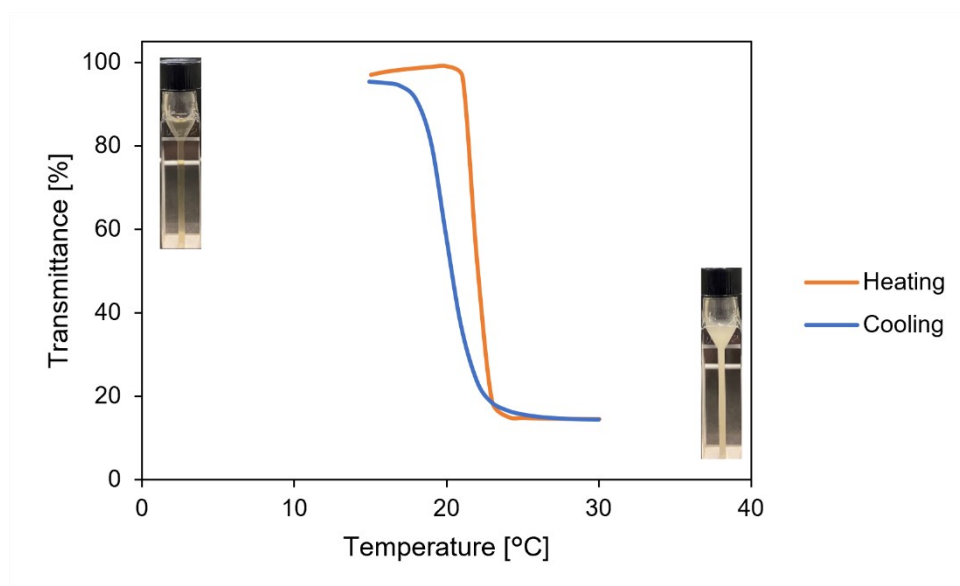


Figure S117. (a) Transmittance change at 800 nm of *N*-Et-4,4 in water (10 mg/mL) by the temperature changes; the orange and blue lines represent the heating and cooling processes, respectively. (b) Dynamic light scattering

(a)



(b)

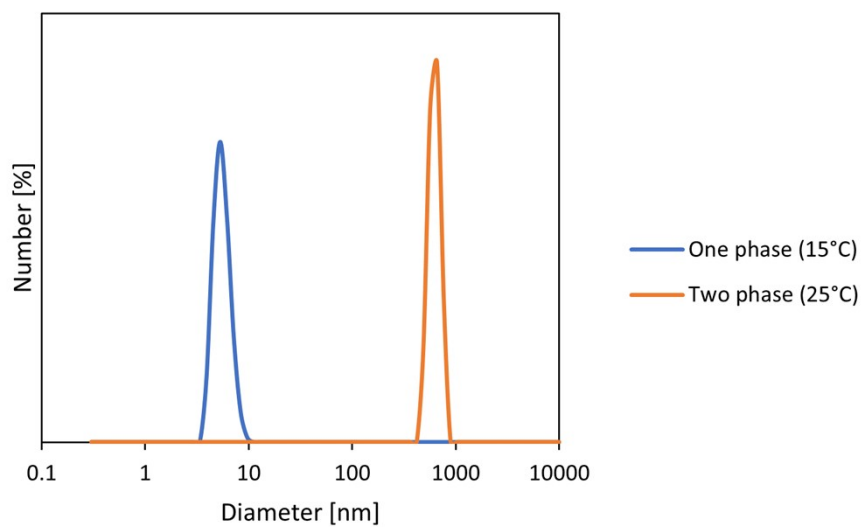
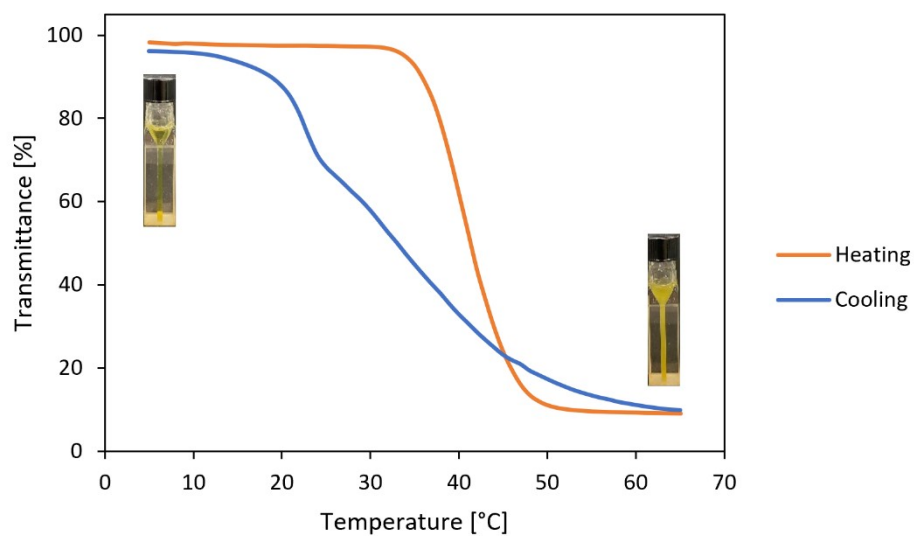


Figure S118. (a) Transmittance change at 800 nm of *N-Et-4,5* in water (10 mg/mL) by the temperature changes; the orange and blue lines represent the heating and cooling processes, respectively. (b) Dynamic light scattering

(a)



(b)

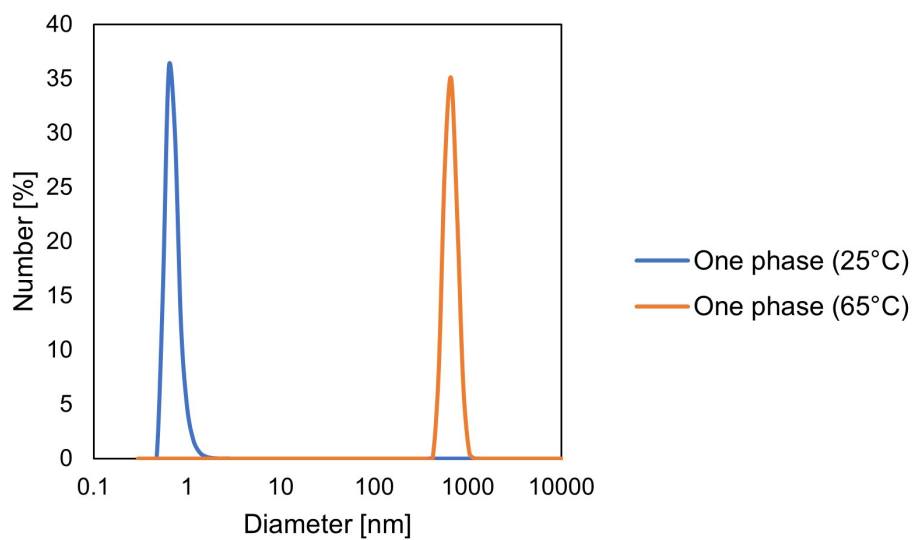
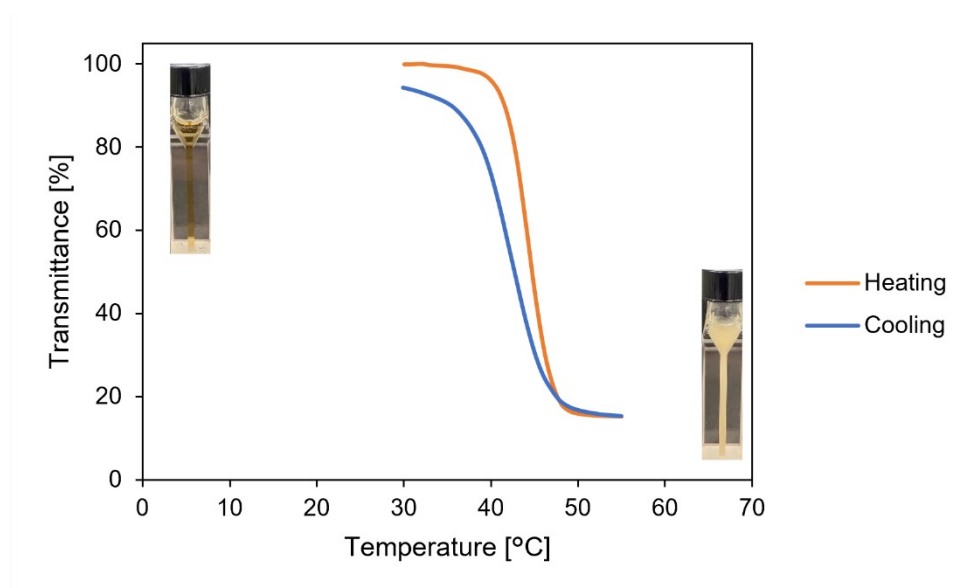


Figure S119. (a) Transmittance change at 800 nm of *N-nPr-2,3* in water (10 mg/mL) by the temperature changes; the orange and blue lines represent the heating and cooling processes, respectively. (b) Dynamic light scattering

(a)



(b)

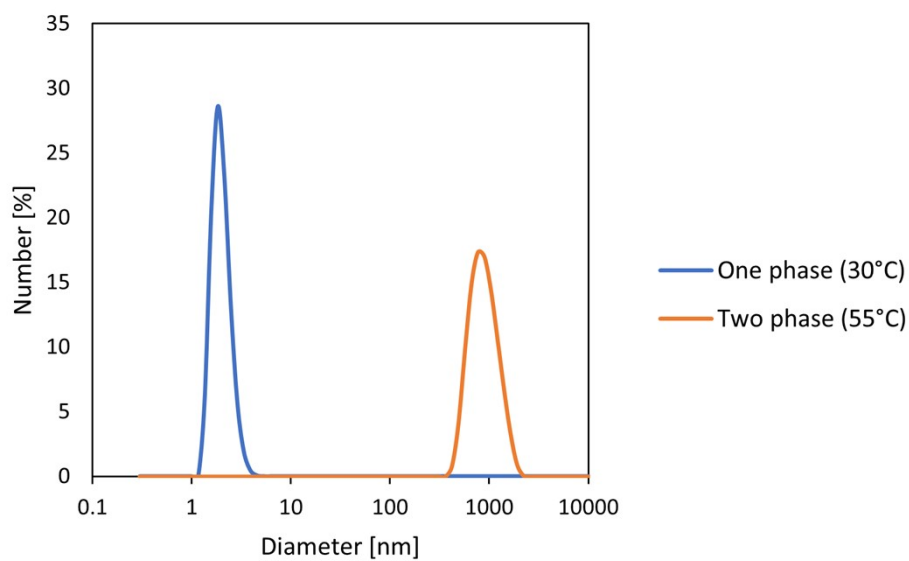
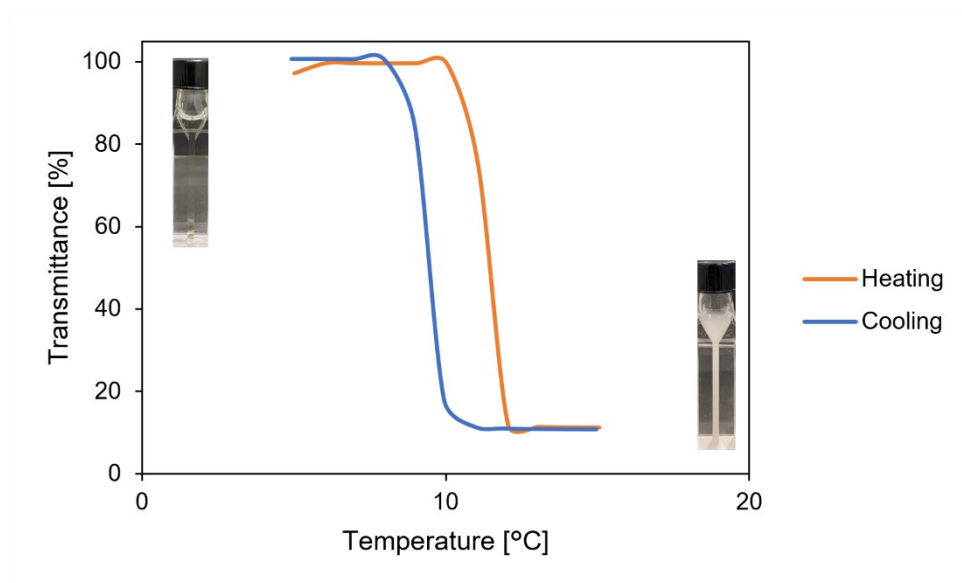


Figure S120. (a) Transmittance change at 800 nm of *N-nPr-2,4* in water (10 mg/mL) by the temperature changes; the orange and blue lines represent the heating and cooling processes, respectively. (b) Dynamic light scattering

(a)



(b)

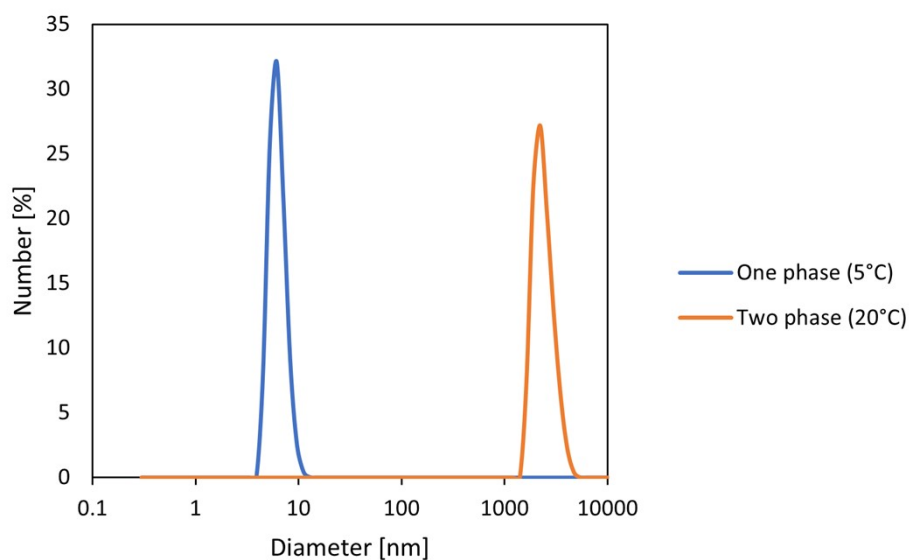
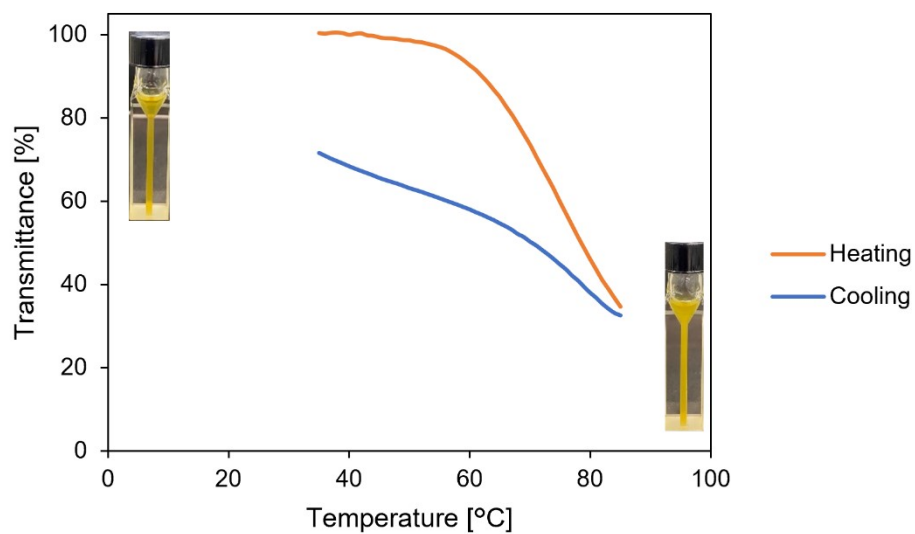


Figure S121. (a) Transmittance change at 800 nm of *N-nPr-2,5* in water (10 mg/mL) by the temperature changes; the orange and blue lines represent the heating and cooling processes, respectively. (b) Dynamic light scattering

(a)



(b)

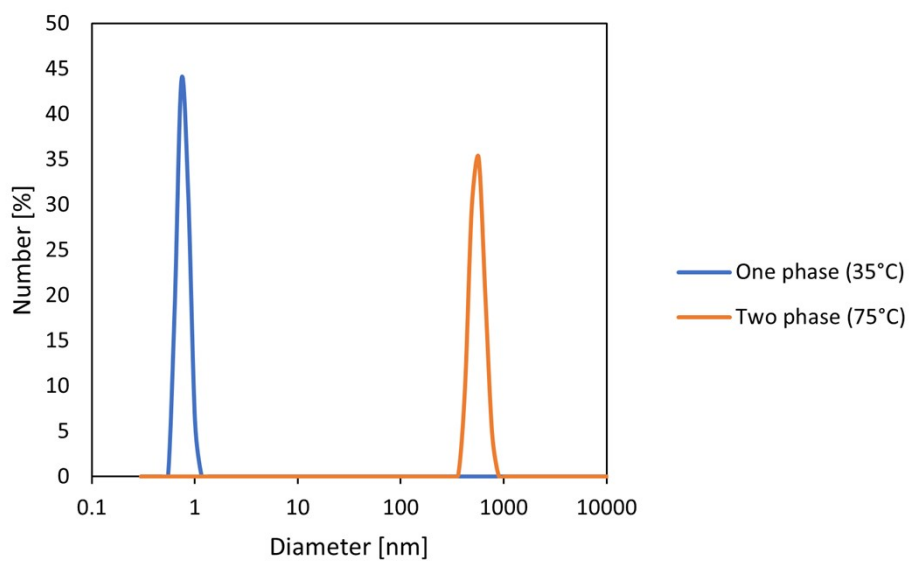
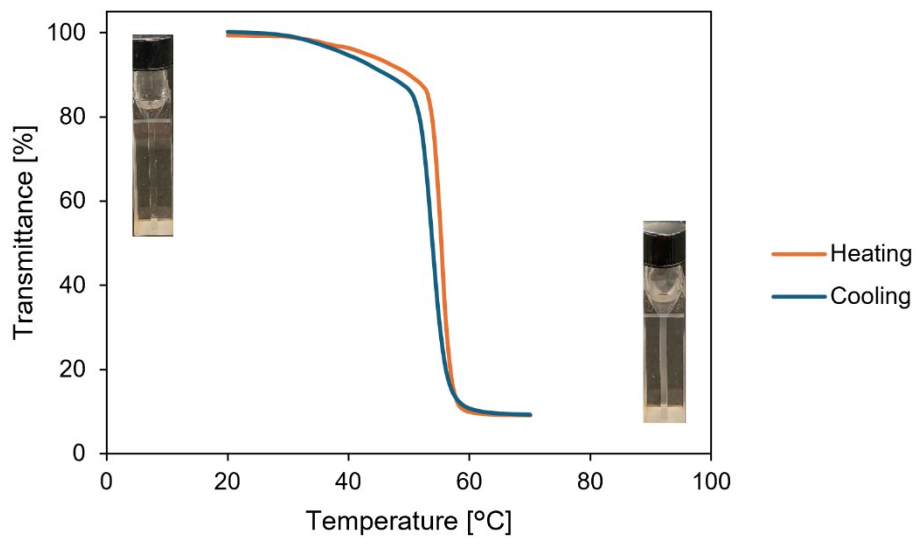


Figure S122. (a) Transmittance change at 800 nm of *N-iPr-2,3* in water (10 mg/mL) by the temperature changes; the orange and blue lines represent the heating and cooling processes, respectively. (b) Dynamic light scattering

(a)



(b)

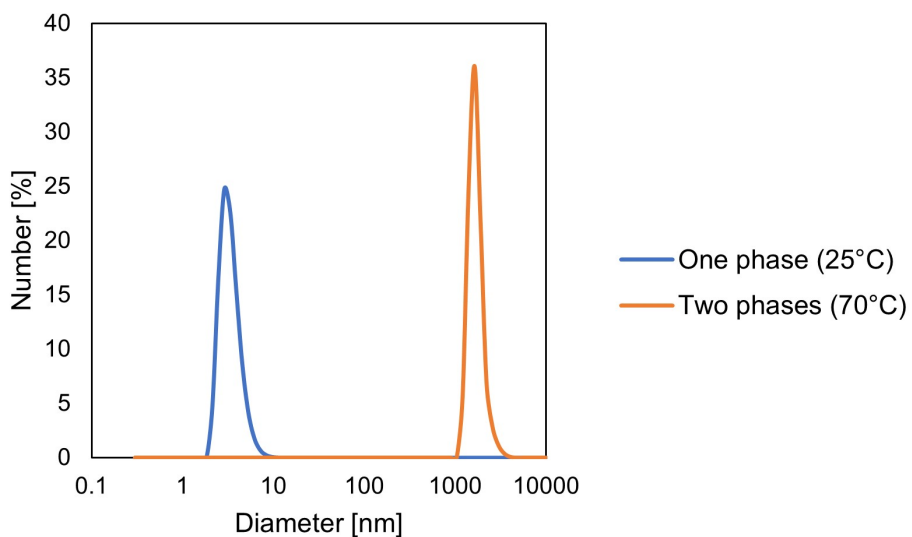
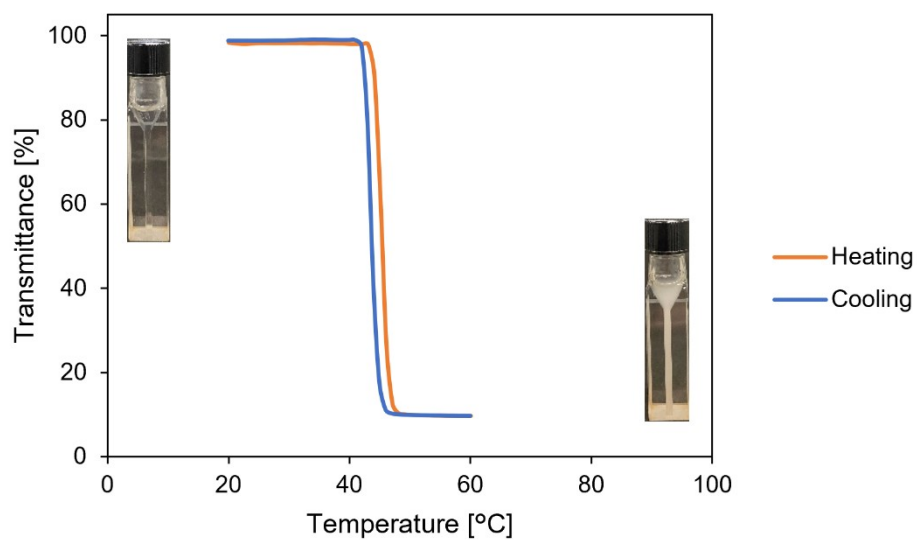


Figure S123. (a) Transmittance change at 800 nm of *N-Me-4,5-Me* in water (10 mg/mL) by the temperature changes; the orange and blue lines represent the heating and cooling processes, respectively. (b) Dynamic light scattering

(a)



(b)

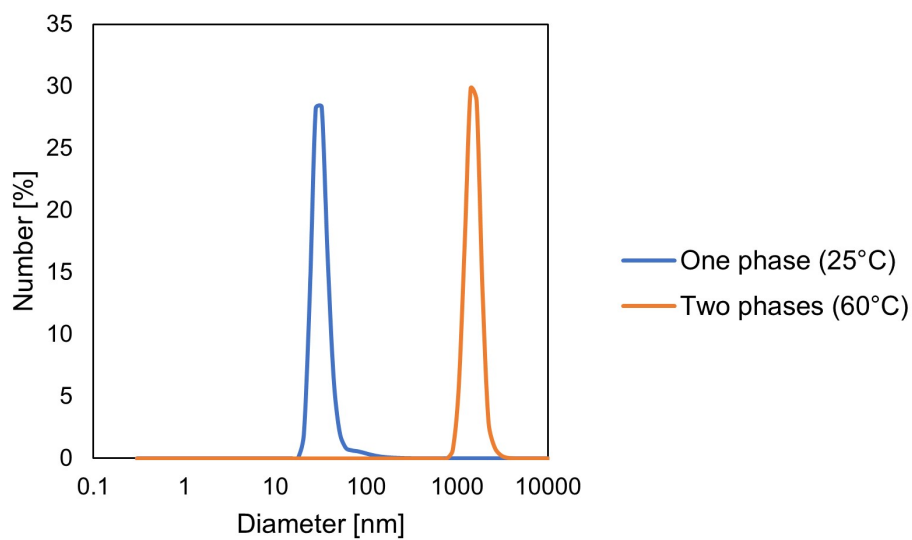
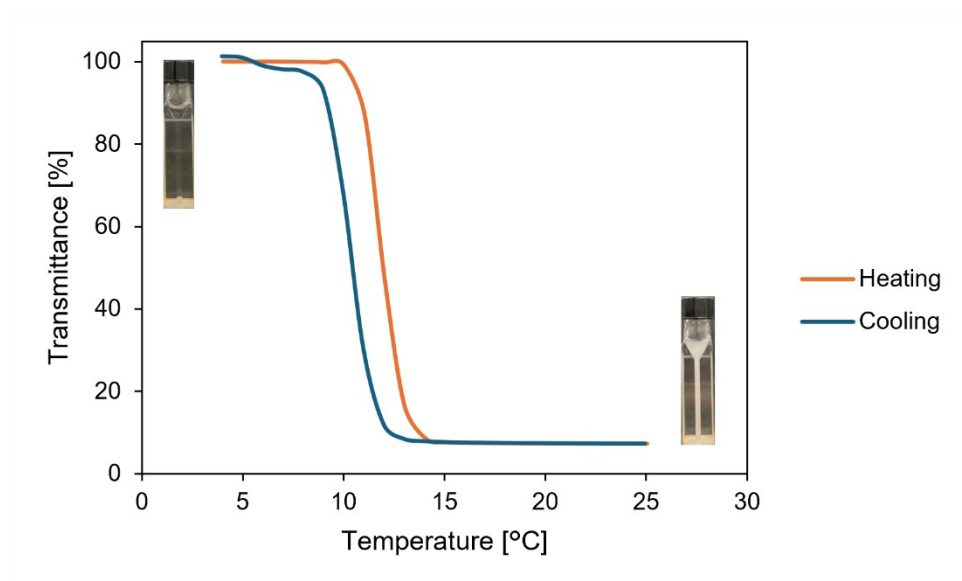


Figure S124. (a) Transmittance change at 800 nm of *N-Et-2,5-Me* in water (10 mg/mL) by the temperature changes; the orange and blue lines represent the heating and cooling processes, respectively. (b) Dynamic light scattering

(a)



(b)

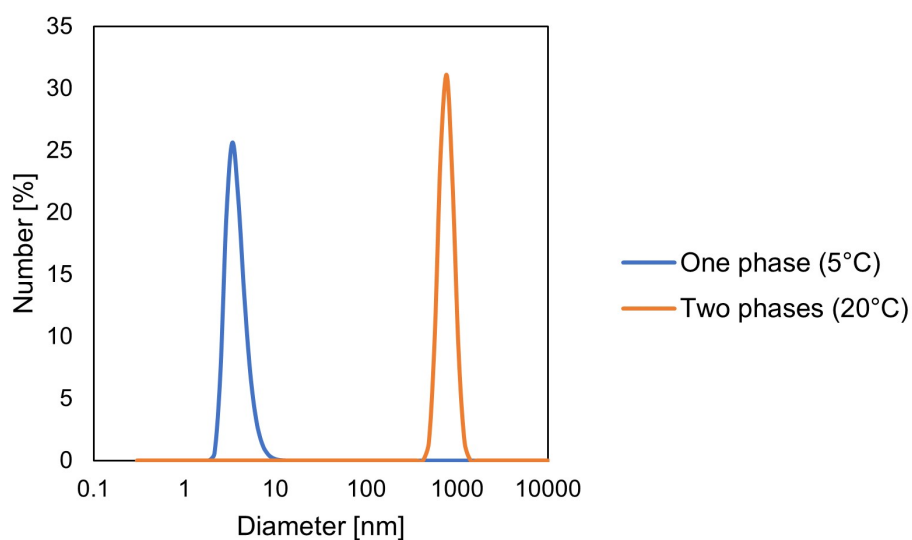
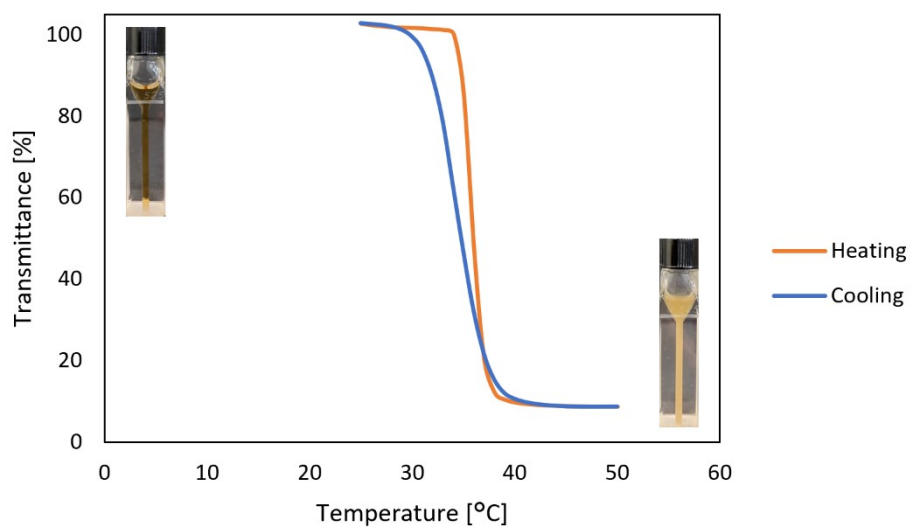


Figure S125. (a) Transmittance change at 800 nm of *N-Me-2,6-ran-N-Me-2,10* in water (10 mg/mL) by the temperature changes; the orange and blue lines represent the heating and cooling processes, respectively. (b) Dynamic light scattering

(a)



(b)

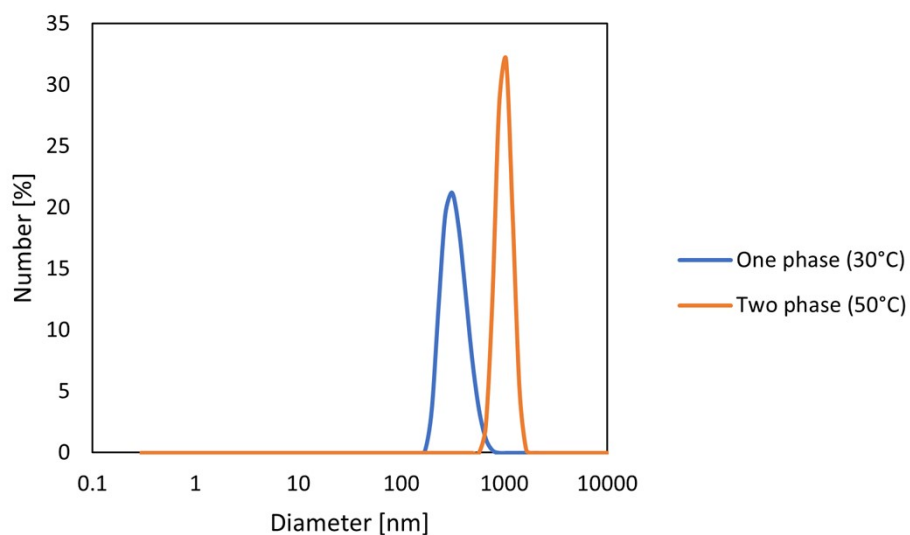


Figure S126. (a) Transmittance change at 800 nm of *N-Et-2,4-ran-N-Et-2,8* in water (10 mg/mL) by the temperature changes; the orange and blue lines represent the heating and cooling processes, respectively. (b) Dynamic light scattering

(a)

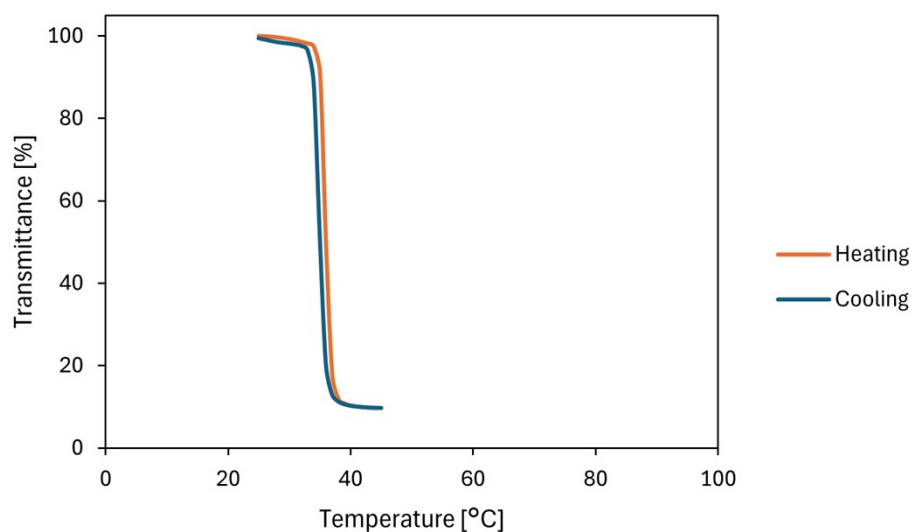


Figure S127. (a) Transmittance change at 800 nm of *N-Me-4,6* in water (10 mg/mL) by the temperature changes; the orange and blue lines represent the heating and cooling processes, respectively.

6 DLS measurement of thermo-responsive behavior of *N-Et-4,4* in H₂O

As shown in **Figure S128**, temperature-dependent DLS measurements for *N-Et-4,4* ($T_{cp} = 32$ °C) during heating revealed a sharp increase in particle size at temperatures slightly below the cloud point, providing insight into the aggregation process associated with LCST-type phase separation.

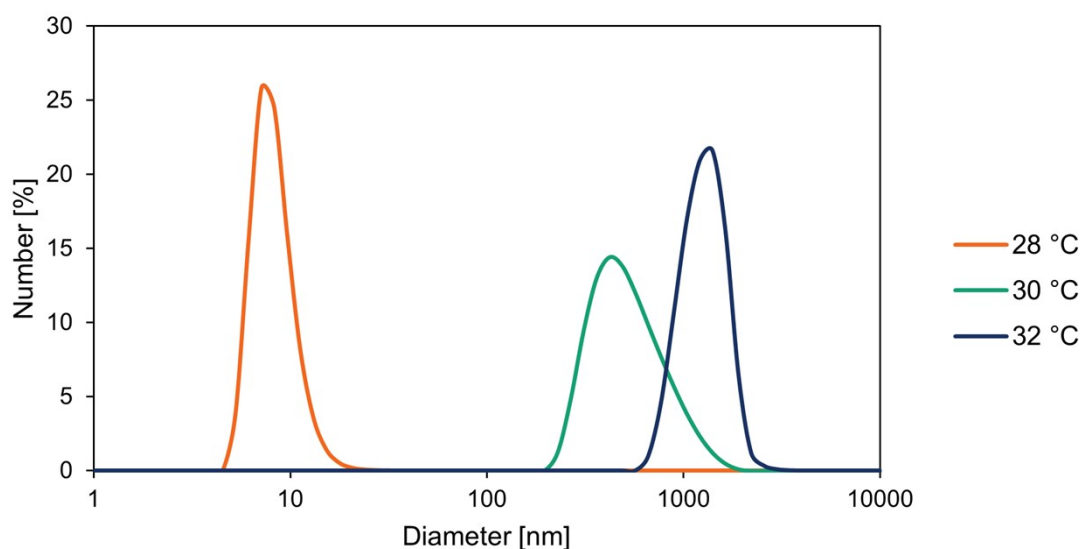


Figure S128. Variable temperature DLS measurement in H₂O (10 mg/mL) at 28 °C to 32 °C.

7 ^1H NMR analysis of thermo-responsive behavior of *N*-Et-4,4 in D_2O

As shown in **Figure S129**, the conformer ratio² of the tertiary amide group (cis:trans = 1.0:1.2) at 1.0 to 1.2 ppm remained unchanged around T_{cp} at 32 °C, indicating that the interconversion between the two conformers would not induce the LCST-type phase separation. Above T_{cp} , all the peaks did not disappear and only slightly shifted downfield. If coil-globule transition occurs above T_{cp} , all polymer peaks should completely disappear. Therefore, these observations can be explained by partial dehydration of the polymer chain inducing the aggregation of an aliphatic group to coacervation³⁻⁵.

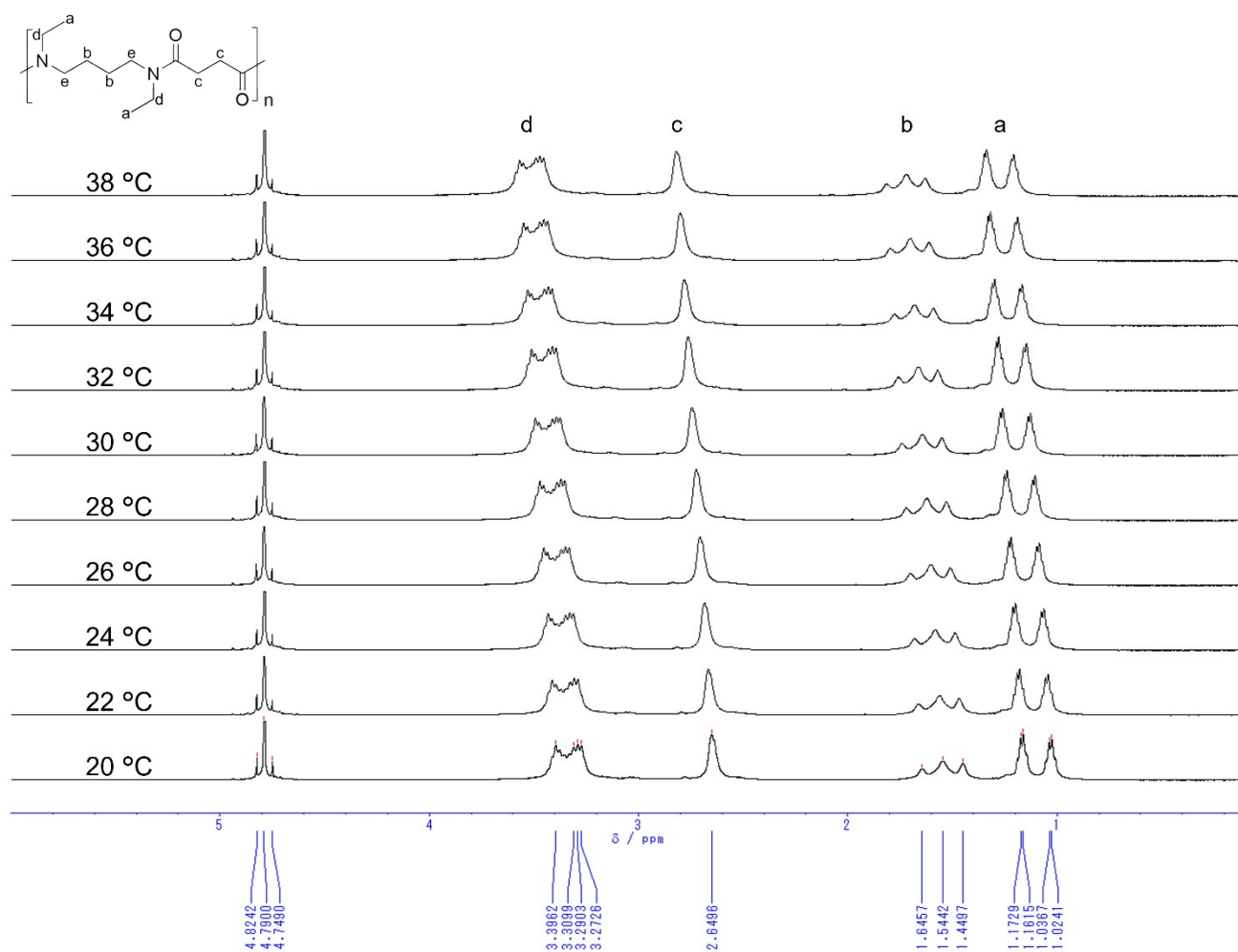
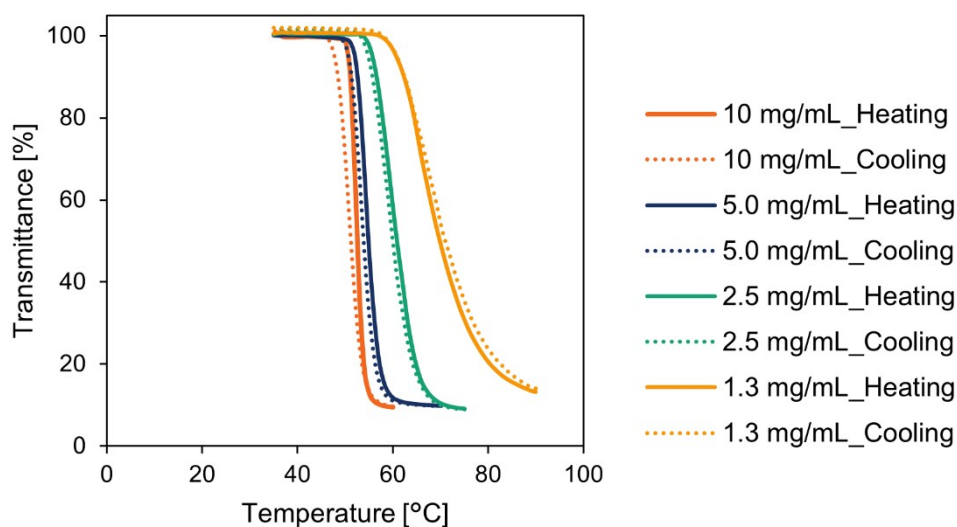


Figure S129. Variable temperature ^1H NMR analysis in D_2O (10 mg/mL) at 20 °C to 38 °C.

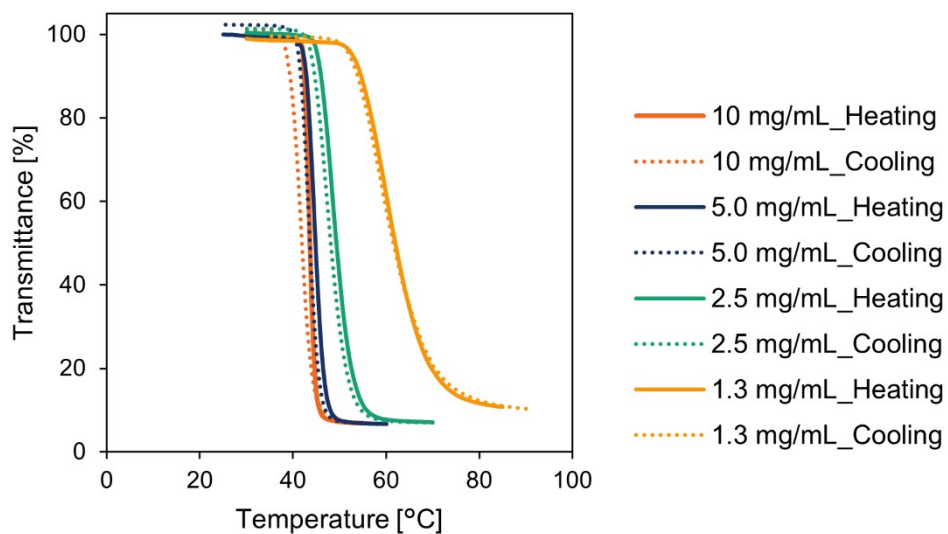
8 Concentration dependence of *N*-alkylated nylons on the LCST-type phase separation

Aqueous solutions of four *N*-Et-2,6, *N*-Et-3,5, *N*-Et-4,4 and *N*-*n*Pr-2,4 were prepared at different concentrations (10 mg/mL, 5.0 mg/mL, 2.5 mg/mL, 1.3 mg/mL), and the transmittance change at 800 nm of each solution was measured (scan rate: 1.5 °C/min). In **Figure S130- S134** shown below, the solid and dotted orange line (10 mg/mL), blue line (5.0 mg/mL), green line (2.5 mg/mL), and yellow line (1.3 mg/mL) represent the heating and cooling processes, respectively.



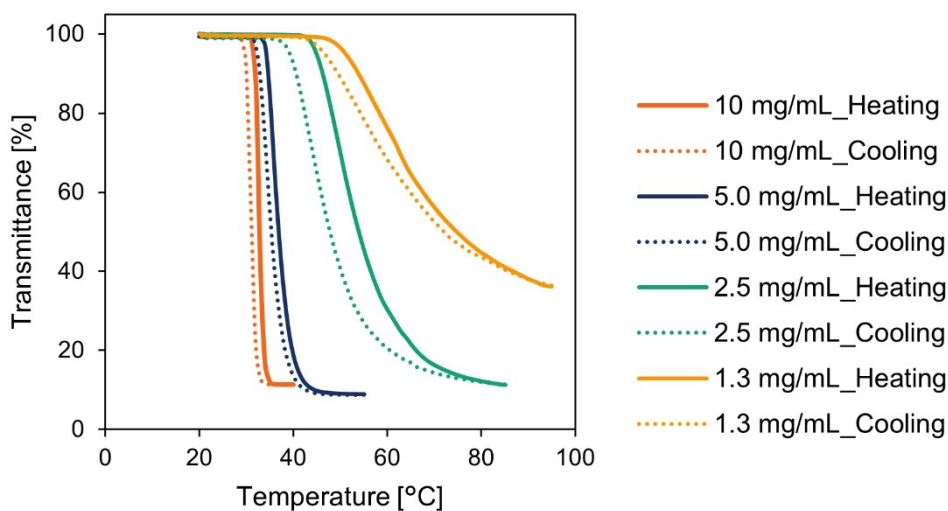
Concentration	T_{cp}
10 mg/mL	51 °C
5.0 mg/mL	52 °C
2.5 mg/mL	56 °C
1.3 mg/mL	62 °C

Figure S130. Transmittance change in water with different concentrations of *N*-Et-2,6.



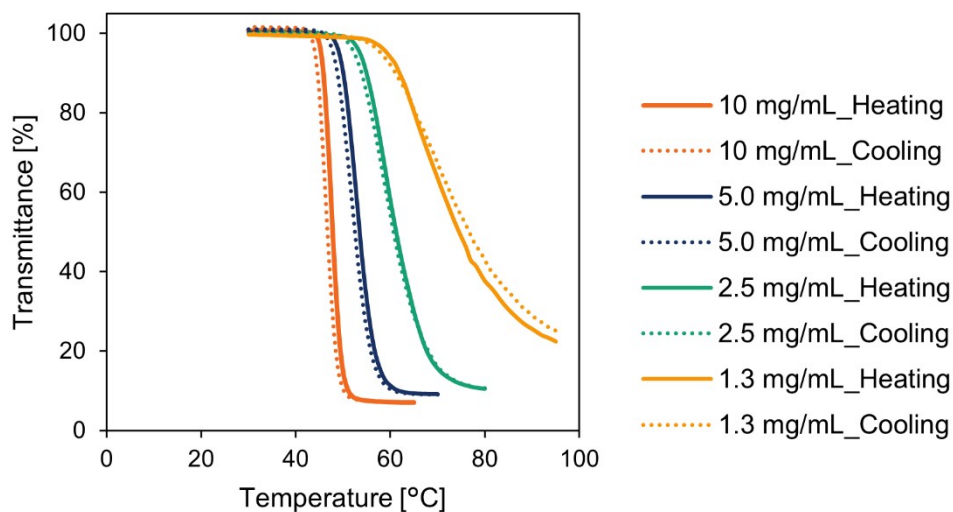
Concentration	T_{cp}
10 mg/mL	42 °C
5.0 mg/mL	42 °C
2.5 mg/mL	46 °C
1.3 mg/mL	54 °C

Figure S131. Transmittance change in water with different concentrations of *N-Et-3,5*.



Concentration	T_{cp}
10 mg/mL	32 °C
5.0 mg/mL	34 °C
2.5 mg/mL	46 °C
1.3 mg/mL	53 °C

Figure S132. Transmittance change in water with different concentrations of *N-Et-4,4*.



Concentration	T_{cp}
10 mg/mL	46 °C
5.0 mg/mL	50 °C
2.5 mg/mL	55 °C
1.3 mg/mL	62 °C

Figure S133. Transmittance change in water with different concentrations of *N-nPr-2,4*.

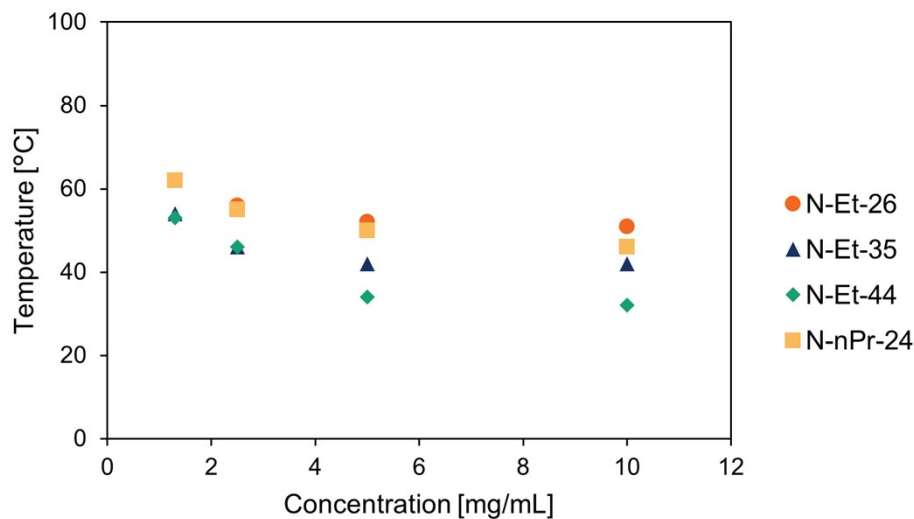


Figure S134. The effect of solution concentration from 10 mg/mL to 1.3 mg/mL for LCST-type thermo-responsiveness of *N-Et-2,6* (red circle), *N-Et-3,5* (blue triangle), *N-Et-4,4* (green diamond), *N-nPr-2,4* (yellow square) in water. T_{cp} was determined by transmittance change at 800 nm (scan rate: 1.5 °C/min). In all cases, the solubility and T_{cp} of *N*-methylated nylons in water increase with decreasing the solution concentration.

9 Supplementary references

1. F. Devínský, I. Lacko, L. Krasnec, *Synthesis*, **1980**, *1980*, 303–305.
2. Q. Sui, D. Borchardt, D. L. Rabenstein, Kinetics and equilibria of cis/trans isomerization of backbone amide bonds in peptoids. *J. Am. Chem. Soc.*, **2007**, *129*, 12042–12048.
3. T. Maeda, M. Takenouchi, K. Yamamoto, T. Aoyagi, Thermoresponsive polymers. *Biomacromolecules*, **2006**, *7*, 2230–2236.
4. J. P. Swanson, L. R. Monteleone, F. Haso, P. J. Costanzo, T. Liu, A. Joy, Thermoresponsive, coacervate-forming biodegradable polyesters. *Macromolecules*, **2015**, *48*, 3834–3842.
5. J. P. Swanson, M. R. Martinez, M. A. Cruz, S. G. Mankoci, P. J. Costanzo, A. Joy, Functional coacervates. *Polym. Chem.*, **2016**, *7*, 4693–4703.